Identification of KSRP as a novel protein regulator of the interferon-inducible RNA-dependent protein kinase (PKR) by quantitative mass spectrometry

DISSERTATION

zur Erlangung des akademischen Grades

DOCTOR RERUM NATURALIUM

(Dr. rer. nat.)

im Fach Biologie

eingereicht an der

Lebenswissenschaftlichen Fakultät
der Humboldt-Universität zu Berlin

von

Sandra Sänger

Präsidentin der Humboldt-Universität zu Berlin

Prof. Dr.-Ing. habil. Dr. Sabine Kunst

Dekan der Lebenswissenschaftlichen Fakultät

Prof. Dr. Richard Lucius

Gutachter:
1. PD Dr. Thorsten Wolff
3. Prof. Dr. Detlev H. Krüger
3. Prof. Dr. Benedikt Kaufer

Tag der mündlichen Prüfung: 27.10.2016

Summary

The RNA-dependent protein kinase (PKR) is an interferon induced protein kinase that plays a significant role in innate antiviral immunity. Activation of PKR can be triggered by binding of viral RNA and results in dimerisation and autophosphorylation of the protein. Downstream effects of PKR include inhibition of translation, initiation of apoptosis and the induction of transcription factors that lead to production of proinflammatory cytokines. Due to its key role in antiviral immunity, many viruses have evolved mechanisms to avoid PKR initiated effects. For influenza viruses, the main antagonist of PKR is the multifunctional non-structural protein 1 (NS1). Over the last decades, extensive research was conducted to identify the whole network of PKR regulators and adaptor proteins, but it is most likely that still some pieces are missing to complete our understanding of PKR functions.

This thesis provides a systematic analysis of PKR binding partners in the context of influenza virus infection by using quantitative mass spectrometry. In total, 47 proteins that bound specifically to PKR after influenza A/Puerto Rico/8/1934 (H1N1) wild type (WT) or ΔNS1 virus infection were identified. The interaction of PKR and a subset of proteins was tested in independent biochemical assays to confirm reliability of the method. The biological impact of identified proteins was examined in overexpression experiments. Hereby, four proteins had a positive effect on the catalytic PKR activity. The most interesting candidate, the KH type-splicing regulatory protein (KSRP), was selected for further analysis to investigate its role in PKR regulation and antiviral immunity in greater detail.

KSRP is an AU-rich element-binding protein that is involved in degradation of various cytokine mRNAs. The results of this thesis show that overexpression of KSRP induced phosphorylation of PKR in a dose-dependent manner. Activation of PKR by KSRP was mediated by direct interaction of KSRP with the N-terminal domain of PKR, but was found to be independent from dsRNA binding. Immunofluorescence experiments showed that upon infection with the influenza A ΔNS1 virus, both proteins were redistributed to antiviral stress granules. In addition to binding of KSRP and PKR, the function of KSRP in PKR dependent signalling was analysed. Knockdown of KSRP impaired PKR activation and consequently rescued viral replication of influenza A mutant viruses by one order of magnitude in cells with reduced IFNβ levels.

It was shown for the first time that KSRP directly supports antiviral signalling by enhancing PKR activation in a process that involves direct protein-protein-interaction. Taken together, this study demonstrates the aptitude of quantitative mass spectrometry for elucidation of cellular antiviral response pathways to reveal potential new targets for antiviral therapy.

Zusammenfassung

Die RNA-abhängige Proteinkinase (PKR) ist eine Interferon-induzierte Proteinkinase mit einer zentralen Rolle in der angeborenen, antiviralen Immunantwort. Eine Aktivierung von PKR wird unter anderem durch Bindung viraler RNA ausgelöst und resultiert in der Dimerisierung und Autophosphorylierung des Proteins. Nachgeschaltete Effekte von PKR umfassen die Inhibierung der Translation, Initiation von Apoptose und die Induktion von Transkriptionsfaktoren, die zur Produktion von proinflammatorischen Cytokinen führen. Aufgrund seiner Schlüsselrolle in der antiviralen Abwehr haben viele Viren Mechanismen entwickelt, um PKR-initiierte Effeke zu vermeiden. In Influenzaviren wird diese Aufgabe vom multifunktionalen Nichtstrukturprotein 1 (NS1) übernommen. In den letzten Jahrzehnten wurde intensiv daran geforscht, das gesamte Spektrum von PKR-Regulatoren und Adaptorproteinen aufzudecken, es ist jedoch sehr wahrscheinlich, dass noch einige Teile zur Vervollständigung unseres Verständnisses der PKR Funktionen fehlen.

In der vorliegenden Arbeit wurde mithilfe von quantitativer Massenspektrometrie eine systematische Analyse von PKR Bindungspartnern im Kontext einer Influenzavirusinfektion durchgeführt. Zusammengenommen wurden 47 Proteine identifiziert, die nach Infektion mit Influenza A/Puerto Rico/8/1934 (H1N1) Wildtyp (WT)- oder ΔNS1-Virus spezifisch an PKR gebunden waren. Die Interaktion von PKR und einem Teil der Proteine und deren biologische Relevanz wurden in weiterführenden Experimenten analysiert. Hierbei wurden vier Proteine mit einem positiven Einfluss auf die katalytische PKR-Aktivität gefunden. Der vielversprechendste Kandidat, das KH-Typ Splicing regulatorische Protein (KSRP), wurde für weiterführende Analysen hinsichtlich seines Einflusses auf PKR-Regulierung und antivirale Immunantwort ausgewählt.

KSRP ist ein AU-reiche-RNA-Elemente-bindendes Protein, das an der Degradation verschiedener Zytokin-mRNA beteiligt ist. Die Ergebnisse dieser Arbeit zeigen, dass die Überexpression von KSRP die Phosphorylierung von PKR dosisabhängig steigert. Die Aktivierung von PKR durch KSRP wurde dabei durch direkte Interaktion der Proteine über die N-terminale Domäne von PKR vermittelt, war jedoch unabhängig von der RNA-Bindungsfunktion. Immunfluoreszenzversuche zeigten, dass die Infektion mit dem ΔNS1-Virus zur Umlagerung beider Proteine in antivirale Stress-Granula führte. Verringerte KSRP-Level beeinträchtigten die PKR-Aktivierung, was zu einer 10-fachen Verbesserung der Replikation von mutierten Influenzaviren in Zellen mit verringerter IFNβ-Expression führte.

In dieser Arbeit konnte zum ersten Mal gezeigt werden, dass KSRP die zelluläre, antivirale Abwehr durch direkte Bindung an PKR und die damit verbundene Steigerung der PKR-Aktivität unterstützt. Zusammenfassend, unterstreichen die Ergebnisse das Vermögen quantitativer Massenspektrometrie, antivirale Antwortmechanismen systematisch aufzuklären, um neue potenzielle Ziele für antivirale Therapien zu finden.

Contents

List of Figures

List of Tables

List of abbreviations

aa	amino acids
ABC	ammonium bicarbonate
ABP	ARE-binding protein
ACN	acetronitrile
ADAR1	double-stranded RNA-specific adenosine deaminase
AKT	RAC-alpha serine/ threonine-protein kinase
AMD	ARE-mediated decay
AP1	activator protein 1
AP-MS	affinity-purification mass spectrometry
APS	ammonium persulfate
ARE	AU-rich element
aSG	antiviral stress granule
ATF	activating transcription factor
ATP	adenosine triphosphate
BCA	bicinchoninic acid
BioGRID	Biological General Repository for Interaction Datasets
BSA	bovine serum albumin
BSL	biosafety level
$CaCl_2$	calcium chloride
$CaPO_4$	calcium phosphate
CARD	caspase activation and recruitment domain
CIAP	calf-intestinal alkaline phosphatase
CID	collision induced dissociation
CLR	C-type lectin receptor
CMV	cytomegalovirus
CPSF	cleavage and polyadenylation specificity factor
cRNA	complementary RNA
CSF	colony-stimulating factor
Da	Dalton
DAPI	4',6-diamidino-2-phenylindole
dd	double destilled
DDB1	DNA damage binding protein 1
DDX5	probable ATP-dependent RNA helicase DDX5
DHX58	probable ATP-dependent RNA helicase DHX58
DHX9	ATP-dependent RNA helicase A
DMEM	Dulbecco's modified Eagle medium
DMSO	dimethyl sulfoxide
DNA	desoxyribonucleic acid
ds	double-stranded
DTT	dithiothreitol
E. coli	*Escherichia coli*
EDTA	ethylenediaminetetraacetic acid
EEF1A1	elongation factor 1 α 1
e.g.	*exempli gratia*
eIF2α	eukaryotic translation initiation factor 2 α
eIF6	eukaryotic translation initiation factor 6
ELISA	enzyme-linked immunosorbent assay
ER	endoplasmatic reticulum
ESI	electrospray ionisation
ExoSC5	exosome complex component RRP46
ExoSC7	exosome complex component RRP42
FA	formaldehyde
FADD	FAS-associated death domain protein
FBS	fetal bovine serum

FDR false discovery rate

FoAc formic acid

For forward

FRET Förster resonance energy transfer

FUBP2 Far upstream element-binding protein 2

G3BP1 Ras GTPase-activating protein-binding protein 1

GCN2 general control nonderepressible 2

GFP green fluorescent protein

GO gene ontology

h hour

HA haemagglutinin

HA haemagglutination

HBS HEPES buffered saline

HCIP high confidence interacting protein

HCMV human cytomegalovirus

HDAC6 histone deacetlyase 6

HIV human immunodeficiency virus

HL heavy to light

hnRNP heterogeneous ribonucleoprotein particle

HPLC high pressure liquid chromatography

HRI haeme-regulated inhibitor

HRP horse raddish peroxidase

HSP90β heat shock protein 90 β

HSPA5 78 kDa glucose-regulated protein

HSV herpes simplex virus

IAA 2-iodoacetamide

IFN interferon

IFNAR interferon-α/ β-receptor

IG immunoglobulin

IGF2BP1 insulin-like growth factor 2 mRNA-binding protein 1

IKK inhibitor of nuclear factor κ-B kinase

IL interleukine

IP immunoprecipitate

IPS-1 interferon β promoter stimulator protein 1

IRAK IL-1 receptor-associated kinases

IRES internal ribosomal entry site

IRF interferon regulatory factor

ISG interferon stimulated gene

ISG15 ubiquitin-like protein ISG15

ISGF3 IFN-stimulated gene factor 3

ISRE IFN-stimulated response element

JAK1 Janus kinase 1

JNK c-Jun N-terminal kinase

KARS lysine-tRNA ligase

KD knockdown

KEGG Kyoto Encyclopedia of Genes and Genomes

KPNA2 importin subunit alpha-1

KSRP KH type-splicing regulatory protein

LC liquid chromatography

LSM laser scanning microscope

LTQ linear ion trap quadrupole

M1 matrix protein 1

M2 matrix protein 2

MALDI matrix-assisted laser desorption/ ionisation

MAPK mitogen-activated protein kinase

MCL Markov Cluster algorithm

MDA5 melanoma differentiation associated protein 5

MDA7 melanoma differentiation associated protein 7

MDCK Madin-Darby canine kidney

ME mercaptoethanol

MEM minimal essential medium

MHC major histocompatibility complex

min minutes

MINT Molecular Interaction Database

miRNA micro RNA

ML medium to light

MOI multiplicity of infection

mRNA messenger RNA

MS mass spectrometry

MS/MS tandem mass spectrometry

MTT 3-(4,5-dimethylthiazol-2-yl)-2,5-diphenyltetrazolium bromide

MX1 myxovirus resistance protein 1

MYBBP1A Myb-binding protein 1A

Myc Myc proto-oncogene protein

MyD88 myeloid differentiation primary response gene 88

NA neuraminidase

$NaPO_4$ sodium phosphate

NCBI National Center for Biotechnology Information

NCR non-coding region

NEP nuclear export protein

NFκB nuclear factor κ B

NLR NOD-like receptor

NLS nuclear localisation signal

NOD nucleotide-binding oligomerisation domain receptors

NP nucleoprotein

NPM nucleophosmin

NS1 non-structural protein 1

NT non-target

OAS 2'-5'-oligoadenylate synthase 1

ON over night

p.i. post infection

p.t. post transfection

PA polymerase acidic protein

PA-X polymerase acidic protein X

PABP poly-A binding protein

PACT protein activator of the interferon-induced protein kinase

PAMP pathogen-associated molecular pattern

PANTHER Protein Analysis Through Evolutionary Relationships

PB1 polymerase basic protein 1

PB1-F2 polymerase basic protein 1 F2

PB1-N40 polymerase basic protein 1 N40

PB2 polymerase basic protein 2

PB2-S1 polymerase basic protein 2 S1

PBS phosphate buffered saline

PCR polymerase chain reaction

Pen penicilline

PERK PKR-like endoplasmic reticulum kinase

PFU plaque-forming unit

pH *pondus hydrogenii*

PI3K phosphoinositide 3 kinase

PKR RNA-dependent protein kinase

PP1 protein phosphatase 1

PP2A protein phosphatase 2A

pPKR phosphorylated PKR

ppm parts per million

PPP triphosphate

PRR pattern recognition receptor

RBD RNA-binding domain

RBM dsRNA-binding motif

Rev reverse

RIG-I retinoic acid inducible gene 1 protein

RIP1 receptor-interacting protein 1

RLR RIG-I-like receptor

RNA ribonucleic acid

RNP ribonucleoprotein particle

rpm rounds per minute

RT room temperature

RVFV Rift Valley fever virus

SDS sodium dodecyl sulfate

SDS PAGE sodium dodecyl sulfate polyacrylamide gel electrophoresis

sec second

SRSF1 serine/ arginine-rich splicing factor 1

SFPQ splicing factor, proline- and glutamine rich

SFTSV severe fever with thrombocytopenia syndrome virus

SG stress granule

siRNA small interfering RNA

SILAC stable isotopic labelling by amino acids in cell culture

SOC super optimal broth with catabolite repression

SOCS suppressors of cytokine signalling

ss single-stranded

STAT signal transducer and activator of transcription

Strep streptomycine

STRING Search Tool for the Retrieval of Interacting Genes/ Proteins

TBK1 TANK-binding kinase 1

TBST tris-buffered saline and Tween20

TEM transmission electron microscopy

TEMED tetramethylethylenediamine

TFA trifluoroacetic acid

TGF transforming growth factor

TIA1 T-cell-restricted intracellular antigen 1

TLR toll-like receptor

TNF tumor necrosis factor

TOF time-of-flight

TPCK tosyl phenylalanyl chloromethyl ketone

TRAF TNF-receptor-associated factors

TRIF TIR-domain-containing adapter-inducing IFNβ

TRIM25 tripartite motif-containing protein 25

Tris tris(hydroxymethyl)aminomethane

TTP tristetraprolin

TYK2 tyrosine kinase 2

UTR untranslated region

vRNA viral RNA

vRNP viral ribonucleoprotein particle

VSV vesicular stomatitis virus

WCL whole cell lysate

WHO World Health Organisation

WT wild type

YFP yellow fluorescent protein

YWHAE 14-3-3 protein epsilon

ZPC Zernike phase contrast

1 Introduction

1.1 Influenza Viruses

1.1.1 Disease

Influenza viruses are the causative agents of the acute respiratory disease “influenza” (colloquially “the flu”) in humans. They can replicate in the upper and lower respiratory tract, including e.g. nose, throat, trachea, bronchial epithelium and lung cells [1]. Influenza occurs in epidemic waves with peak infection rates during the winter season, presenting global annual infection rates of in average 5 % to 10 % in adults and 20 % to 30 % in children. The virus causes three to five million cases of severe illness and approximately 250,000 to 500,000 deaths per year according to World Health Organisation (WHO) [2].

Influenza viruses are transmitted via droplet infection by coughing or sneezing, direct contact or via contaminated surfaces. Typical influenza disease is characterised by a sudden onset of high fever and additionally involves respiratory symptoms, such as cough, sore throat, runny nose, as well as headache, muscle and joint pain and often extreme fatigue [3]. The incubation time can vary between one and four days, with a usual onset of disease two days post infection. Most people recover from symptoms within a week without medical treatment. However, severe illness with hospitalisation and death can occur, especially among people with high risk, such as children under two years, elderly over 65 years, pregnant women and chronically ill people [2].

1.1.2 Taxonomy

Influenza viruses belong to the family of *Orthomyxoviridae* and are further classified into the four genera Influenza A, B, C and the recently identified influenza D viruses according to antigenic differences in their nucleo- and matrix proteins [4]. Influenza viruses can be distinguished by their ability to infect different hosts. Hereby, influenza A viruses are characterised by a wide host range. They can infect birds and several mammalian species, including humans or bats (reviewed in [5]). In contrast, the host spectrum of Influenza B, C and D viruses is more limited. Influenza B virus infections are restricted to humans and occasionally seals while influenza D viruses were only found in cattle and pigs so far [4]. Influenza C viruses infect humans, pigs and dogs, but cause only mild disease symptoms in humans [2].

Influenza A viruses are further divided into subgroups according to their surface proteins haemagglutinin (HA) and neuraminidase (NA). To date, 18 different HA and 11 NA subtypes have been identified [6]. However, only some of these subtypes have been found in human

infections and only H1N1 and H3N2 viruses are circulating during seasonal epidemics [2]. To facilitate the denotation of influenza viruses, common guidelines for influenza virus nomenclature were established by the WHO. The name is comprised of the influenza virus genus, the species from which it was isolated (except in the case of human virus isolates), the origin of isolation, the isolation number, the year of isolation and the subtype of HA and NA protein. For example, influenza A/Puerto Rico/8/1934 (H1N1) stands for a human H1N1 virus isolated in Puerto Rico in 1934. In this thesis, the influenza A/Puerto Rico/8/1934 (H1N1) virus will be denoted as influenza A/PR/8.

1.1.3 Morphology and structure

Influenza viruses are enveloped viruses with a single-stranded (ss) segmented ribonucleic acid (RNA) genome of negative polarity. The envelope is a lipid membrane which is derived from the host cell during budding of newly formed virus particles [7]. Virions have a spherical or pleiomorphic structure with a diameter of 80 nm to 120 nm (figure 1.1 A) and contain the viral genome, packaged as ribonucleoprotein particles (RNPs). Viral RNPs (vRNPs) are composed of the eight different segments of the negative-sense ssRNA genome associated with multiple copies of nucleoprotein (NP) and one copy of the viral polymerase proteins polymerase acidic protein (PA), polymerase basic protein 1 (PB1) and polymerase basic protein 2 (PB2) [8, 9]. The coding sequences of all eight segments are flanked by highly conserved segment-specific non-coding regions (NCRs) which contain the promoter recognition sites for the viral polymerase [10, 11]. The termini of the genome segments are partially complementary resulting in formation of an approximately 15-base-pair-long panhandle and a circular conformation of the viral RNA [12–14].

The eight segments of the viral genome encode for a minimum of ten viral proteins dependent on the viral strain. Hereby, each viral RNA segment encodes a major viral protein. Additional proteins are expressed from segments 1, 2, 3, 7 and 8 by splicing (matrix protein 2 (M2), nuclear export protein (NEP), polymerase basic protein 2 S1 (PB2-S1)), usage of alternative translation initiation sites (polymerase basic protein 1 F2 (PB1-F2), polymerase basic protein 1 N40 (PB1-N40)) or ribosomal frameshifts (polymerase acidic protein X (PA-X)) [15]. In the case of Influenza A/PR/8, 14 proteins (ten structural and four putative non-structural proteins) are expressed (figure 1.1 B and table 1.1). The differentiation between structural and non-structural proteins involves two characteristics: Presence in the incoming virus particles and participation in the formation of the virion structure. For influenza A/PR/8, PB2, PB1, PA, HA, NP, NA, matrix protein 1 (M1) and M2 are structural proteins. Interestingly, non-structural protein 1 (NS1) and NEP were first described to be non-structural proteins, but were shown to be present in purified virus particles in a mass spectrometric screen by Hutchinson *et al.* in 2014 [16]. So, even if a participation of NS1 and NEP in formation of the virion structure has not been shown yet, they were proposed as novel structural proteins [16]. In infected cells, additional non-structural proteins are expressed, namely PA-X, PB1-F2, PB1-N40 and PB2-S1 for the influenza A/PR/8 strain. These proteins contribute to virulence

and can have inhibitory effects on the antiviral host cell response, but their detailed function remains to be elucidated [15, 17–19].

Genome segment	Protein name	Protein length (aa)	Protein function
1	PB2	759	Subunit of the viral polymerase; directly involved in the recognition of 5'-capped host pre-mRNAs
	PB2-S1	508	Contributes to inhbition of RIG-I mediated IFN signaling
2	PB1	757	Catalytical subunit of the viral polymerase; responsible for RNA chain elongation
	PB1-F2	87	Virulence factor for induction of mitochondria-associated apoptosis; influences polymerase activity
	PB1-N40	718	Maintains balance between PB1 and PB1-F2 expression to ensure stable replication
3	PA	716	Subunit of the viral polymerase; RNA endonuclease activity
	PA-X	252	Virulence factor; modulates host response
4	HA	565	Receptor binding function; mediates membrane fusion for release of vRNPs
5	NP	498	Major component of the vRNP; controls the nucleo-cytoplasmic vRNA transport
6	NA	454	Cleaves sialic acids for release of progeny viruses
7	M1	252	Main component of virus membrane; role in virion assembly
	M2	97	Membrane protein; forms a proton channel; role in genome unpacking during virus entry
8	NS1	230	Antagonist of antiviral host cell response; regulates host and viral gene expression
	NEP	121	Mediates vRNP export from nucleus

Table 1.1. Viral RNA segments and encoded proteins of Influenza A/PR/8 virus. Adapted from [20].

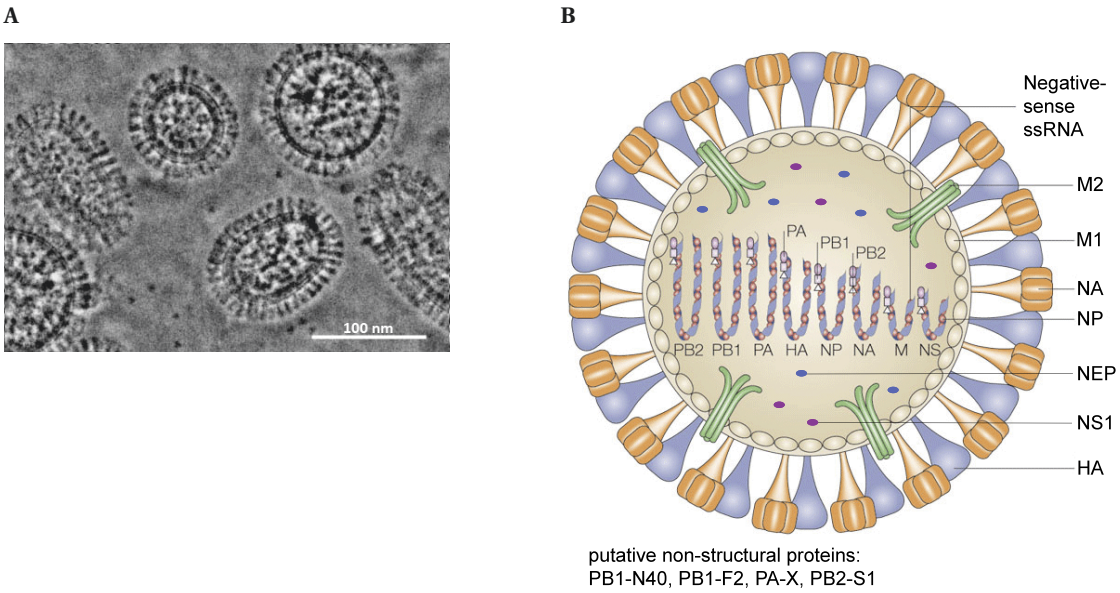

Figure 1.1. Electron microscopy and schematic model of influenza A virus particles. A ZPC cryo-TEM picture of inactivated purified influenza A/NewCaledonia/20/99 (H1N1) virus. Scale bar is equivalent to 100 nm. Adapted from [21]. **B** Schematic representation of the influenza A/PR/8 virion with the structural proteins PB2, PB1, PA, HA, NP, NA, M1 and M2 and the putative structural proteins NS1 and NEP. The non-structural proteins PA-X, PB1-F2, PB1-N40 and PB2-S1 are expressed in infected cells and cannot be found in the incoming virus particle. The vRNPs within the virion are composed of the eight different segments of the negative-sense ssRNA genome associated with NP and the viral polymerase proteins PA, PB1 and PB2. Adapted from [22].

In the Zernike phase contrast (ZPC) cryo-transmission electron microscopy (TEM) picture, the two viral surface proteins NA and HA become clearly visible (figure 1.1 A). They look like spikes protruding from the lipid envelope. The HA protein forms trimers that bind to sialic acids on the surface of the host cells, which act as cellular receptors for influenza viruses [23]. It also mediates the fusion of the viral and the endosomal membrane during virus entry, resulting in the release of the vRNPs into the cytoplasm [24]. The NA forms tetramers and is responsible for the release of newly formed virus particles from the cell surface by cleavage of sialic acids [25]. The third viral surface protein M2 forms homotetramers to build a proton channel that leads to the acidification of the virus particle and thereby facilitates the uncoating of the virions resulting in the release of the vRNPs [26]. On the inside of the virion, the lipid membrane is covered with M1 protein. It mediates the contact between the outer lipid membrane, the surface proteins and the vRNP complexes [27].

1.1.4 Viral replication

Viruses are obligate intracellular pathogens that rely on the host cell metabolism for replication. Virus replication involves different steps, the major ones being viral attachment to the host cell, entry, uncoating, viral gene expression and replication, virion assembly, budding and release of progeny viruses (figure 1.2).

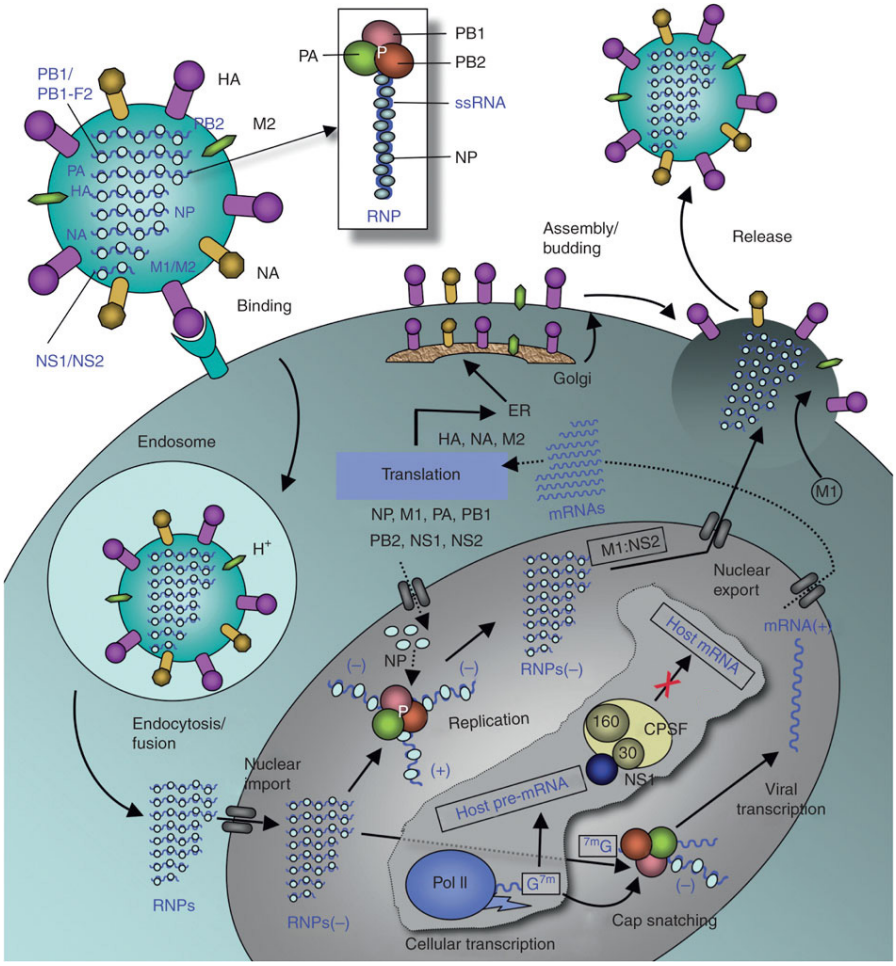

Figure 1.2. Replication cycle of influenza A viruses. Virus replication involves viral attachment to the host cell, entry, uncoating, viral gene expression and replication, virion assembly, budding and release of progeny viruses. For details see text. Adapted from [28].

During virus infection, the incoming virus particles attach to host cells by binding of the viral HA protein to sialic acid conjugates on the cell surface [29]. Species specificity of human and avian influenza A viruses is partially caused by the different binding preferences of the respective HA proteins to either α-2,3-linked sialic acids, mainly present in the intestine of birds, or α-2,6-linked sialic acids, present in the upper respiratory tract of humans [30]. After attachment, the virus enters the cell by clathrin-mediated endocytosis [31]. The acidification of the endosome triggers a pH-dependent conformational change in the HA protein that leads to exposure of the fusion peptide and hereby fusion of the viral and endosomal membranes [32, 33]. The low pH in the endosome also leads to activation of the viral proton channel formed by M2 homotetramers, resulting in the dissociation of the vRNPs from the M1 proteins and release of vRNP into the host cell cytoplasm [34]. The vRNPs are transported into the nucleus by recognition of the nuclear localisation signal (NLS) within the NP and viral polymerase proteins and interaction with cellular importins [35, 36].

Viral genome transcription and replication take place in the nucleus of host cells. Viral messenger RNA (mRNA) synthesis is initiated with capped RNA primers cleaved off from the 5'-end of host pre-mRNAs [37]. Hereby, the PB2 subunit binds the 5'-cap of host pre-mRNA

and the endonucleolytic function of the PA subunit allows cleavage of the pre-mRNA ten to thirteen nucleotides downstream of the cap [38]. The resulting cap-structure serves as a primer for transcription initiation by the PB1 subunit with the vRNA as a template [39]. The transcription of a uridine-rich sequence at the 5' end of the vRNA leads to the generation of a 3'-polyadenylated tail for the viral mRNA [40, 41]. This means, that the polyadenylated tail of influenza virus mRNA is directly encoded in the vRNA. In contrast, host cell mRNAs need a specific poly(A) polymerase for generation of the 3'-polyadenylated tail. This process can be inhibited by interaction of the viral NS1 protein with the 30 kDa subunit of the cellular cleavage and polyadenylation specificity factor (CPSF), resulting in the block of e.g. antiviral interferon (IFN) mRNA translation [42, 43].

Viral mRNAs are subsequently exported into the cytoplasm for translation by the host cell translation machinery. After translation, viral proteins bearing an NLS are reimported into the nucleus [44]. The viral surface proteins HA, NA and M2 are further processed while they are transported from the endoplasmatic reticulum (ER) via the Golgi apparatus and trans-Golgi network to the host cell membrane. Modifications include glycosylation, palmitoylation and grouping into homotrimers (for HA) or homotetramers (for NA and M2) [45]. At the plasma membrane, HA and NA accumulate in lipid rafts [46].

In the course of infection, rising levels of NP, NEP and polymerase proteins facilitate the synthesis of regulatory small viral RNAs, which results in a switch from viral transcription to replication of viral RNA (vRNA) [47]. Hereby, the vRNA is first transcribed into complementary RNA (cRNA) with positive polarity which then serves as a template for vRNA synthesis [48, 49]. The newly formed vRNA is complexed with NP and binds to the viral polymerase proteins PA, PB1 and PB2. The resulting vRNPs are subsequently exported to the cytoplasm in a process involving M1 and NEP [50, 51].

Assembly and budding of progeny virions occur at cholesterol-rich lipid raft domains in the host cell plasma membrane. The process is not completely understood, but clustering of HA and NA in the lipid rafts is thought to cause a deformation of the membrane for the initiation of the virus budding event. M1 is presumed to interact with both the vRNPs and the cytoplasmic tails of HA, NA, and M2, herein acting as a bridge between them at the budding site. This is believed to facilitate incorporation of the vRNPs into the newly formed virion [27, 52, 53]. Progeny virions are released from the host cell surface by cleavage of cellular sialic acids by the viral NA protein [25].

1.2 The innate immune system

To protect themselves from pathogenic agents like bacteria, viruses and funghi, vertebrates have developed the immune system. The expression "immune system" hereby provides a simple generic term for a highly complex network of various proteins, cells and organs and their interactions.

The immune system can be subdivided into two major forms, the innate and the adaptive immune system. The innate immune system is often referred to as the first line of host defence. It is evolutionary older than the adaptive immunity and comparable systems can also be found in plants, fungi, insects and even primitive multicellular organisms. It is responsible for the early detection of invading pathogens and provides immediate, but non-specific responses. Unlike the adaptive immune system, the innate immune response does not confer long-lasting immunity to the host. It consists of humoral and cell-mediated response mechanisms and includes the following major functions [54]:

- Acting as a physical barrier to prevent entry of pathogens
- Secretion of cytokines
- Recruitment of specialised immune cells to the sites of infection
- Clearance of foreign matter and dead cells
- Activation of the complement system
- Activation of the adaptive immune response by antigen presentation.

The first obstacle, pathogens have to overcome for effective infection, is a physical barrier consisting of epithelia cells, which cover the body on all outer parts including the respiratory tract. They often contain special defence mechanisms such as antimicrobial peptides or have developed characteristics like cilia to support the clearance of incoming pathogens. If a pathogen succesfully passed the physical barrier, it is recognised by specialised cells. In addition to the epithelial cells, the innate immune system includes a wide range of leukocytes with different functions, as for example natural killer cells, mast cells, eosinophils, basophils and phagocytic cells like macrophages, neutrophils and dendritic cells. Cells of the innate immune system can spot pathogens by detection of conserved molecular structures that are unique to microorganisms, so called pathogen-associated molecular patterns (PAMPs), with specialised pattern recognition receptors (PRRs). PRRs are divided into four major families: RIG-I-like receptors (RLRs), toll-like receptors (TLRs), NOD-like receptors (NLRs) and C-type lectin receptors (CLRs) that detect different pathogen structures. Activation of the PRRs employs complex signalling mechanisms to finally result in transcription of genes for the expression of proinflammatory cytokines, as among others tumor necrosis factor (TNF) α for the regulation of inflammation and apoptosis, interleukines which control the proliferation of B and T cells or IFNs which are further discussed in section 1.2.1 [55]. These factors are responsible for the coordination of local and systemic inflammation and the regulation of the adaptive immune response.

Unlike the innate immune system, the adaptive immunity confers a highly specific, acquired immune response that can induce lifelong protection to encountered pathogens. The adaptive immune system relies on two main cell types: T cells, responsible for the cell-mediated immunity, and B cells, performing the humoral immune response. B and T cells express a

broad diversity of clonal receptors for recognition and discrimination of antigens. Recognition of antigens initiates proliferation and differentiation of the lymphocytes into effector and memory cells. Activated B cells mature into plasma cells and secrete high levels of antigen-specific antibodies. Binding of the antibody to the antigen leads to neutralisation and clearance of the opsonised structure. T cells can be further subdivided into T helper cells and cytotoxic T cells. T helper cells recognise peptide antigens presented by the major histocompatibility complex (MHC) class II on the surface of infected cells. This leads to secretion of cytokines that attract phagocytic cells for the elimination of the infected cell. Cytotoxic T cells recognise infected or cancer cells by binding to antigen presented by MHC class I on the cell surface. Activated cytotoxic T cells secrete cytotoxins that subsequently induce apoptosis of the infected cell. Following activation, B and T cells produce memory cells, which enable increased speed and effectiveness of immune responses if an antigen is detected again [56].

1.2.1 The antiviral interferon response

The IFN system is a powerful system with antiviral, antiproliferative, antitumoral and immunomodulatory functions. It comprises three groups, namely IFNs type I, II and III. The type I IFNs are a large group of IFNs and contain different forms of IFNα as well as IFNβ, IFNδ, IFNϵ, IFNκ, IFNν, IFNω, IFNτ and IFNζ [57]. Type I IFNs are highly induced by viral infections and can be secreted from a broad variety of cell types. The group of type II IFNs only includes one member, IFNγ. It is released by immune cells like activated T cells and NK cells and plays a role in the induction of the adaptive immune response [55]. IFNλ 1, 2 and 3 belong to the group of type III IFNs. Comparable to type I IFNs, they are expressed upon viral infection and their expression is regulated by similar mechanisms [58]. The IFN response is a major part of the innate and adaptive cellular antiviral immunity. The expression of type I and III IFNs is a consequence of the detection of viral RNA by specialised PRRs, such as TLRs and RLRs.

The main PRR, responsible for the detection of viral RNAs in the cytoplasm, is the retinoic acid inducible gene 1 protein (RIG-I), a member of the RLR family. RIG-I is an IFN-inducible RNA helicase that consists of an N-terminal caspase activation and recruitment domain (CARD) and a central helicase domain. It is activated by binding of dsRNA or 5'-triphopsphate-ssRNA to the C-terminal domain, making it to one of the key players in the antiviral defence against influenza viruses [59, 60]. Binding of viral RNA results in a conformational change of the RIG-I molecule, which facilitates ubiquitinylation of the CARD domains by adaptor proteins as for example the E3 ubiquitin ligase tripartite motif-containing protein 25 (TRIM25) [61]. RIG-I then oligomerises and triggers CARD-CARD mediated interaction with the downstream factor interferon β promoter stimulator protein 1 (IPS-1), which is predominantly located on the outer membranes of mitochondria [62]. The IPS-1 signalling cascade leads to phosphorylation of TANK-binding kinase 1 (TBK1) and inhibitor of nuclear factor κ-B kinase (IKK)ε, followed by the activation of transcription factors IRF3 and 7, ultimately re-

sulting in an antiviral response mediated by type I IFN and interferon stimulated gene (ISG) production (figure 1.3) [63, 64].

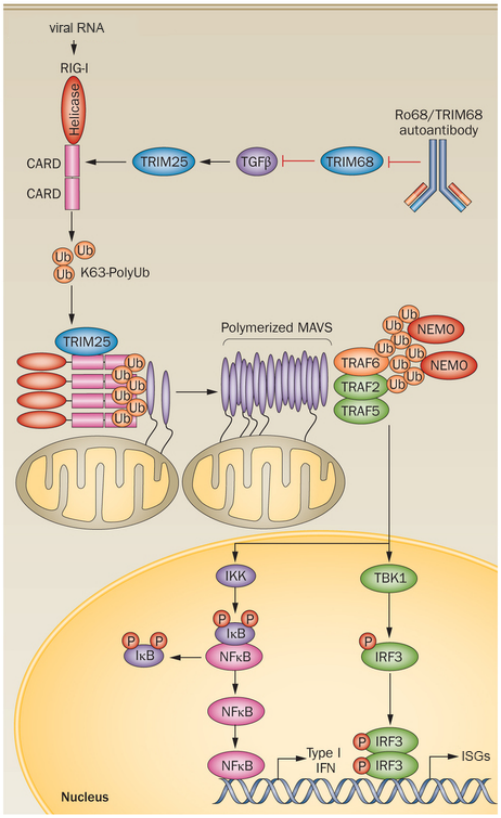

Figure 1.3. RIG-I signalling cascade. RIG-I is a cytoplasmatic PRR that is able to recognise virus-specific RNA structures. Activation of RIG-I involves adaptor molecule mediated ubiquitinylation and oligomerisation and leads to signalling via the IPS-1 pathway, resulting in upregulation of transcription factors for expression of antiviral IFNs and ISGs. Adapted from [65].

Another group of PRRs for the detection of viral PAMPs are TLRs. TLRs are evolutionarily conserved membrane-spanning receptors. They are predominantly expressed on leukocytes and epithelial cells of the lung or the gastrointestinal tract. So far, ten human forms of TLRs have been characterised, which are able to recognise a broad spectrum of ligands (figure 1.4 A) [66]. Viral PAMPs, such as viral ss or double-stranded (ds)RNA, are detected by the intracellular, endosomal TLRs 3, 7, 8 and 9. It was shown previously that the detection of influenza viruses in plasmacytoid dendritic cells and B cells is mediated by TLR7, among others [67]. Activation of TLR3, 7, 8 and 9 initiates overlapping signalling cascades in conventional or plasmacytoid dendritic cells and macrophages, resulting in the production of proinflammatory cytokines and type I IFN (figure 1.4 B). TLR7 and 8 signalling involves the adaptor protein myeloid differentiation primary response gene 88 (MyD88), followed by recruitment and phosphorylation of different IL-1 receptor-associated kinases (IRAK) proteins and activation of TNF-receptor-associated factors (TRAF) family members. This results in the release of transcription factors like interferon regulatory factor (IRF) 5 and 7, nuclear factor κ B (NFκB) or activator protein 1 (AP1). Translocation of the transcription factors to the nucleus leads to transcription of pro-inflammatory cytokines and to induction of large amounts of type I IFNs to counteract infection. The TLR3 signalling cascade is not dependent on MyD88,

but on the adaptor proteins TIR-domain-containing adapter-inducing IFNβ (TRIF), TRAF 6 and receptor-interacting protein 1 (RIP1). Upon TLR3 activation, IRF3, NFκB and different members of the mitogen-activated protein kinase (MAPK) family are released, which in turn induce transcription of IFNβ and proinflammatory cytokines (figure 1.4 B) [68].

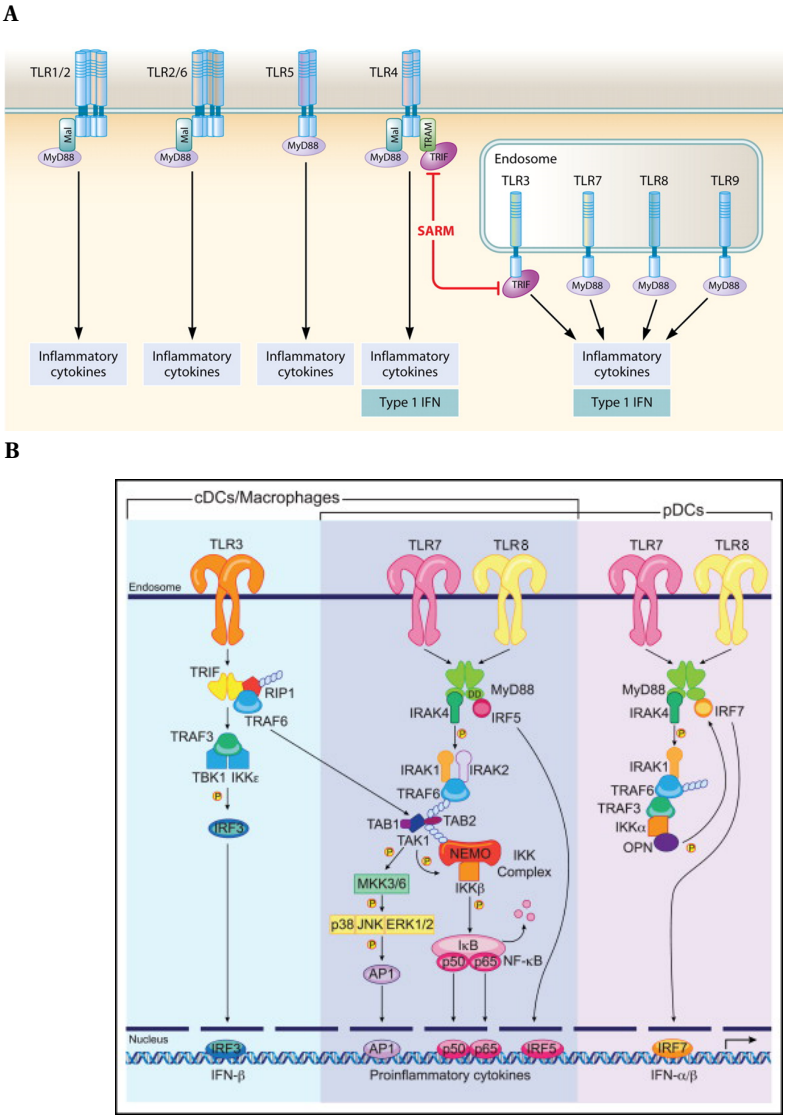

Figure 1.4. TLR signalling cascade. A Overview of human TLR1 to 9. TLR1, 2, 4, 5, 6 are located in the cell membrane and lead to production of inflammatory cytokines and type I IFN via MyD88 mediated signalling. TLR3, 7, 8 and 9 are intracellular PRRs located in the endosomal membrane. Activation induces release of proinflammatory cytokines and type I IFN via MyD88 or TRIF dependent signalling. Adapted from [69]. **B** Detailled signalling cascade of viral sensors TLR3, 7 and 8. TLR3, 7 and 8 are intracellular receptors located within the endosomal membrane. Activation by viral ssRNA or dsRNA is followed by TRIF or MyD88 dependent signalling, resulting in the release of factors triggering the transcription of IFN type I and pro-inflammatory cytokines. Adapted from [68].

Expressed IFNs are secreted and can be bound by distinct IFN receptors on susceptible cells in an autocrine and paracrine fashion, which leads to the establishment of a general antiviral state not only in infected but also in non-infected cells [70]. Herein, type I IFNs bind to the interferon-α/ β-receptor (IFNAR), which results in the recruitment of Janus kinase 1 (JAK1) and tyrosine kinase 2 (TYK2) and consequently in the phosphorylation of

signal transducer and activator of transcription (STAT) 1 and 2. The STAT1/ 2 complex recruits the adaptor molecule IRF9 for the formation of the IFN-stimulated gene factor 3 (ISGF3) complex, which then translocates to the nucleus. Here it binds to the IFN-stimulated response elements (ISREs) in the promoter regions of ISGs, consequently leading to their transcription (figure 1.5) [71]. ISG is a collective term for a varied group of genes that are transcribed as a result of IFN expression to counteract viral infection. Important members of the ISG family are myxovirus resistance protein 1 (MX1), 2'-5'-oligoadenylate synthase 1 (OAS) and RNA-dependent protein kinase (PKR). In a positive feedback loop, expression and activation of ISGs can lead to further induction of type I IFNs [72].

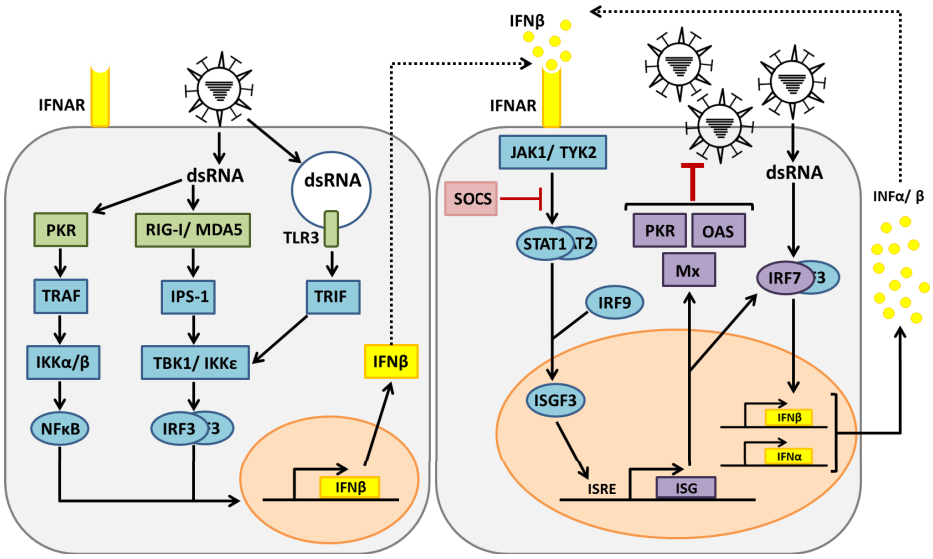

Figure 1.5. Type I IFN induction and signalling. Viral infection is detected by intracellular PRRs like PKR, RIG-I or TLR3, leading to NFκB and IRF3-dependent expression of type I IFN, such as IFNβ. IFNβ is detected by IFNARs on neighbouring cells or in an autocrine way and activates the expression of various ISGs, such as PKR or OAS, via the JAK/ STAT pathway. Adapted from [72].

KH type-splicing regulatory protein

Due to the essential role of IFNs and their manifold modes of action, the production of IFNs needs to be strictly regulated. Prolonged exposure to high levels of IFN can have detrimental effects on healthy cells, so that depletion of IFN after clearance of pathogen infection is crucial to return to homeostasis [73].

Many cytokines, including different type I IFNs such as IFNβ and most forms of IFNα, carry special AU-rich elements (AREs) in the 3'-untranslated region (UTR) of their mRNA, designating them for rapid decay [74–76]. AREs are recognised by ARE-binding proteins (ABPs), which can interact with intracellular exosomes to promote mRNA degradation [77, 78]. This process is termed ARE-mediated decay (AMD). ABPs can be divided into two groups with opposite functions, namely mRNA-stabilising ABPs and destabilising ABPs. Binding of an ABP to the ARE of mRNA molecules is not exclusive, meaning that more than one ABP can bind simultaneously to the same ARE in an additive or competitive manner [79]. ABPs themselves can be regulated by post-translational modifications like phosphorylation,

which was reported to affect their subcellular localisation and ability to interact with target mRNAs [80–82]. For the destabilising ABP tristetraprolin (TTP) it was shown that the p38 MAPK pathway regulates the subcellular localisation and stability of the protein in a process involving phosphorylation of TTP at serines 52 and 178 [83]. Herein, Brook and colleagues showed that a p38 inhibitor caused dephosphorylation of TTP, which resulted in relocalisation of the protein from the cytoplasm to the nucleus followed by proteasomal degradation.

KH type-splicing regulatory protein (KSRP), also known as Far upstream element-binding protein 2 (FUBP2), is an ABP that is involved in the degradation of various cytokine mRNAs [84, 85]. It was shown to play an important role in maintaining basal cellular levels of type I IFN by binding to IFNβ and IFNα4 mRNA, among others. KSRP hereby interferes with their mRNA stability and promotes their degradation [86]. Human KSRP is a 75 kDa protein, comprised of a central region with four KH domains responsible for ARE-recognition and nucleic acid binding as well as N- and C-terminal regions with low sequence complexity that contain sites for post-translational modifications and protein-protein-interaction (figure 1.6 A) [87]. In addition to regulation of AMD, KSRP is involved in repression of cytokine transcription, translational silencing by dissociation of the mRNA from the polysome and micro RNA (miRNA) maturation (figure 1.6 B) [88, 89].

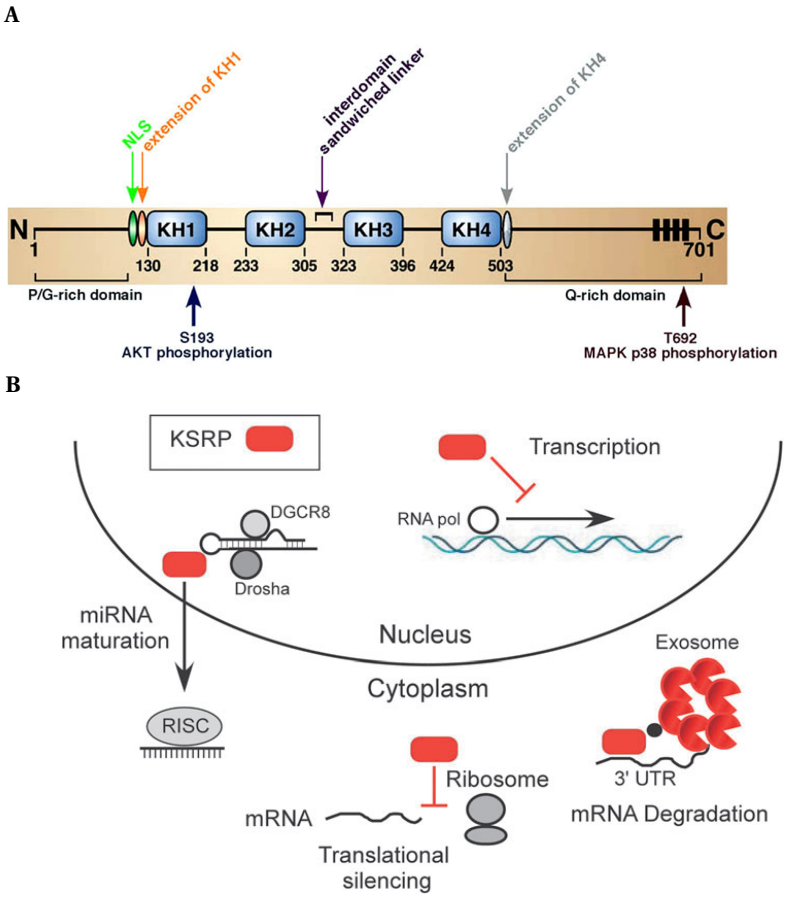

Figure 1.6. KSRP structure and functions. A KSRP consists of a central region with four KH domains and an N- and C-terminal region with low complexity. Localisation of the protein is regulated by the NLS and phosphorylation by AKT or p38. Adapted from [90]. **B** KSRP is involved in transcription and translation regulation, mRNA degradation and miRNA maturation. Adapted from [85].

KSRP activity is dependent on its localisation. Under normal conditions, KSRP shows a predominantly nuclear distribution [79]. KSRP phosphorylation by RAC-alpha serine/ threonine-protein kinase (AKT) at serine 193 promotes the unfolding of the unstable KH 1 domain, which creates a binding site for the 14-3-3 ζ protein and consequently results in relocalisation of KSRP to the nucleus [81]. This prevents its mRNA decay promoting function and decreases the ability to interact with exosomes. Phosphorylation of the serine residue at position 692 in the C-terminal domain by p38 MAPK was shown to lower the affinity of KSRP for AREs thus stabilising short-lived mRNA transcripts [80, 91]. The exact mechanism underlying this finding has not been described in detail yet, but since it was shown that p38 MAPK is involved in determining the localisation of other ABPs such as TTP, a similar process was suggested for KSRP regulation by p38 [91]. KSRP is also able to associate with antiviral stress granules (aSGs) upon cellular stress induced by viral infection [79, 92].

Since KSRP strongly influences type I IFN and ISG levels, an involvement of KSRP in antiviral signalling has been analysed. For infections with the positive stranded ssRNA Enterovirus 71, an antiviral effect of KSRP could be shown. Upon Enterovirus infection, KSRP is enriched in the cytoplasm and interacts with the viral internal ribosomal entry site, hereby negatively influencing viral translation [93]. In contrast to these findings, Lin *et al.* showed a type I IFN mediated positive effect of KSRP on viral replication of herpes simplex virus (HSV) type 1 and vesicular stomatitis virus (VSV) [86]. They demonstrated that KSRP knockdown cells and mice produce higher amounts of type I IFN and other cytokines that affect viral replication, which results in lower viral titers. Taking these contradictory findings into account, the role of KSRP in antiviral host defense needs to be clarified further.

1.2.2 The RNA-dependent protein kinase

One of the key factors for recognition and elimination of viral infection, especially influenza virus infection, is the RNA-dependent protein kinase (PKR). PKR is a member of the family of eukaryotic translation initiation factor 2 α (eIF2α) phosphorylating kinases. Other members include general control nonderepressible 2 (GCN2), PKR-like endoplasmic reticulum kinase (PERK) and haeme-regulated inhibitor (HRI). The kinases of this family phosphorylate eIF2α, which leads to a block of translation, as a result of cellular stress such as amino acid deprivation (GCN2), ER stress (PERK), the presence of viral RNA (PKR) or haeme deficiency (HRI) [94].

PKR is constitutively expressed at low levels in various cell types, including epithelial cells [95]. It is localised mainly in the cytoplasm, where it is associated with ribosomes, and to a much lesser extent in the nucleus [96, 97]. Expression of PKR is upregulated by type I IFNs after detection of viral pathogens. Therefore, PKR is also referred to as an ISG [98].

Human PKR is an 68 kDa protein, comprised of 551 amino acids (aa). It consists of two consecutive dsRNA-binding motifs (RBMs) (aa 9-77 and 100-167) at the N-terminus that form the RNA-binding domain (RBD) and a serine/ threonine kinase domain (aa 267-538)

at the C-terminus. N- and C-terminus are connected by an unstructured linker (figure 1.7 A) [99, 100]. As stated before, PKR is constitutively expressed at a basal level, but it is not functional before activation due to its autoinhibitory conformation. Activation of PKR during viral infection leads to a conformational change of the protein, disbanding the interaction between the RBM 2 and the kinase domain. Subsequently, the PKR protein can homodimerise and autophosphorylate its critical threonine residues 446 and 451 in the activation loop (figure 1.7 B) [101–103]. Active PKR can then bind to and phosphorylate downstream adaptor and effector proteins, such as eIF2α [104]. A mutation in the catalytic domain at position 296 from lysine to arginine results in a complete loss of kinase activity, as binding of adenosine triphosphate (ATP) is abolished, inhibiting the phosphotransfer to downstream proteins [105, 106].

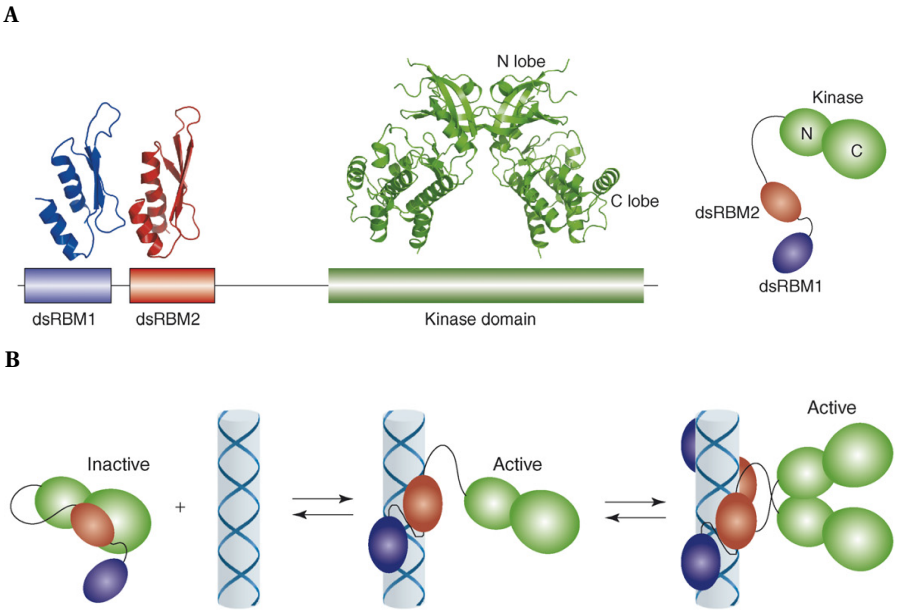

Figure 1.7. PKR domain structure and mode of activation. A PKR consists of an N-terminal regulatory domain with two consecutive RBMs, RBM 1 and 2, an unstructured linker domain and the C-terminal effector domain containing the serine/ threonine kinase with typical bilobal form. Molecule structures of the single domains derived from NMR (RBDs, PDB code 1QU6) or crystallographic experiments (kinase domain, PDB code 2A1A) are depicted above. Adapted from [99]. **B** Inactive PKR is in an autoinhibitory state, where interaction of RBM 2 with the kinase domain blocks the activity of latent PKR. Binding of dsRNA abrogates interaction of RBM 2 and the kinase domain, allowing homodimerisation and activation of PKR. Adapted from [99].

PKR activation is mediated by binding of viral PAMPs, such as dsRNA or, in the case of influenza virus infection, recognition of highly structured 5'-triphosphate stem-loop RNA molecules [107–109]. Binding of viral RNA to PKR hereby is pivotal for its activation, because it brings two or more PKR monomers in close proximity to support homodimerisation via the kinase domain [110]. A mutation of lysine to alanine at position 60 in the RBM 1 was described to result in the complete loss of RNA-binding function [109, 111]. PKR can also be activated RNA-independently by TLR and RLR mediated signalling, polyanionic molecules, as e.g. heparin, caspases and protein activators, resulting in similar downstream effects (figure 1.8) [112–114]. Protein activators of PKR include the protein activator of the interferon-induced protein kinase (PACT) and melanoma differentiation associated protein 7 (MDA7) among

others [115, 116]. For example, PACT was shown to facilitate PKR activation and subsequent phosphorylation of eIF2α in the absence of dsRNA by direct protein interaction that involves the dsRNA BMs of PKR [115].

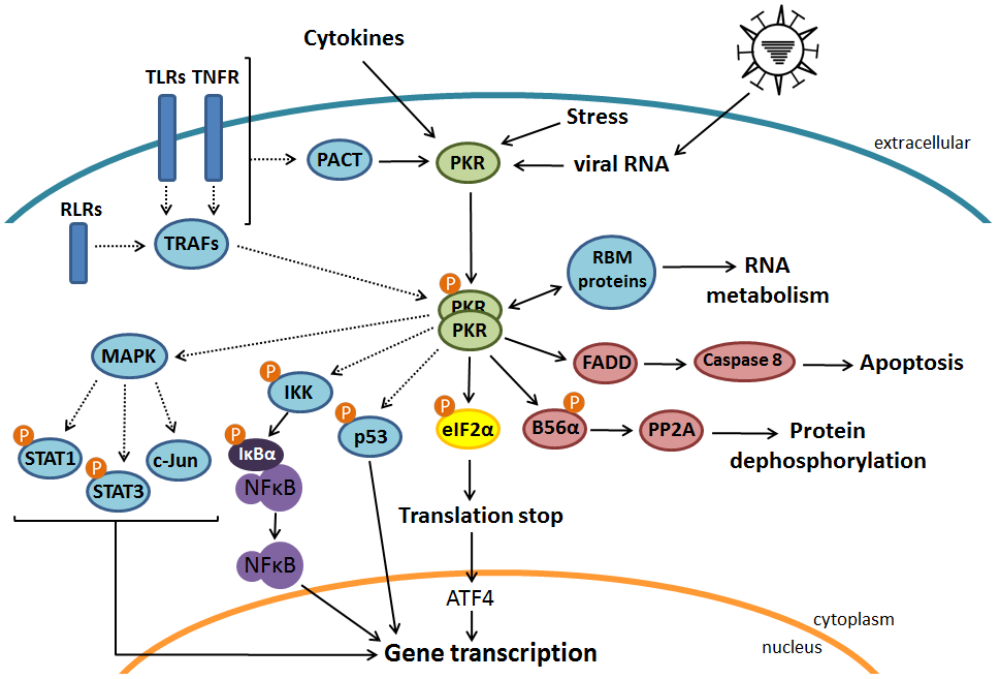

Figure 1.8. PKR antiviral signalling pathways. PKR is activated by different stimuli, such as cytokines, cellular stress, detection of viral RNA or protein activators. Activation of PKR involves, homodimerisation and autophosphorylation and results in induction of cellular processes to counteract harmful conditions, as e.g. phosphorylation of eIF2α to block translation, release of transcription factors for additional cytokine response or induction of apoptosis. For detailed description see text. Adapted from [117, 118].

One of the best studied targets of PKR is eIF2α. Main function of eIF2 is the delivery of Met-tRNA to ribosomes for the initiation of translation [119]. At the ribosome, GTP is hydrolysed, the protein complex resolves and Met-tRNA is set free. Free eIF2-GDP is then regenerated by the GTP-exchange factor eIF2B to reinitiate the circle. Phosphorylation of eIF2α at serine 51 leads to an increased affinity of eIF2α for eIF2B, consequently resulting in sequestration of eIF2B and stop of translation initiation. As many viruses, including influenza viruses, strongly depend on the host cell translation machinery for viral protein production, the inhibition of translation initiation by PKR strongly affects viral reproduction. In addition, phosphorylation of eIF2α leads to the formation of aSGs, cytoplasmic aggregates containing stalled mRNA and proteins with antiviral functions [120]. Contradictory to the block of general translation, phosphorylation of eIF2α enhances the transcription of genes associated to the cellular stress response via alternative pathways, as for example via activating transcription factor (ATF) 3 and 4 [121, 122]. Hereby, ATF 4 was shown to be involved in processes associated with amino acid metabolism and regulation of autophagy [123, 124].

PKR also regulates various other pathways (figure 1.8). Hereby, it can either function by phosphorylating downstream molecules or, phosphorylation-independent, as an adaptor protein [118]. PKR plays a role in the transcriptional induction of antiviral genes such as IFNβ

for the establishment of an antiviral state. For example, PKR plays a role in transcriptional regulation via pathways involving different members of the MAPK family [72]. MAPKs are a large group of evolutionary conserved kinases, that regulate many cellular events. Members of the MAPK family, that are regulated by PKR, include e.g. p38 and c-Jun N-terminal kinase (JNK) [125, 126]. MAPK activation by PKR leads to STAT1/ 3 and c-Jun mediated transcription of a variety of antiviral genes [127]. PKR also directly regulates NFκB mediated transcription in a reaction involving interaction of PKR and IKK [128]. NFκB controls the expression of genes involved in immune and inflammatory responses, cell differentiation, apoptosis and more, underlining its prominent role in antiviral immunity [129]. Another major transcription factor, regulated by PKR phosphorylation upon cellular stress, is the tumor suppressor p53 [130, 131]. Moreover, PKR has been demonstrated to bind to numerous proteins that contain RBMs such as ILF3 and double-stranded RNA-specific adenosine deaminase (ADAR1), which are associated with inhibition of viral replication [132, 133]. PKR is also involved in induction of apoptosis. Hereby, PKR on the one hand regulates transcription of genes coordinating apoptotic functions, as e.g. via p53 and on the other hand directly interacts with protein factors mediating programmed cell death [134, 135]. As an example, PKR can interact with the B56α regulatory subunit of protein phosphatase 2A (PP2A) proteins. It herein blocks B56α-mediated inhibition of PP2A, which results in enhanced PP2A activity and consequently influences induction of apoptotic processes. PKR is also involved in FAS-associated death domain protein (FADD) mediated caspase 8 activation, equally resulting in apoptosis [136, 137].

1.2.3 Antiviral Stress Granules

Recently, a new mode of counteracting viral infection, was discovered: The intracellular assembly of antiviral stress granules (aSGs). Stress granules (SGs) as a consequence of cellular stress induced by heat shock were described in the 1980s by Nover and collegues, but their participation in antiviral immunity was first investigated by Onomoto *et al.* in 2012 [120, 138]. SGs are dynamic aggregations of RNA and proteins, located in the cytoplasm. They selectively store translationally silenced mRNAs [139]. Their assembly is a consequence of the inhibition of translation initiation, ocurring after phosphorylation of eIF2α by PKR or other eIF2α phosphorylating kinases while opposing viral infection or cellular stress [140]. The accumulation of untranslated mRNAs in SGs is reversible. That means, the translationally stalled mRNAs are vital and can be translated, when the cell recovers from non-lethal stress [140]. The core factors of SGs are [141, 142]:

- Translationally stalled mRNA
- Components of the translationally silent 48S pre-initiation complex, like eIF4E or eIF3
- RNA-binding proteins that regulate mRNA translation and stability, like poly-A binding protein (PABP) or T-cell-restricted intracellular antigen 1 (TIA1)

- Proteins linked to mRNA metabolism, like Ras GTPase-activating protein-binding protein 1 (G3BP1)
- Signalling proteins, like TRAF 2.

SGs resulting from viral infection additionally contain multiple forms of antiviral signalling proteins as RIG-I, IPS-1 and PKR [120, 143, 144]. In this context, it could be shown, that IPS-1 not only serves as an adaptor protein for RLR signalling, but also as an enhancer for PKR activation, demonstrating a crosstalk between both antiviral pathways [143]. Based on these findings, aSGs have been proposed as antiviral signalling platforms [120].

1.3 Viral inhibition of the host IFN response

Many viruses have evolved strategies to prevent their recognition by host cells and to counteract the effects of the antiviral IFN response. For this, viral intervention at two key nodes of the IFN system is possible: Inhibition of cytokine transcription to reduce IFN production or post-transcriptional inhibition of IFN signalling by targeting IFN receptors and effector proteins [70].

The first action in induction of the antiviral IFN response is the recognition of viral RNA by PRRs. Viruses employ different mechanisms to mask their PAMPs, e.g. many RNA viruses assemble special membrane vesicles for viral replication to shield nascent vRNAs from activating RLRs [145]. Influenza viruses prevent newly generated viral mRNA from degradation, by hijacking host cell pre-mRNA 5'-cap structures in a process called "cap-snatching", which is mediated by the viral polymerase complex (see section 1.1.4) [37]. Viruses can also directly inhibit PRR signalling by sequestering cellular receptors or their adaptor proteins (figure 1.9 A). The NS protein of the severe fever with thrombocytopenia syndrome virus (SFTSV) for example can sequester RIG-I, TRIM25 and TBK1 into distinct cytoplasmic structures [146, 147]. Another example are the influenza A virus proteins PB2 and PB1-F2. They can interfere with the type I IFN production by inhibition of the RIG-I adaptor protein IPS-1 [148, 149]. Another target mechanism is located further downstream, at the level of transcription induction. The multifunctional ebola virus polymerase cofactor (VP35) for example can prevent IRF3 activation and translocation [150]. Moreover, influenza and corona viruses have been shown to inhibit NFκB activation by suppressing IKKα/ β [151, 152].

The second way, to avert the antiviral IFN response is to post-transcriptionally inhibit IFN signalling and effector proteins (figure 1.9 B). IFN signalling is transduced via binding to distinct IFN receptors. Type I IFNs bind to IFNAR, which results in the recruitment of JAK1 and TYK2 and the phosphorylation of STAT1/ 2 to regulate transcription of a variety of ISGs (see figure 1.5). The nonstructural proteins NS4B and NS5 of West Nile viruses are able to block the activation of JAK1 and TYK2 [153]. Moreover, some viral pathogens like ebola or influenza increase the expression of suppressors of cytokine signalling (SOCS) proteins to inhibit the IFN signalling pathway [154, 155]. Viruses also directly antagonise STAT1 and 2

function by inhibiting their phosphorylation or translocation [156–158]. This is executed for example by the influenza virus NS1 protein or NS4B and NS5 proteins of Dengue viruses. Finally, many viruses also directly target ISGs, such as OAS or PKR [72].

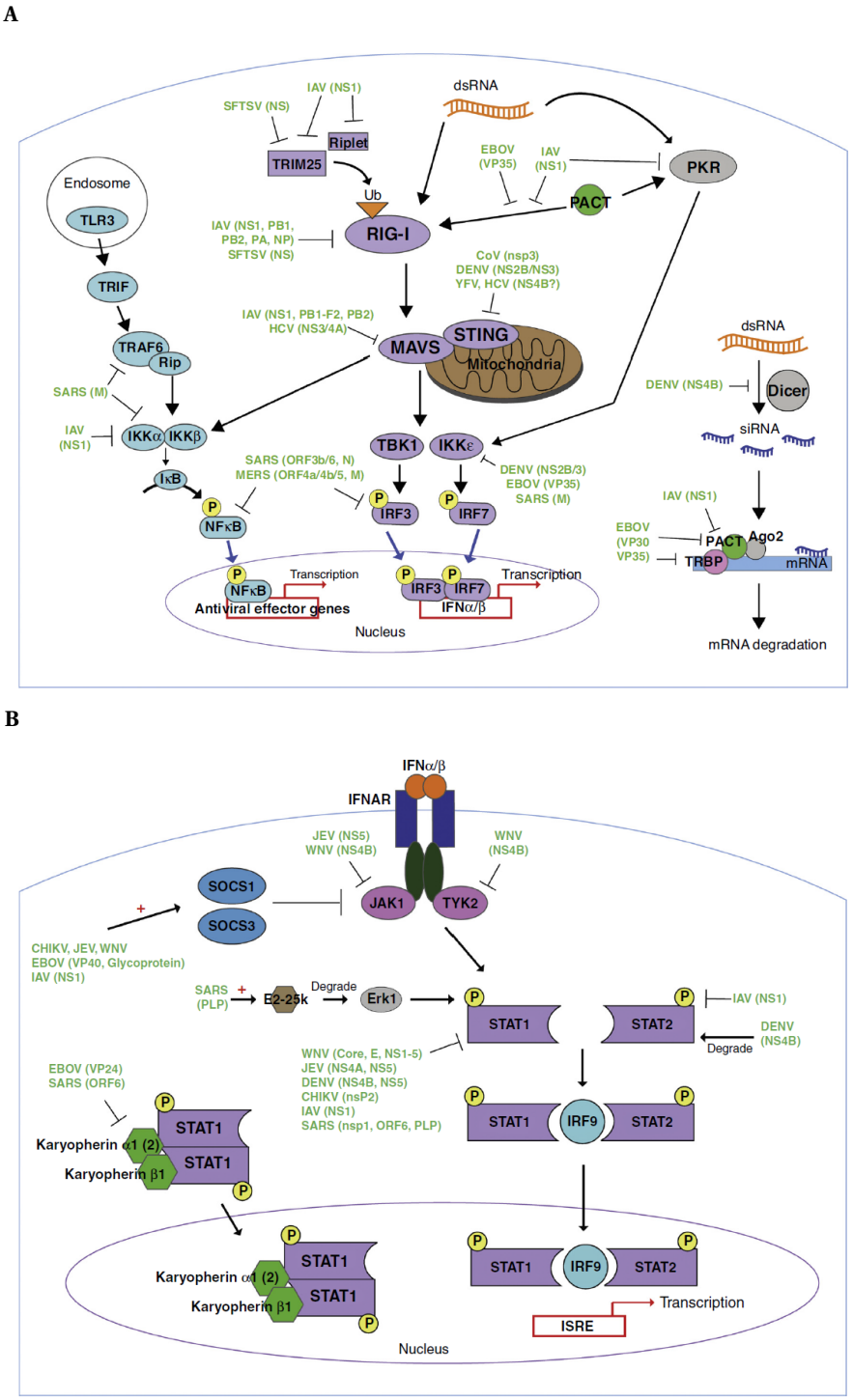

Figure 1.9. Viral inhibition of innate immune signaling pathways. A Viral countermeasures against cytosolic signalling pathways leading to the transcription of cytokines. **B** Viral inhibition of post-transcriptional type I IFN signalling. Viral antagonists are highlighted in light green. For details, see text. A and B adapted from [159].

Many viruses inhibit PKR activation and downstream effects by manifold strategies (reviewed

in [112, 160]). Hereby, some viruses express proteins that directly interact with PKR, thus blocking its ability to homodimerise and autophosphorylate. Examples for this are the influenza virus NS1 protein, the US11 protein of HSV type 1 or the vaccinia virus E3 protein, among others [161–163]. The vaccinia virus E3 protein was also described to inhibit PKR activation by sequestration of viral RNA [164, 165]. This strategy is employed in a similar manner by the human cytomegalovirus (HCMV) TRS1 protein [166]. In addition, some viral proteins as e.g. the influenza virus NS1 protein and the ebola virus VP35 are able to interact with protein regulators of PKR, such as PACT, to inhibit PKR activation [167–169]. Some viruses as for example the human immunodeficiency virus (HIV) type 1 synthesize PKR pseudosubstrates that act as substrate homologues of eIF2α to prevent PKR mediated inhibition of protein translation [170]. Another way to inhibit PKR mediated effects is the activation of antagonist phosphatases. This strategy was shown to be employed by the HSV type 1 $\gamma_1$34.5 protein [171]. It inhibits PKR downstream effects by recruiting the cellular protein phosphatase 1 (PP1) to form a high-molecular-weight complex which can dephosphorylate the PKR substrate eIF2α. For Rift Valley fever virus (RVFV) it could be shown that expression of the NS protein facilitates the proteasomal degradation of PKR [172].

1.3.1 The influenza virus non-structural protein 1

One of the major antagonists of the cellular IFN-mediated immune response in influenza viruses is the multifunctional NS1 protein. It is highly expressed in infected cells and plays an important supportive role in virus replication, since NS1 deficient mutant viruses display strongly attenuated replication [173]. The influenza A virus NS1 is a 26 kDa protein with a length of about 230 aa depending on the strain. It consists of three domains, an N-terminal RNA-binding domain, a linker domain and a C-terminal effector domain (figure 1.10 A). The RNA-binding domain mediates binding to a variety of RNA species with variable affinity including viral RNA, polyadenylated RNA and dsRNA [174–176]. The effector domain is mainly involved in direct protein interaction, mediating its antagonistic functions (figure 1.10 B). The NS1 protein can inhibit IFN expression by blocking RIG-I activation. It can for example either directly interact with RIG-I and its adaptor protein IPS-1 or inhibit ubiquitination of RIG-I by interaction with TRIM25 [177, 178]. Moreover, NS1 can limitate the antiviral effects of IFN-induced proteins as PKR and OAS [179]. Hereby, it was shown that NS1 inhibits dsRNA and PACT mediated PKR activation by binding to the N-terminal domain of PKR [161, 167]. By binding to PKR and thus inhibiting PKR activation, the NS1 protein is also able to block aSG formation to avert translational arrest that would be detrimental for viral replication [180]. Moreover, NS1 can block the maturation of cellular mRNAs such as IFN mRNAs by interacting with the 30 kDa subunit of CPSF and it interferes with the export of cellular mRNAs [42, 43, 181]. Contrary to the block of cellular mRNA maturation, NS1 is able to promote viral mRNA translation by associating with PABP1 and the translation initiation factor eIF4GI [182]. Another host cell process modulated by NS1 is the phosphoinositide 3 kinase (PI3K) mediated signalling [183, 184].

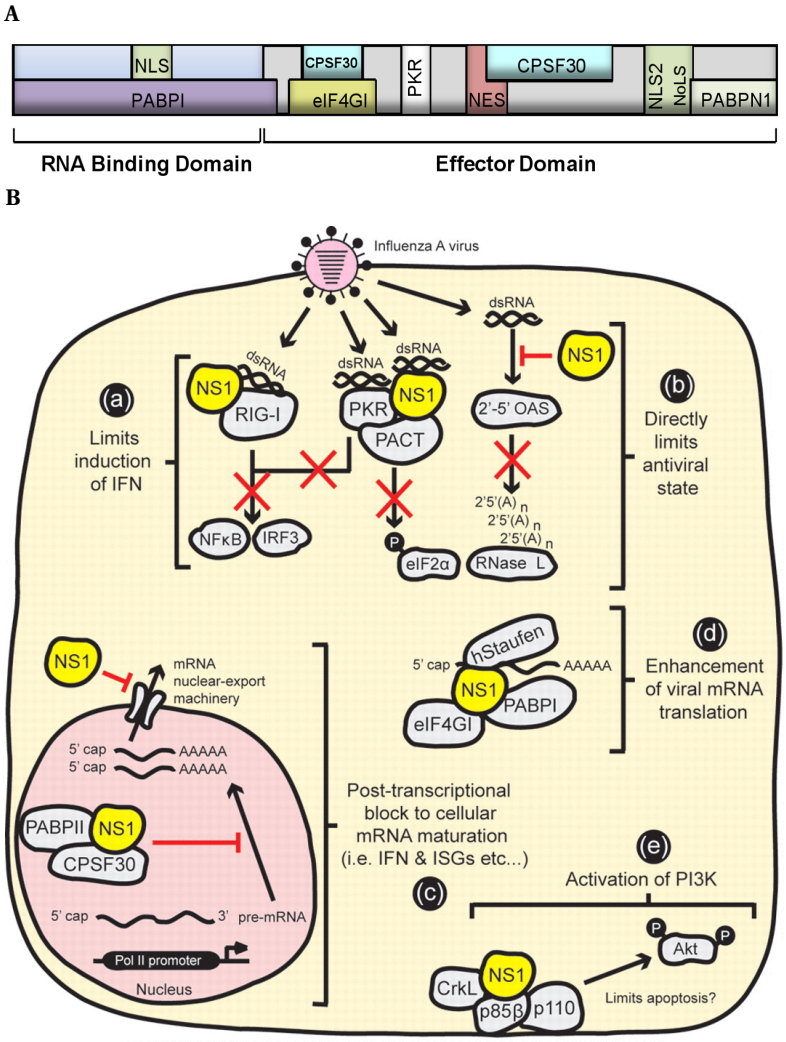

Figure 1.10. Domain structure and main functions of the influenza virus NS1 protein. A NS1 consists of an N-terminal RBD and a C-terminal effector domain connected by a linker. Binding sites of cellular proteins are indicated. Adapted from [185]. **B** NS1 can inhibit the cellular IFN induction (a) and limits the antiviral state by interaction with PKR and OAS (b). It can block the maturation and export of cellular mRNAs (c) and promotes viral mRNA translation (d). NS1 can also regulate PI3K mediated signalling (e). For details, see text. Adapted from [179].

In this thesis, two influenza A/PR/8 derived NS1 loss-of-function mutant viruses were employed in addition to the wild type (WT) virus: A mutant completely lacking the NS1 protein coding sequence, thus not expressing the viral NS1 protein (A/PR/8 ΔNS1) and a virus expressing an NS1 with a point mutation from arginine to alanine at position 46 of the RNA-binding domain (A/PR/8 R46A). The arginine at position 46 was shown to be essential for the RNA-binding function of the NS1 protein. Accordingly, the NS1 R46A mutant is not able to bind RNA and additionally lacks the ability to inhibit PKR activation [186, 187].

1.4 Mass spectrometry

Mass spectrometry is an analytical method to analyse the composition of small molecule compounds and complex protein mixtures such as whole cellular proteomes with the help of a mass spectrometer. The technique can be used for proteomic approaches, because it allows rapid detection, identification and quantitation of high amounts of peptide sequences with good accuracy and sensitivity [188]. The proteome of an organism is hereby defined as the complete set of proteins expressed in the given organism at a given time point [189]. A derivation from proteomic studies are "interactomics" that analyse the network of protein-protein-interactions of a protein of interest.

A mass spectrometer is an instrument that ionises molecules and measures their mass-to-charge ratio (m/z). It consists of three major components: an ion source, a mass analyser and an ion detector. The ion source ionises the molecules which is a prerequisite for the following analysis. The most common types of ionisers are electrospray ionisation (ESI), where the sample is in a liquid phase, and matrix-assisted laser desorption/ ionisation (MALDI) that employs samples associated to a solid matrix. Following ionisation, mass analysers separate the ionised analytes according to their m/z ratio, based on their behaviour in an electric or magnetic field [190]. There are several forms of mass analysers differing in resolution, dynamic range, sensitivity, mass accuracy, speed and the ability to perform tandem mass spectrometry (MS/MS) analyses. Hereby, the most common combination with an ESI source is an ion trap mass analyser, whereas MALDI ionisers are often used with time-of-flight (TOF) analysers [191].

In proteomics, two different approaches for the identification of proteins exist: In top-down proteomics, the whole, intact protein is analysed, allowing the detection of degradation products and sequence variants. It is mainly used for the analysis of individual proteins or simple mixtures, since the method suffers from a dynamic range challenge [192]. For complex mixtures of proteins, the bottom-up approach is employed. Hereby, the proteins are proteolytically digested into peptides before the analysis. By comparing the masses of the detected peptides with those predicted from a sequence database or alignment of peptide spectra with a peptide spectral library, peptides can be identified and proteins can accordingly be assembled from multiple peptide identifications by using computational tools [193].

By this means, the problem arises, that peptides with a different sequence can have the same mass. To unambiguously identify peptides, the peptide ion is fragmented and the resulting peptide fragments are further analysed in a second mass analyser. This technique is called tandem mass spectrometry (MS/MS). It employs the principle, that peptide ions are formed in the ion source and their m/z ratio is determined in a first mass spectrometric scan (M1). Then, a subset of peptides is selected according to their m/z values and further fragmented by collision induced dissociation (CID). The resulting fragment ions are separated and analysed in detail in a second scan (MS2). Combined information from MS1 and MS2 spectra allows the sequence identification of the peptides with high accuracy [191].

The experiments in this thesis were conducted with a linear ion trap quadrupole (LTQ)-Orbitrap with an ESI ion source using tandem mass spectrometric analysis. Thus, following explanations of the method refer to this instrumental setup. The LTQ-Orbitrap is a hybrid mass spectrometer with two sequential mass analysers, a linear ion trap quadrupole and an Orbitrap. Hereby, the Orbitrap used for the full scan has a high dynamic range, mass accuracy and resolution, whereas the linear ion trap is very sensitive and fast, which is important for the second scan of fragmented peptide ions. The technical process of the analysis is as follows: Peptides are first ionised by ESI, resulting in the production of positively charged peptide ions. These ions are analysed in the Orbitrap. Hereby, they are trapped in the Orbitrap's electrostatic field and oscillate around a central elctrode. The oscillation frequency allows determination of the m/z values, whereas the oscillation amplitude represents the signal intensity. The signals, related to time, are used for generation of the precursor ion spectrum (M1) by Fourier transformation analyses [194]. The precursor ions with the five most intense peaks are isolated and fragmented by collision with inert gas molecules (CID). The m/z ratios of the peptide fragments are further analysed in the LTQ, generating the MS2 spectra. MS1 and MS2 raw data are subsequently processed by automated search engine software. The experiments in this thesis were evaluated with the Sequest algorithm embedded in the Proteome Discoverer v1.4 software. The Sequest algorithm compares each spectrum individually to theoretical spectra created by in silico digestion of an input protein database. Data from the MS2 spectra are merged with the known mass of the intact peptide to identify proteins [195]. To avoid false positives, Sequest creates a random decoy database for comparison with the mass spectrometric data. On assuming, that a false peptide assignment can occur in both, input and decoy, databases with the same probability, the number of identifications in the decoy database is used to estimate the total number of incorrect assignments, denoted as "False discovery rate (FDR)". The FDR is the percentage of random identifications and represents an index number for the quality of protein identification [196].

1.4.1 Stable isotopic labelling by amino acids in cell culture

Stable isotopic labelling by amino acids in cell culture (SILAC) is a method for quantitative mass spectrometry analyses, which allows to detect differences in protein abundance among two or more samples using non-radioactive isotopic labelling [197]. The basic principle relies on the in vivo incorporation of tagged amino acids into cellular proteins during cell growth. Since there is hardly any chemical difference between the labelled and the natural amino acids, the cells behave the same and there is no difference in protein composition [198, 199]. For the SILAC analysis, cells are grown in media lacking an essential amino acid that is replaced with an isotopically labelled form of the same amino acid. Labelled proteins from different cell cultures are identical except for a small mass difference. In the mass spectrometry (MS) analysis, pairs of chemically identical peptides from differentially labelled cells can be differentiated by their mass shifts.

In this thesis, media with labelled lysine and arginine species were used and proteins were digested with trypsin (see section 2.11 for composition of SILAC media and section 3.6.5 for protocol of trypsine digestion). Trypsin cuts after lysine and arginine residues, ensuring that all peptides carry one isotopic label (except the peptide at the C-terminus).

For a triplex-SILAC assay, which was used in this study, three cell populations are either grown in medium containing light (R0K0), intermediate (R6K4) or heavy (R10K8) amino acid isotopes of lysine and arginine. After complete incorporation of the tagged amino acids, cells are lysed and lysates are mixed in a proportion of 1:1:1 regarding the protein amount. Proteins are fractionated to lower the complexity of the sample and proteins are digested into peptides, which are analysed by LC-MS/MS. In the resulting peptide spectra, a triplet of peaks appears for every peptide, because intermediate and heavy labelled amino acids create a distinct, known mass difference of a few Dalton (Da) (figure 1.11). The relation of signal intensities of the peptides from different cell populations allows a direct comparison of the protein abundance, hence facilitates relative protein quantification [200]. In this study, SILAC was used for the comparison of the PKR interactomes of cells infected with influenza A/PR/8 WT or ΔNS1 virus to non-infected cells to enable the exclusion of false positives.

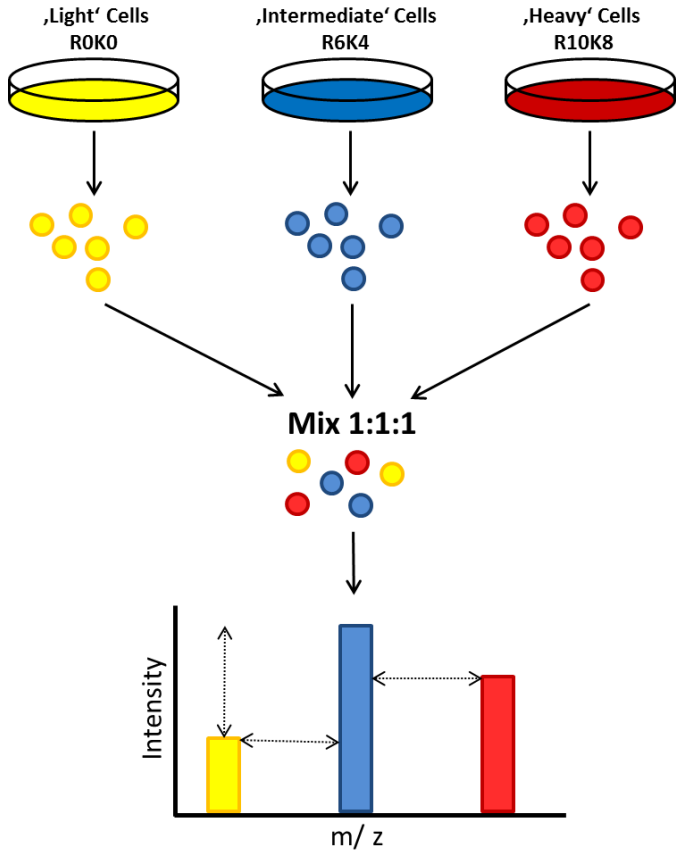

Figure 1.11. SILAC principle. Cells are cultivated in medium containing light (R0K0), intermediate (R6K4) or heavy (R10K8) amino acid isotopes of arginine and lysine. After cell lysis, equal amounts of protein lysates are mixed and digested with trypsin. The resulting peptide mixture is analysed by LC-MS/MS. Peptides of proteins from differently labelled cells are identical except for a distinct mass shift (horizontal arrow), which allows relative quantification of protein abundance according to signal intensities (vertical arrow).

1.5 Aim of study

PKR is a key regulatory factor of the antiviral immune response. Upon activation by recognition of viral RNA, PKR affects a broad range of antiviral proteins either by phosphorylation or direct protein-protein interaction. PKR mediated antiviral signalling is highly complex and includes diverse modes of action such as translation inhibition, induction of apoptosis and release of factors for the transcription of antiviral genes. Due to its importance in the cellular antiviral immunity, many viruses have evolved mechanisms to prevent PKR mediated effects. In influenza virus infection, this role is excerted by the viral NS1 protein, but the exact mechanism of PKR inhibition by NS1 is not completely understood. Over the last decades, extensive research has been conducted to identify the full pattern of PKR regulatory mechanisms, but recent studies employing advanced techniques were able to uncover novel PKR binding partners, thereby suggesting that the PKR interactome is still not fully uncovered.

The main aim of this study was, to systematically identify PKR binding partners in the context of influenza virus infection and to analyse the role of cellular and viral factors in regulating PKR activation. To address this, a quantitative mass spectrometric screen was conducted to determine the interactome of PKR in influenza WT and NS1 mutant virus infected cells. Identified interaction partners were validated and their role in regulating PKR functions was further analysed in independent biochemical assays.

It was hoped that the functional analysis of novel PKR interaction partners would further our understanding of cellular antiviral mechanisms and their modulation by influenza A virus, which could support the identification of new, promising antiviral targets for future drug development.

2 Materials

2.1 Chemicals and Consumables

0.5 ml reaction tubes	Sarstedt, Nümbrecht
1.5 ml reaction tubes	Sarstedt, Nümbrecht
15 ml reaction tubes	Roth, Karlsruhe
50 ml reaction tubes	TPP, Trasadingen (Switzerland)
6-well plates	TPP, Switzerland
12-well plates	PAA Laboratories, Cölbe
24-well plates	PAA Laboratories, Cölbe
48-well plates	Greiner, Solingen
96-well plates	BRAND GmbH, Wertheim
Acetic acid	Roth, Karlsruhe
Acetonitril	Roth, Karlsruhe
Acrylamide/Bis-acrylamide solution 30 % (29:1)	Roth, Karlsruhe
Agarose NEEO Ultra Quality	Roth, Karlsruhe
Ammonium carbonate	Roth, Karlsruhe
Ammonium chloride	Roth, Karlsruhe
APS	Roth, Karlsruhe
Ampicillin	Roche, Mannheim
Bacto-Agar	Becton-Dickenson, Heidelberg
β-Mercaptoethanol	Roth, Karlsruhe
Boric acid	Roth, Karlsruhe
Bovine Albumin Fraction V	Roth, Karlsruhe
BSA, 30 %	PAA Laboratories, Cölbe
Calcium chloride	Merck, Darmstadt
Cell culture dishes	Nunc, Roskilde (Denmark)
Cell culture flasks and dishes	TPP, Trasadingen (Switzerland)
Cell culture dishes	Greiner, Solingen
Cell Dissociation Buffer	Gibco (Life Technologies), Darmstadt
Cell scraper	TPP, Trasadingen (Switzerland)
CL-XPosure film	Thermo Scientifc, Bonn
Coomassie Brilliant Blue R250	Roth, Karlsruhe
DEAE-Dextran	Sigma-Aldrich, Taufkirchen
Dialyzed FBS	Invitrogen (Life Technologies), Darmstadt
DMSO	Sigma-Aldrich, Taufkirchen
DNA Fast Ruler	Fermentas, St. Leon-Rot
DNA Mass Ruler	Fermentas, St. Leon-Rot
DNA 6x loading buffer	Fermentas, St. Leon-Rot
DTT	Roth, Karlsruhe
EASY-Column, 2 cm, C18-A1	Proxeon (Thermo Fisher Scientifc), Dreieich
EASY-Column, 10 cm, C18-A2	Proxeon (Thermo Fisher Scientifc), Dreieich

EDTA	Roth, Karlsruhe
Embryonated Chicken Eggs	Valo Biomedia GmbH, Osterholz Scharmbeck
Ethanol	Roth, Karlsruhe
Ethidium bromide	Roth, Karlsruhe
FBS	Biochrom, Cambridge (UK)
Formaldehyde 10 % (methanol-free)	Polysciences Inc., Eppelheim
Formaldehyde 37 %	Roth, Karlsruhe
Formic acid	Sigma-Aldrich, Taufkirchen
GFP-Trap® matrix	Chromotek, Martinsried-Planegg
Glutamine	Roth, Karlsruhe
Glycerol	Roth, Karlsruhe
Glycin	Roth, Karlsruhe
HEPES	Roth, Karlsruhe
IGEPAL® CA-630	Fluka Biochemika, Milano (Italy)
Iodoacetamide	Sigma-Aldrich, Taufkirchen
Isopropanol	Roth, Karlsruhe
Kanamycine	Roth, Karlsruhe
L-Arginine (non labelled) Cat. #201004102	Silantes, München
L-Arginine ($^{13}C_6$) Cat. #201204102	Silantes, München
L-Arginine ($^{13}C_6$, $^{15}N_4$) Cat. #201604102	Silantes, München
L-Lysine (non labelled) Cat. #211004102	Silantes, München
L-Lysine (D_4) Cat. #211104112	Silantes, München
L-Lysine ($^{13}C_6$, $^{15}N_2$) Cat. #211604102	Silantes, München
Lipofectamine® 2000	Invitrogen, Darmstadt
Lipofectamine® RNAiMAX	Invitrogen, Darmstadt
Methanol	Roth, Karlsruhe
Midori Green Advance	Biozym Diagnostik, Oldendorf
Milk powder	Roth, Karlsruhe
Mowiol 4-88	Roth, Karlsruhe
Nitrocellulose-membrane	Whatman (GE Healthcare), Freiburg
Opti-MEM®	Gibco® , Darmstadt
Parafilm	American National Can, Chicago (USA)
Paraformaldehyde	Roth, Karlsruhe
Pefabloc	Roth, Karlsruhe
Penicillin/Streptomycin	PAA Laboratories, Cölbe
PicoTip Emmiter SilicaTip	New Objective Inc., Woburn (USA)
Ponal (glue)	Henkel, Düsseldorf
Ponceau S	Sigma-Aldrich, Taufkirchen
Prestained protein ladder	Fermentas, St. Leon-Rot
Protein A Agarose	Roche, Mannheim
Protein G Agarose	Roche, Mannheim
ProteoMass Cal Mix	Sigma-Aldrich, Taufkirchen
SDS	Serva, Heidelberg
Sodium acetate	Roth, Karlsruhe
Sodium chloride	Roth, Karlsruhe
Sodium deoxycholat	Roth, Karlsruhe
Sodium orthovanadate	Sigma-Aldrich, Taufkirchen
Super Signal Dura chemiluminescence	Pierce, Bonn

TEMED	Serva, Heidelberg
TPCK-Trypsin	Sigma-Aldrich, Taufkirchen
Trifluoroacetic acid	Roth, Karlsruhe
Tris	Roth, Karlsruhe
Triton-X 100	Serva, Heidelberg
Trypsin (cell culture)	Gibco® , Darmstadt
Tween® 20	Roth, Karlsruhe
Whatman paper	Whatman (GE Healthcare), Freiburg

2.2 Kits

BCA Protein Assay Kit	Pierce (Thermo Scientific), Bonn (Germany)
BigDye® Terminator 3.1 Kit	Applied Biosystems, Darmstadt (Germany)
Cell Proliferation Lit I (MTT)	Roche, Mannheim (Germany)
Expand™ High Fidelity PCR System	Roche, Mannheim
IFNβ ELISA Kit	Fujirebio® Inc., Tokyo (Japan)
Invisorb® Spin Plasmid Mini Two Miniprep Kit	STRATEC Molecular GmbH, Berlin (Germany)
QIAfilter Plasmid Maxi Kit	QIAGEN, Hilden (Germany)
QIAquick® PCR Purification Kit	QIAGEN, Hilden (Germany)
VeriKine™ Human IFNβ ELISA Kit	PBL Assay Science, New Jersey (USA)

2.3 Enzymes

BamHI (FastDigest)	Fermentas, St. Leon-Rot
CIAP	Fermentas (Thermo Fisher Scientific), St. Leon-Rot
DpnI	Fermentas, St. Leon-Rot
RNasin	Promega, Mannheim
T4 DNA Ligase	Fermentas (Thermo Fisher Scientific), St. Leon-Rot
XhoI (FastDigest)	Fermentas, St. Leon-Rot

2.4 Cell lines

A549 cells	Human alveolar epithelial cells
HEK293T cells	Human Embryonic Kidney cells
HeLa cells	Human adenocarcinoma epithelial cells
MDCKII cells	Madin-Darby Canine Kidney cells

2.5 Bacterial strains

Escherichia coli (*E. coli*), strain *BL26*	*[F^- ompT $hsdS_B(r_B{}^- m_B{}^-)$gal dcm]*
E. coli, strain *DH5α*	*fhuA2 lac(del)U169 phoA glnV44 Φ80' lacZ(del)M15 gyrA96 recA1 relA1 endA1 thi-1 hsdR17*
Escherichia coli (*E. coli*), strain *XL1-Blue* (Stratagene)	*recA1 endA1 gyrA96 thi-1 hsdR17 supE44 relA1 lac [F' proAB $lacI^q ZδM15$ Tn10 (Tet^r)]*

2.6 Virus strains

A/PuertoRico/8/1934	H1N1	recombinant	
A/PuertoRico/8/1934 ΔNS1	H1N1	recombinant	A/PuertoRico/8/1934 derived virus with deletion of NS1 protein coding sequence
A/PuertoRico/8/1934 R46A	H1N1	recombinant	A/PuertoRico/8/1934 derived virus with R46A point mutation in NS1 protein

2.7 Plasmids

pcDNA3.1	Invitrogen (Life Technologies)
pcDNA3.1-HA-HSP90β	Addgene Plasmid #22487
pcDNA3.1-HA-YWHAE	Addgene Plasmid #48797
pcDNA3.1-Flag-DDB1	Addgene Plasmid #19981
pcDNA3.1-Flag-HDAC6	Addgene Plasmid #30482
pcDNA3.1-IGF2BP1	S. Hüttelmaier, Department of Medicine, Martin Luther University Halle-Wittenberg, Halle
pcDNA3.1-V5/His-PKR	B. Dauber, FG17, RKI, Berlin
pcDNA3.1-V5/His-PKR 1-265	B. Dauber, FG17, RKI, Berlin
pcDNA3.1-V5/His-PKR 266-551	B. Dauber, FG17, RKI, Berlin
pcDNA3.1-V5/His-PKR K296R	B. Dauber, FG17, RKI, Berlin
pcDNA3.1-V5/His-PKR K60A	B. Dauber, FG17, RKI, Berlin
pcDNA5-FRT/TO-Venus/Flag	Addgene Plasmid #40999
pcDNA5-FRT/TO-Venus/Flag-ExoSC5	S. Sänger, FG17, RKI, Berlin
pcDNA5-FRT/TO-Venus/Flag-ExoSC7	S. Sänger, FG17, RKI, Berlin
pCMV-Myc-HSPA5	Addgene Plasmid #27164
pCMV-Myc-PACT	J. Schneider, FG17, RKI, Berlin
pCMV-Myc-SFPQ	Addgene Plasmid #35103
pCMV-T7-KPNA2	Addgene Plasmid #26678
pEGFP-C1	Clontech
pEGFPC1-6XHis-FLKSRP	Addgene Plasmid #23001
pEGFP-C1-PKR	S. Sänger, FG17, RKI, Berlin

pEGFP-C1-SRSF1	Addgene Plasmid #17990
pEZY-Flag	Addgene Plasmid #18700
pEZY-Flag-DDX5	S. Sänger, FG17, RKI, Berlin
pEZY-Flag-EEF1A1	S. Sänger, FG17, RKI, Berlin
pEZY-Flag-KARS	S. Sänger, FG17, RKI, Berlin
pFRT/TO-His/Flag/HA-MYBBP1A	Addgene Plasmid #38084
pMIG-Flag-PP2A	Addgene Plasmid #10884

2.8 Antibodies

Primary antibodies

Identifier	Species/ Feature	Source
α-A-Influenza virion	goat/ polyclonal	AbD Serotec
α-A-NP	mouse/ monoclonal	AbD Serotec
α-A-NS1 (#9102)*	rabbit/ polyclonal	Biogenes
α-β-actin	mouse/ monoclonal	Sigma-Aldrich
α-cMyc (A14)	rabbit/ polyclonal	Santa-Cruz
α-Exo7	mouse/ monoclonal	Santa-Cruz
α-Exo5	mouse/ monoclonal	Abcam
α-Flag M2	mouse/ monoclonal	Sigma
α-G3BP1	mouse/ monoclonal	Becton Dickinson
α-GFP	mouse/ monoclonal	Santa-Cruz
α-HA	rabbit/ polyclonal	Abcam
α-HSP90β	mouse/ monoclonal	Acris
α-IGF2BP1 (6A9)	mouse/ monoclonal	S. Hüttelmaier, Department of Medicine, Martin Luther University Halle-Wittenberg, Halle
α-ISG15 (#9461)*	rabbit/ polyclonal	Biogenes
α-KSRP	rabbit/ polyclonal	Abcam
α-PKR	rabbit/ monoclonal	Abcam
α-Phospho-PKR (pT446)	rabbit/ monoclonal	Abcam
α-Stat1	mouse/ monoclonal	Santa-Cruz
α-Stat2	rabbit/ polyclonal	Santa-Cruz

$*$ Immunization of rabbits with GST-A-NS1 or GST-ISG15 protein, respectively

Secondary antibodies

Identifier	Species	Source
Alexa 488 α-mouse IgG	donkey	Molecular Probes
Alexa 594 α-goat IgG	donkey	Molecular Probes
Alexa 647 α-rabbit IgG	donkey	Molecular Probes
α-mouse IgG-HRP	goat	Dako
α-rabbit IgG-HRP	swine	Dako

2.9 Primer

Identifier	Feature	Target sequence 5' →3'
BamHI-PKR Rev	cloning primer	CGATGGATCCCTAACATGTGTGTCG
CMV-Seq For	sequencing primer	AACAACTCCGCCCCATTGAC
T7-Seq Rev	sequencing primer	TAATACGACTCACTATAGGG
XhoI-PKR For	cloning primer	CGATCTCGAGTGATGGCTGGTGATCTTTCAGC
YFP-Seq For	sequencing primer	CGAGAAGCGCGATCACATGG
YFP-Seq Rev	sequencing primer	GCTGCAATAAACAAGTTAAC

2.10 siRNA

Identifier	Source	Target sequence 5' →3'
AllStars Negative Control siRNA	Qiagen FlexiTube	
siRNA KHSRP #2	Qiagen FlexiTube	CAGAGGAGGTGAACAAATTAA
siRNA KHSRP #5*	Qiagen FlexiTube	AAGATGATGCTGGATGACATT
siRNA KHSRP #7*	Qiagen FlexiTube	AGGACGGATCTCAGAATACGA
siRNA KHSRP #4*	Qiagen FlexiTube	CAGGATTCAGGCTGCAAAGTA
siRNA KHSRP #3*	Qiagen FlexiTube	CTGGAGTGAAGATGATCTTAA

∗ component of KSRP-siRNA Mix

2.11 Cell culture media

DMEM/ MEM culturing medium	FBS	10 %
	Glutamin	2 mM
	Pen/ Strep	50 mg/ml
	DMEM or MEM	ad 500 ml
Transfection DMEM/ MEM	FBS	10 %
	Glutamin	2 mM
	DMEM or MEM	ad 500 ml
Infection DMEM/ MEM	BSA	0.2 %
	Glutamine	2 mM
	Pen/ Strep	50 mg/ml
	DMEM or MEM	ad 500 ml
SILAC DMEM	dialyzed FBS	10 %
	Glutamine	2 mM
	L-Lysine (non-labelled), (D_4) or ($^{13}C_6$, $^{15}N_2$)	150 mg/l
	L-Arginine (non-labelled), ($^{13}C_6$) or ($^{13}C_6$, $^{15}N_4$)	84 mg/l
	SILAC DMEM	ad 500 ml
SILAC Infection DMEM	Glutamine	2 mM
	L-Lysine (non-labelled), (D_4) or ($^{13}C_6$, $^{15}N_2$)	150 mg/l

	L-Arginine (non-labelded), ($^{13}C_6$) or ($^{13}C_6$, $^{15}N_4$)	84 mg/l
	SILAC DMEM	ad 500 ml
Avicel overlay medium	2.5 % Avicel RC-581 in H_2O	4.86 ml
	2x MEM	4.86 ml
	30 % BSA	66.7 µl
	5 % $NaHCO_3$	100 µl
	1 % DEAE-Dextran	100 µl

2.12 Media for bacteria

2x YT medium	Trypton	16 g/l
	Yeast extract	10 g/l
	NaCl	10 g/l
	pH 7,2	
SOC medium	Trypton	20 g/l
	Yeast extract	5 g/l
	NaCl	10 mM
	KCl	2.5 mM
	autoclaving	
	$MgCl_2$	20 mM
$MgCl_2$-Stock	$MgCl_2$ x 6 H_2O	1 M
	$MgSO_4$ x 7 H_2O	1 M
	Glucose	0.4 % (w/ v)
2x YT-agar with antibiotics	2x YT medium	
	Bacto-Agar	1.5 % (w/ v)
	autoclaving and cooling down	
	ampicillin or kanamycin	100 g/l or 50 g/l

2.13 Buffer and solutions

PBS	NaCl	137 mM
	KCl	2.7 mM
	Na_2HPO_4	80.9 mM
	KH_2PO_4	1.5 mM
$PBS^{+/+}$	PBS	
	BSA	0.2 %
	$MgCl_2$	0.1 g/l
	$CaCl_2$	0.13 g/l
10x SDS buffer	Tris	250 mM
	Glycin	1.92 M
	SDS	10 g/l
10x TBE buffer	Tris	0.89 M
	Boric acid	0.89 M

	EDTA (pH 8.0)	10 mM
10x Crystal violet solution	ddH_2O	
	Ethanol	20 % (v/ v)
	Crystal violet	1 % (w/ v)
1x Crystal violet solution	10x Crystal violet solution diluted in 4 % Formaldehyde/ PBS	
2x SDS sample buffer	H_2O	1.2 ml
	0.5 M Tris/ HCl (pH 6,8)	8.3 ml
	10 % SDS (w/ v)	6 ml
	Glycerol	1.5 ml
	Bromphenolblue	9 g/l
	β-Mercaptoethanol	5 %
6x SDS sample buffer	H_2O	1.2 ml
	0.5 M Tris/ Cl (pH 6.8)	9.8 ml
	1 M Tris/ Cl (pH 7.5)	1.2 ml
	1 M HCl	0.4 ml
	SDS	1.7 g
	0.5 M EDTA	0.5 ml
	Glycerol	5 ml
	Bromphenolblue	9 g/l
	β-Mercaptoethanol	5 %
Semi-dry blotting buffer	Tris	40 mM
	Glycin	30 mM
	SDS	1.3 mM
	Ethanol	20 %
Coomassie staining solution	Coomassie Roti® Blue (5x)	20 %
	Ethanol	20 %
	H_2O	60 %
Coomassie destaining solution	Methanol in H_2O	10 %
Coomassie fixation solution	Acetic acid	10 %
	Ethanol	30 %
6x DNA sample buffer	Bromphenolblue	0.1 % (w/ v)
	Xylencyanol	0.1 % (w/ v)
	Glycerol	30 %
Mowiol	Mowiol 4-88	2.4 g
	Glycerol	6 ml
	ddH_2O	6 ml
	incubation over night	
	0.2 M Tris/ Cl (pH 8.5)	12 ml
	heating to 60 °C while stirring	
	centrifugation for 15 min 1300 g	
	DABCO	10 %
GFP-Trap Dilution buffer	Tris/ Cl (pH 7.5)	10 mM
	NaCl	150 mM

	EDTA	0.5 mM
GFP-Trap Lysis buffer	Tris/ Cl (pH 7.5)	10 mM
	NaCl	150 mM
	EDTA	0.5 mM
	NP-40	0.5 %
Kinase binding buffer	HEPES/ Cl (pH 7.5)	20 mM
	NaCl	300 mM
	$MgOAc_2$	5 mM
	Sodium-β-glycerophosphate	25 mM
	Glycerol	10 %
	NP-40	0.5 %
2x HBS	HEPES/ Cl (PH 7.0)	50 mM
	NaCl	280 mM
	Na_2HPO_4	1.5 mM
$CaCl_2$	$CaCl_2$	2.5 M
ABC buffer	NH_4HCO_3 in H_2O (pH 8.0)	200 mM
Alkylation buffer	Iodoacetamide in H_2O	50 mM
Extraction buffer	Trifluoroacetic acid	3 %
	Acetonitrile	30 %
Buffer A	Acetonitrile in 0.1 % formic acid (in H_2O)	1 %
Buffer B	Acetonitrile in 0.1 % formic acid (in H_2O)	80 %

2.14 Technical equipment

Centrifuges

Biofuge pico	Heraeus (Thermo Scientific)
Centrifuge 5417 R	Eppendorf
Centrifuge RC5C (rotors: SS-34, SLA1500)	Sorvall Instruments
Labofuge 400R (rotor: 8179)	Heraeus (Thermo Scientific)
Megafuge 1.0R (rotor: 2704)	Heraeus (Thermo Scientific)
Multifuge 1S-R (rotor: 75002000)	Heraeus/Sorvall (Thermo Scientific)
SpeedVac Univapo 150 H	Uniequip

Thermocycler

Personal Cycler	Biometra
Primus 96	PEQLAB
Uno Thermoblock	Biometra

Microscopes

Eclipse TS100	Nikon
Olympus CKX41	Olympus
Confocal laser scan microscope LSM 780	Zeiss

Other devices

ABI Prism 3100 Genetic Analyzer	Applied Biosystem
Advanced Fluorescence Imager	Intas
Binder (incubator)	Thermo Fisher Scientific
FLUOstar® Omega Plate Reader	BMG Labtech
HeraSafe HSP15 clean bench	Heraeus
HeraSafe KS12	Heraeus
Curix 60 developer machine	Agfa
Easy Nano-LC 2	Proxeon
Gel chamber Mini-Sub Cell GT	Biorad
Gel documentation	Intas UV-systems
LTQ Orbitrap Discovery mass spectrometer	Thermo Fisher Scientific
Mini-Protean 3	Biorad
NanoDrop 8000	Thermo Fisher Scientific
Phero-Temp 40	BioTec Fisher
Power Pack 200 and 300	BioRad
Spectrafluor Plus ELISA-Reader	Tecan
Tecan Genios Pro ELISA-Reader	Tecan
Thermomixer compact	Eppendorf
Trans-Blot SD Semi-Dry Transfer Cell	Biorad
Varocell 150 (incubator)	Varolab

2.15 Software and webtools

Software

Adobe Photoshop CS5	image processing
ChemoStar Proffessional software (Intas)	gel documentation
DNASTAR Lasergene 10	sequence analysis
Endnote X5	reference manager
Geneious R8	sequence analysis
GraphPad Prism 5	tables and statistics
LabImage 1D	Quantification of immunoblot protein bands
MARS data analysis software	data analysis
Microsoft Office 2010	text and presentations
MikTex	LaTeX distribution
Proteome Discoverer 1.4	Analysis of MS data
TeXnicCenter	LaTeX text processing
Xcalibur 2.1	Control and process of LC-MS

Webtools

NCBI Gene Database	`http://www.ncbi.nlm.nih.gov/gene/`
NCBI PubMed	`http://www.ncbi.nlm.nih.gov`
PANTHER Classification System online tool, v10.0	`http://pantherdb.org`
STRING database network analysis tool, v10	`http://string-db.org`

Venn diagram calculation tool	`http://bioinformatics.psb.ugent.be/webtools/Venn/`

3 Methods

3.1 Cell culture

3.1.1 Cell passaging

Cell culture work was performed under sterile conditions at room temperature (RT). All cell lines were cultivated at 5 % CO_2 and 37 °C under humidified condition in specific media in T75 or T25 cell culture flasks. 293T and A549 cells were cultured in complemented Dulbecco's modified Eagle medium (DMEM), Madin-Darby canine kidney (MDCK) cells in complemented minimal essential medium (MEM) medium. See section 2.11 for exact composition of media. Cells were subcultured each three to four days at 90 % to 95 % confluency. Therefore, cells were washed with phosphate buffered saline (PBS) and detached with Trypsin-ethylenediaminetetraacetic acid (EDTA) solution. Detached cells were resuspended in fresh media and transferred into new flasks at needed density.

3.1.2 Transfection of eukaryotic cells

The introduction of foreign desoxyribonucleic acid (DNA) or RNA in eukaryotic cells is called transfection. This section describes the transfection of cells using Lipofectamine® 2000. For transfection of cells using calcium phosphate see section 3.6.2.

In this thesis, DNA was transiently transfected into 293T cells using lipofection by employing Lipofectamine® 2000 reagent. Lipofectamine® 2000 consists of cationic lipids. Adding negatively charged nucleic acids results in formation of positively charged liposomes with incorporated DNA. These liposomes can fuse with the negatively charged plasma membrane and enter the cell through endocytosis. Inside the cell, the DNA is released and coded proteins are expressed using the cellular transcription- and translation apparatus.

The day prior to transfection, cells were subcultured to keep them in dividing stage. On the day of transfection, cells were washed with PBS, detached with Trypsin-EDTA solution and resuspended in transfection medium. Cells were pelleted at 800 g for 3 minutes (min) and resuspended in 10 ml fresh transfection medium. For 1×10^6 cells in one well of a 6-well-plate 900 µl of cells were seeded in 1 ml of fresh transfection medium. Meanwhile, plasmid DNA was diluted in 25 µl Opti-MEM and Lipofectamine® 2000 was diluted in 125 µl Opti-MEM at a rate of 1.5 µl per 1 µg of plasmid DNA. The Lipofectamine® 2000-Opti-MEM mixture was incubated at RT for 5 min before combining with the DNA-Opti-MEM mixture and incubating for another 20 min at RT. The DNA-Lipofectamine® 2000-solution was added to the cells and distributed well by shaking gently. Cells were incubated at 5 % CO_2 and 37 °C for 24 h to 30 h before further analysis.

3.1.3 Transfection of siRNAs

To study the specific functions of cellular proteins in vitro, the expression of the corresponding target gene can be inhibited by employing small interfering RNA (siRNA) knockdown techniques. siRNA are short double-stranded RNA molecules that can be introduced into eukaryotic cells by transfection (see section 3.1.2). In the cell, the siRNA molecules bind specifically to the complementary sequence of the target gene which leads to cleavage or translational repression of the target genes' mRNA. These post transcriptional gene silencing processes involve the cellular RNA interference pathway.

In this thesis, the effect of KSRP knockdown was examined by transfection of A549 cells with KSRP siRNA using Lipofectamine® RNAiMAX reagent according to the manufacturer's instructions. Briefly, A549 cells were seeded in transfection DMEM, so that they were approximately 60 % to 80 % confluent on the day of transfection. For 1 well of a 12-well-plate 25 pmol, 50 pmol and 100 pmol of KSRP siRNA or non-target (NT) control siRNA, that is not complementary to human mRNA, were diluted in 50 µl Opti-MEM. In parallel, 5 µl Lipofectamine® RNAiMAX was diluted in 50 µl Opti-MEM. Both solutions were mixed and incubated at RT for 5 min before adding to the cells. 5 h to 6 h post transfection (p.t.) medium was replaced by fresh transfection DMEM. Efficiency of the knockdown was tested at different time points p.t. by SDS PAGE and immunoblotting.

3.2 Infectious work

All experiments involving infectious influenza viruses were performed under BSL2 conditions.

3.2.1 Infection of eukaryotic cells with influenza A viruses

For the infection with influenza A viruses, cells were seeded one day in advance, so that they were 80 % to 90 % confluent on the day of infection. Then, cells were washed with PBS and overlaid with PBS^{++} for mock treatment or influenza A virus diluted in PBS^{++} for 45 min at RT with occasional gentle shaking. Cells were always infected with a defined number of infectious particles per cell (multiplicity of infection (MOI)). For most of the experiments in this thesis, including PKR phosphorylation, coprecipitation and immunofluorescence assays, cells were infected with virus at an MOI of 1.5. For replication experiments and corresponding IFNβ ELISAs, cells were infected at an MOI of 0.1. Inoculation volume of PBS^{++} or virus dilution was chosen according to the minimum volume that could still cover the dish to prevent the cells from running dry. After incubation, virus solution was discarded and cells were washed with PBS to remove unbound viral particles before overlaying the cells with fresh infection media. For 293T and A549 cells infection DMEM and for MDCK cells infection MEM media was used.

For multicyclic infection, medium was supplemented with tosyl phenylalanyl chloromethyl ketone (TPCK) trypsin, which assists cleaving of the viral HA protein and thereby leads to enhanced virus propagation. TPCK trypsin was added depending on employed cell type: 1 µg/ml for MDCK and 293T cells and
0.225 µg/ml for A549 cells. Infected cells were incubated at 5 % CO_2 and 37 °C. For growth curve analysis 10 % of supernatant per well was removed and replaced by fresh infection medium supplemented with TPCK trypsin at different time points post infection (p.i.). Supernatants were stored at −80 °C until further analysis.

To examine the effect of NFκB signaling in infected cells, A549 cells were pretreated with 50 µM of NFκB inhibitor BAY 11-7085 (Enzo® Life Sciences) for 1 h at 37 °C, 5 % CO_2 in infection DMEM. Inhibitor containing medium was collected prior to infection, stored at RT and added again to the cells after infection.

3.2.2 Infection of embryonated chicken eggs for virus propagation

Influenza viruses replicate well in the allantoic cavity of embryonated chicken eggs. So, for generation of influenza virus stocks, ten day old eggs for Influenza A/PR/8 WT and seven day old eggs for Influenza A/PR/8 ΔNS1 or R46A mutant were used. Seven day old eggs have not developed a functional IFN system yet, allowing the replication of viruses with restricted IFN antagonistic properties such as the Influenza A/PR/8 ΔNS1 or R46A mutants.

For infection of embryonated chicken eggs, eggs were candled first, to check for fertilization and to mark the position of the allantoic cavity. Then, eggs were inoculated with 1000 PFU per 100 µl for ten day old eggs or 1000 PFU per 50 µl for seven day old eggs, diluted in PBS^{++}. Eggs were incubated for 48 h at 37 °C under humidified conditions. Eggs were cooled over night (ON) at 4 °C before opening the egg shells and collecting the allantoic fluid without injuring the yolk sac. Harvested virus supernatant was cleared of debris by centrifugation (3000 rpm, 5 min, 4 °C) and a haemagglutination assay (section 3.2.3) was performed to estimate virus titres. Allantoic fluids of eggs with similar haemagglutination titres were pooled, aliquoted and stored at −80 °C. Viral titers were determined by plaque-forming assay as described in section 3.2.4.

3.2.3 Haemagglutination assay

The haemagglutination assay is a test for the estimation of viral titers. It uses the capacity of the viral HA protein to bind to sialic acids on the surface of erythrocytes and agglutinate them. It cannot distinguish between infectious and non-infectious particles and therefore only serves as a rough approximation of the viral titer.

To conduct the haemagglutination test, virus-containing solutions, such as cell supernatants or allantoic fluids, were serially diluted in PBS in a 96-well microtitre plate (V-bottom). Then, equal amounts of a 1 % chicken erythrocyte solution was added and the plate was incubated

at 4 °C for at least 30 min. If the concentration of viruses in the tested solution is high enough, the erythrocides are agglutinated which results in a diffuse red staining, otherwise the erythrocides sink to the bottom of the well. The haemagglutination titer denotes the reciprocal value of the dilution at which hemagglutination can still be observed.

3.2.4 Viral titration by plaque-forming assay

To determine the amount of infectious virus particles in solutions as cell supernatants or allantoic fluids, a plaque-forming assay was performed. When infecting a confluent cell monolayer with influenza virus, the cytopathic lytic effect of the virus on infected cells results in the formation of visible plaques that can be counted, to determine viral titers.

One day prior to virus titration, MDCK cells were seeded in 12-well plates, so that they were confluent on the day of titration. MDCK cells were then infected with serial dilutions of virus containing solutions as described in section 3.2.1 and overlaid with Avicel medium containing 1 µg/ml TPCK trypsin for 48 h at 37 °C, 5 % CO_2. Avicel medium was removed and cells were washed twice with PBS following fixation and staining with 0.1 % crystal violet in 10 % formaldehyde for at least 15 min at RT. Staining solution was removed by water washes and cells were dried at RT. Viral titers were determined by multiplying the number of plaques per dilution with the reciprocal dilution factor times 10 (for infection with 100 µl virus dilution) and are displayed as PFU/ml.

3.3 Molecular biology methods

3.3.1 Polymerase chain reaction

The polymerase chain reaction (PCR) is a technique for amplification of specific DNA-segments by using two short oligonucleotides (primers) that are complimentary to the 3' ends of the sense and antisense strand of the target gene. The techincal process is as follows: In a first step, the DNA template is denatured by heat to facilitate binding of the primers to the DNA strands. Then, beginning from the hybridized primer sequences, a special thermostable DNA polymerase synthesizes new DNA strands complementary to the DNA template by adding dNTPs in 5' to 3' direction. These three steps, denaturation, annealing and elongation, are repeated for a defined number of cycles to amplify the target DNA sequence exponentially.

To generate the pEGFP-C1-PKR plasmid for the expression of GFP-tagged PKR, the human PKR-gene was amplified from pcDNA3.1-V5-PKR template and BamHI and XhoI restriction sites were added in a PCR reaction using the Expand™ High Fidelity PCR System (Roche) according to the manufacturer's instructions. The following reaction parameters were employed:

5 x reaction buffer with 15 mM $MgCl_2$	10 µl
Template DNA pcDNA3.1-V5-PKR ($c = 50$ ng/µl)	1 µl
Primer 1 XhoI-PKR-For ($c = 10$ µM)	2 µl
Primer 2 BamHi-PKR-Rev ($c = 10$ µM)	2 µl
Nucleotide Mix ($c = 10$ mM)	0.5 µl
Expand High Fidelity Enzyme Mix	0.5 µl
ddH_2O	ad 50 µl

PCR programme:

Number of cycles	Temperature	Time	Step
1x	95 °C	30 s	Initial denaturation
35x	95 °C	30 s	Denaturation
	55 °C	30 s	Primer annealing
	72 °C	4 min	Elongation
1x	72 °C	10 min	Final elongation
1x	4 °C	∞	Cooling

3.3.2 PCR purification and DpnI digestion

PCR products were purified from excessive primers, nucleotides and enzymes after PCR or restriction enzyme digestion using the QIAquick® PCR Purification Kit according to the manufacturer's instructions. Purified DNA was eluted with 30 µl to 50 µl double destilled (dd)H_2O.

To degrade remaining template DNA, a DpnI digestion was performed following the PCR reaction. DpnI is a restriction enzyme that specifically degrades methylated DNA. The parental template DNA is from bacterial origin and is therefore methylated. In contrast to that, the newly PCR-generated DNA does not have any methylation modification and will not be degraded in the DpnI reaction. To perform the restriction analysis, 2 µl DpnI, 6 µl 10x Tango buffer and 2 µl were added to 50 µl PCR reaction and incubated for 2 h at 37 °C.

3.3.3 Agarose gel electrophoresis

DNA and RNA segments can be separated according to their size and form by agarose gel electrophoresis. To generate 1 % agarose gels, 1 g agarose was boiled in 100 ml 1x TBE buffer, cooled down and 6 µl of Midori green were added to stain DNA. Samples were supplemented with 6x loading buffer. Separation of samples was performed at a constant voltage of 100 V and DNA was visualized on a transilluminator with UV light. Size and concentration of samples was determined by comparison to commercially available DNA ladders.

3.3.4 Restriction enzyme digestion

Retriction endonucleases are bacterial enzymes that cut the phosphodiester bonds of the dsDNA backbone at specific DNA sequences, referred to as “enzyme recognition sequences”. By separating the phosphodiester bonds between two nucleotides, the enzymes generate blunt ends or 3’-overhangs, creating the possibility of ligating two separate DNA segments with complementary overhangs.

In this thesis, restriction enzyme digestion of PCR products or plasmid vectors was perfomed according to the manufacturer’s protocol in a total volume of 20 µl with 2 µl restriction enzyme and 2 µl of the corresponding 10x digestion buffer at 37 °C.

3.3.5 Vector dephosphorylation

To further prepare the plasmid vector for ligation with the PCR-generated DNA fragment, 5’-phosphate groups were removed by applying calf-intestinal alkaline phosphatase (CIAP) to prevent religation of the linearised vector DNA and to increase the yield of insert containing expression vector.

Dephosphorylation reaction was performed according to manufacturer’s instructions in a 50 µl reaction volume with 5 µl CIAP enzyme ($c = 20\,\mathrm{U}/\mu\mathrm{l}$) and 5 µl 10x reaction buffer for 30 min at 37 °C.

3.3.6 Ligation

DNA fragments with complimentary nucleotide overhangs, created by restriction enzyme digestion (see section 3.3.4), can be ligated by employing a DNA ligase. In this thesis, purified XhoI and BamHI digested PKR-DNA was ligated with equally treated pEGFP-C1 plasmid vector at a ratio of 1:1. Taking into account the different sizes of plasmid vector and DNA insert, 50 ng of pEGFP-C1 vector were ligated with 18 ng insert. Ligation was performed ON at 16 °C by following protocol:

DNA insert	18 ng
plasmid vector	50 ng
T4 DNA ligase	2 µl
10x ligase buffer	1 µl
ddH_2O	ad 10 µl

3.3.7 Transformation of competent bacteria

Transformation is the process of taking up circular plasmid DNA in competent bacterial cells. To facilitate selective growth of transformed bacteria, the inserted plasmids contain antibiotic resistence genes, so that only bacteria carrying the plasmid DNA can grow in media supplemented with the corresponding antibiotic.

For one transformation reaction, 50 µl competent *E. coli XL-1 Blue* or *BL26* cells were thawed on ice, mixed with 5 µL of ligation reaction (see section 3.3.6) or 0.5 µL expression plasmid and inubated on ice for 30 min. Then, heat shock for the induction of DNA uptake was performed for 90 s at 42 °C, cells were incubated on ice for 2 min and 500 µl super optimal broth with catabolite repression (SOC) medium was added, followed by incubation at 37 °C for 30 min with gentle shaking. Bacteria were plated on 2xTY agar plates supplemented with antibiotic (100 µg/ml Ampicillin or 50 µg/ml Kanamycin) and incubated ON at 37 °C.

3.3.8 Plasmid preparation

To isolate plasmid DNA, single colonies of transformed bacteria were picked and grown ON at 37 °C, 200 rpm in 5 ml ("mini culture") or 200 ml ("maxi culture") 2x TY medium containing appropriate antibiotic (100 µg/ml Ampicillin or 50 µg/ml Kanamycin). Bacteria were pelleted and plasmid DNA was isolated employing the Invisorb® Spin Plasmid Mini Two Kit (Stratec) for mini cultures or the QIAfilter Plasmid Maxi Kit for maxi cultures according to the manufacturer's instructions. DNA was eluted with 50 µL ddH_2O (mini culture) or 200 µL ddH_2O (maxi culture) and DNA concentration was determined using the NanoDrop 8000 machine (Thermo Fisher Scientific).

3.3.9 DNA sequencing

DNA was sequenced by Sanger sequencing using the BigDye® Terminator 3.1 Cycle Sequencing Kit (Applied Biosystems) according to the manufacturer's instructions. Following protocol and PCR programme were used:

5 x ABI reaction buffer	1.5 µl
Template DNA	200 ng
Sequencing primer ($c = 10\,\mu M$)	0.5 µl
BigDye 3.1 Mix	1 µl
ddH_2O	ad 10 µl

PCR programme:

Number of cycles	Temperature	Time	Step
1x	90 °C	1 min	Initial denaturation
25x	96 °C	10 s	Denaturation
	55 °C	5 s	Primer annealing
	60 °C	4 min	Elongation
1x	4 °C	∞	Cooling

3.4 Biochemical methods

3.4.1 Preparation of cell lysates

To prepare cell lysates, cells were washed with ice-cold PBS and collected by scraping from the cell culture dish. Cells were pelleted and resuspended in designated lysis buffer supplemented with protease- and phosphatase-inhibitor. Lysis was performed for 30 min on ice with recurrent resuspension. Lysates were centrifuged for 10 min at 15.000 g and cleared supernatants were transferred to a new reaction tube. Following lysis buffers were used: GFP-Trap-Lysis buffer for GFP-trap experiments and detection of cellular and viral proteins, Kinase-binding buffer for PKR-immunoprecipitation experiments.

3.4.2 SDS PAGE

Proteins can be separated according to their molecular weight by sodium dodecyl sulfate polyacrylamide gel electrophoresis (SDS PAGE). Polyacrylamide gels were prepared in two steps employing the Mini-PROTEAN® 3 gel casting equipment (Biorad). First, the separation gel was prepared. After complete polymerisation, the stacking gel was produced in a second step and lanes were generated by insertion of a plastic comb with the designated number of lanes. For a 1.5 mm gel, 10 ml of separation gel with desired concentration and 5 ml of a 5 % stacking gel were generated according to table 3.1. Samples were prepared by mixing with 6x sample buffer and incubation at 95 °C for 5 min. Samples were loaded and proteins were separated in a vertical gel chamber (Biorad) in SDS-running buffer by application of an electric field at a constant current of 25 mA per gel.

3.4.3 Coomassie staining of polyacrylamide gels

Separated proteins in polyacrylamide gels can be visualized by staining with Coomassie Brilliant Blue R-250 dye, which unspecifically binds to basic amino acid side chains.

In a first step, proteins were fixed in the gel with fixing solution consisting of 3 % ethanol and 10 % acetic acid for 20 min RT. Then, proteins were stained with Coomassie Brilliant

	separation gel			stacking gel
	7.5 %	10 %	12.5 %	5 %
30 % Acrylamide/ Bisacrylamide (29:1)	2.5 ml	3.3 ml	4.1 ml	0.83 ml
ddH_2O	4.8 ml	4.0 ml	3.2 ml	2.8 ml
1.5 M Tris/ Cl pH 8.8		2.5 ml		-
0.5 M Tris/ Cl pH 6.8		-		1.25 ml
10 % SDS/		100 µl		50 µl
10 % APS/		100 µl		50 µl
TEMED		6 µl		6 µl

Table 3.1. Composition of SDS polyacrylamid gels. Composition of SDS polyacrylamid gels with different acrylamid concentrations is given. Amounts are sufficient for one gel of 1.5 mm.

Blue R-250 solution for at least 1 h at RT, followed by removal of unbound dye by repeated washing of the gel with 10 % methanol.

3.4.4 Western transfer and immunoblot analysis

To specifically detect separated proteins with corresponding antibodies, proteins were transferred on a nitrocellulose membrane by semi-dry western blotting. The Trans-Blot® SD Semi-Dry Transfer Cell apparatus (Biorad) was used with the following setup: Anode, 2x Whatman paper, SDS acrylamidgel, nitrocellulose membrane, 2x Whatman paper, cathode. Proteins were transferred from the acrylamid gel to the nitrocellulose membrane by applying a constant current of 75 mA per gel for approximately 80 min (for a 1.5 mm gel). Membranes were blocked with a solution of 3 % milk powder in 1x TBST or 5 % bovine serum albumin (BSA)/ TBST (for detection of phospho-proteins) for at least 30 min RT. Primary antibodies were diluted in 0.5 % milk powder in TBST or 1 % BSA/ TBST (for phospho-proteins) and membranes were incubated with antibody dilutions ON at 4 °C with gentle shaking to prevent membranes from running dry. Membranes were washed with 1x TBST for at least three times before incubation with secondary horse raddish peroxidase (HRP)-coupled antibodies, diluted in 0.5 % milk powder in TBST or 1 % BSA/ TBST (for phospho-proteins) for 1 h RT. Membranes were washed six times or more with TBST before visualisation of staining using an enhanced chemiluminiscence protocol with the SuperSignal™ West Dura Extended Duration Substrate (Thermo Scientific). Luminescence was detected using CL-XPosure™ x-ray films developed with the Curix 60 processor (Agfa) or with the Advanced Fluorescence Imager (INTAS) operated with the corresponding ChemoStar software (INTAS).

3.4.5 Coimmunoprecipitation analysis

To analyse protein-protein-interactions of endogenous PKR and binding partners, Coimmunoprecipitation experiments were conducted in non-infected and infected cells.

For one experiment, 7×10^6 A549 cells were seeded in a 10 cm-dish one day prior to infection with influenza A/PR/8 WT, ΔNS1 or R46A virus (see section 3.2.1) at an MOI of 1.5. 16 h p.i., cells were lysed with 1 ml kinase-binding buffer (see section 3.4.1) and lysates were pre-cleared with 30 µl Protein G Agarose rotating for 3 h at 4 °C. 100 µl of cell lysates were mixed with 6x SDS sample buffer and stored at −20 °C as a sample for whole cell lysate (WCL). Meanwhile, coupling of PKR-specific primary antibody to Protein G Agarose was conducted. For one reaction, 50 µl Protein G Agarose were incubated with α-PKR-antibody or α-Myc-antibody (as negative control) and 500 µl kinase-binding buffer rotating for 3 h at 4 °C. Pre-cleared cell lysates and antibody-coupled Protein G Agarose were combined and incubated rotating ON at 4 °C. To remove non-bound proteins, Protein G Agarose was washed three times with kinase-binding buffer by centrifugation for 3 min at 2000 g. Immunoprecipitated proteins and interaction partners were eluted by incubation with 2x SDS sample buffer for 10 min at 95 °C. Samples of WCL and immunoprecipitate (IP) were analysed by SDS PAGE and immunoblotting (see section 3.4.2, section 3.4.4).

3.4.6 GFP-Trap® -analysis

To analyse the interaction of green fluorescent protein (GFP)-tagged proteins with endogenous or co-transfected proteins, GFP-tagged proteins and binding partners were precipitated using a GFP-Trap® -matrix (Chromotek) according to the manufacturer's instructions.

Briefly, 1×10^6 293T cells were transfected with 1 µg pEGFP-C1-PKR or pEGFP-C1-KSRP using Lipofectamine® 2000 (see section 3.1.2) for 30 h at 37 °C, 5 % CO_2, followed by infection with influenza A/PR/8 WT, ΔNS1 or R46A virus (see section 3.2.1) at an MOI of 1.5. 16 h p.i. cells were lysed with 1 ml GFP-Trap-lysis buffer (see section 3.4.1) and 100 µl of cell lysate were mixed with 6x SDS sample buffer as WCL control. Remaining cell lysate was incubated with at least 20 µl GFP-Trap® slurry rotating for 1 h at 4 °C. GFP-Trap® beads were washed three times with GFP-dilution buffer by centrifugation (3 min, 2000 g) and bound proteins and interaction partners were eluted by incubation with 2x SDS sample buffer for 10 min at 95 °C. Samples of WCL and precipitate were analysed by SDS PAGE and immunoblotting (see section 3.4.2, section 3.4.4).

3.4.7 Interferon β ELISA

To measure IFNβ expression and to confirm the inhibitory effect of NFκB inhibitor BAY 11-7085 (Enzo® Life Sciences) on IFNβ production, concentration of secreted IFNβ in the supernatants of infected cells was determined by enzyme-linked immunosorbent assay (ELISA).

Supernatants of treated cells were collected, cleared of debris by centrifugation and stored at −80 °C. IFNβ levels were measured with the VeriKine™ Human IFNβ ELISA Kit (PBL) or with the Fujirebio® Inc. IFNβ ELISA Kit according to the manufacturers' instructions.

3.5 Cell biology methods

3.5.1 Cell viability assay

To examine possible cell cytotoxic effects of siRNA treatment, cell viability was examined by MTT test. This colorimetric assay is based on the capability of cellular, mitochondrial dehydrogenase enzymes to reduce the tetrazolium dye 3-(4,5-dimethylthiazol-2-yl)-2,5-diphenyltetrazolium bromide (MTT) to its insoluble formazan form, which has a purple color. After solubilisation, the concentration of the formazan, which directly corresponds to cell viability, can be determined by photometric measurement at 570 nm.

A549 cells were seeded in transfection DMEM in 96-well plates, so that they were approximately 60 % to 80 % confluent on the day of transfection. KSRP- or NT-siRNA were transfected as described in section 3.1.3. In addition, control samples were generated by treatment of cells with different dimethyl sulfoxide (DMSO)-concentrations. At 24 h, 48 h, 72 h, 96 h and 120 h p.t., cell viability was analysed using the "Cell Proliferation Kit I (MTT)" (Roche).

3.5.2 Immunofluorescence analysis

Subcellular localisation and colocalisation of cellular proteins can be visualized in fixed cells by indirect immunofluorescence analysis using fluorochrome-coupled antibodies.

HeLa cells were seeded on cover slips and infected with influenza A/PR/8 WT or ΔNS1 virus at an MOI of 3 (see section 3.2.1). 16 h p.i., cells were washed with PBS and fixed with 0.5 % formaldehyde (FA)/ PBS for 15 min RT. Possible autofluorescence from aldehyde fixation was quenched by incubation with 50 mM NH_4Cl/ PBS for 10 min RT, following cell permeabilisation with 0.2 % Triton X-100/ PBS for another 10 min RT. Cells were washed three times with PBS and incubated with primary antibodies diluted in 3 % BSA/ PBS for 1 h RT. Cells were washed repeatedly with PBS and complexes of protein and primary antibody were detected with suitable fluorescence-labelled secondary antibody (diluted in 3 % BSA/ PBS) for 1 h RT in the dark. Cells were washed three times with PBS and cell nuclei were stained with 4',6-diamidino-2-phenylindole (DAPI)-working-solution for 10 min RT in the dark. Cells were washed once with PBS and two times with ddH_2O before mounting of cover slips on glass slides with 5 µl mowiol.

Antibody-staining of cellular proteins was visualized using a Zeiss 780 confocal laser scanning microscope (LSM) equipped with a 63x oil immersion objective with a numerical aperture of 1.4. Images were obtained and processed with Zeiss ZEN imaging software.

3.6 Mass spectrometric SILAC analysis

To further analyse the antiviral abilities of PKR in the context of viral infection and the role of cellular and viral factors in regulating PKR activation, a stable isotopic labelling by amino acids in cell culture (SILAC) approach followed by high-resolution liquid chromatography (LC) tandem mass spectrometric analysis was employed to identify immunoprecipitable PKR interaction partners in influenza A virus infected cells.

SILAC was conducted according to the protocol published by Ong and Mann [201]. The detailed workflow of SILAC experiments, conducted in this thesis, is described in figure 4.2. Briefly, 293T cells were labelled by cultivation in medium containing light (R0K0), intermediate (R6K4) or heavy (R10K8) amino acid isotopes of lysine and arginine. Cells were transfected with a GFP-PKR construct and either mock infected or infected with influenza A/PR/8 WT or ΔNS1 virus. After cell lysis, same amounts of proteins were mixed and affinity-precipitated with GFP-Trap® matrix. The eluted proteins were fractionated and digested with trypsin. The resulting peptide solution was analysed using an LTQ-Orbitrap (Discovery; Thermo Scientific) equipped with a Nano-LC (Thermo Scientific). Differences in mass and intensity of peptide signals were used to specifically determine PKR interacting proteins from influenza A WT or ΔNS1 virus infected cells.

3.6.1 Passaging of SILAC labelled cells

SILAC labelled 293T cells, generated in our lab by R. Daviña-Nuñez, were cultivated at 5 % CO_2 and 37 °C under humidified condition in SILAC R0K0, R6K4 or R10K8 DMEM supplemented with the corresponding L-arginine and L-lysine amino acid isotopes in T75 cell culture flasks [202, p.43-44]. Cells were subcultured each three to four days, when confluency reached 90 % to 95 %. Therefore, cells were washed with PBS and detached with enzyme-free Cell Dissociation Buffer (Gibco® , Life Technologies). Detached cells were resuspended in fresh medium and transferred into new flasks at needed density.

3.6.2 Transfection of SILAC labelled cells with $CaPO_4$

In contrast to other cell lines, SILAC labelled 293T cells were transfected using calcium phosphate ($CaPO_4$). Hereby, in a solution containing calcium chloride ($CaCl_2$) and sodium phosphate ($NaPO_4$), DNA binds to precipitated $CaPO_4$ and can be delivered into cells by endocytosis [203].

For one experiment, SILAC labelled 293T cells were seeded in corresponding SILAC transfection DMEM media in four 15 cm dishes per state (light, intermediate and heavy) one day prior to transfection. On the day of transfection, cells were washed with PBS and fresh SILAC transfection DMEM medium was added. Per state, 240 µg pEGFP-C1-PKR (corresponds to 60 µg per dish) was mixed with 6 ml HEPES buffered saline (HBS) and incubated at RT for

5 min. Then, 240 µl $CaCl_2$ was added to the transfection solution, mixed and incubated at RT for another 20 min. Per dish, 1.62 ml transfection solution was added dropwise to the cells and distributed well by gentle shaking. Cells were incubated at 5 % CO_2 and 37 °C for 30 h.

3.6.3 Infection of SILAC labelled cells with Influenza A virus

For SILAC experiments, transfected SILAC 293T cells were either mock infected (light labelled cells) or infected with influenza A/PR/8 WT or ΔNS1 (intermediate or heavy labelled cells) at an MOI of 1.5 for 16 h, 37 °C, 5 % CO_2. Therefore, cells were washed with PBS and infected with virus diluted in PBS for 45 min RT. Virus solution was discarded and cells were washed with PBS before addition of SILAC infection media, respectively.

3.6.4 Cell lysis, BCA-test and GFP-trap® analysis of SILAC labelled cells

Transfected and infected SILAC labelled 293T cells were washed with PBS and lysed with GFP-Trap-lysis buffer as described in section 3.4.1. Protein concentration of lysates was determined using Pierce™ bicinchoninic acid (BCA) Protein Assay Kit (Thermo Scientific) according to the manufacturer's protocol. Cell lysates of the light, intermedate and heavy state were mixed at a protein concentration ratio of 1:1:1 and GFP-PKR was precipitated with 450 µl GFP-Trap® matrix (see section 3.4.6) and bound proteins were eluted with 500 µl 0.2 M glycine (pH 2.5) for 1 min RT, following neutralisation with 1 M Tris/ Cl pH 10.8 by 2 min centrifugation at 2000 g.

3.6.5 In-gel-digestion and preparation of SILAC samples

Eluted proteins from GFP-Trap® analysis were concentrated by membrane ultrafiltration using Vivaspin 500 Columns (Sartorius Stedim Biotech) with a molecular cutoff of 3000 Da. Concentrated eluate was mixed with 6x SDS sample buffer containing β-mercaptoethanol (ME) for reduction of disulfide-bonds (95 °C, 5 min) and free thiol groups were alkylated with 50 mM 2-iodoacetamide (IAA) for 20 min RT in the dark. Proteins were separated by SDS PAGE (section 3.4.2) and stained with Coomassie Brilliant Blue R-250 as described in section 3.4.3. The gel lane with separated proteins was cut into ten slices. Each slice was further cut to small pieces and destained with 200 mM ammonium bicarbonate (ABC) in 40 % acetronitrile (ACN). Gel slices were dehydrated with 100 % ACN, resuspended in 50 µl freshly prepared trypsin solution (40 mM ABC in 9 % ACN containing 20 ng/µl trypsin) per gel piece and incubated ON at 37 °C for tryptic digestion of proteins. Supernatants were transferred to new reaction tubes and residual peptides were extracted from gel pieces by incubation with 50 % ACN in 0.1 % trifluoroacetic acid (TFA) (30 min, 37 °C). Supernatants were combined, dried in a vacuum concentrator and stored at −20 °C. On the day of measurement, samples

were redissolved in 25 µl 0.1 % formic acid (FoAc) by centrifugation (10 min, 15.000 g) and loaded into separate wells of a 96-well plate.

3.6.6 Nano-LC and mass spectrometric analysis

12 µl of each sample were separated by online reverse phase nano-LC (EASY-nLC II, Proxeon Biosystems) using a ReproSil-Pur® C C18-A column (75 µm × 10 cm). The LC setup was connected to a LTQ Orbitrap Discovery™ mass spectrometer (Thermo Scientific) equipped with a nanoelectrospray ion source (Proxeon Biosystems). Peptides were separated and eluted by applying a 65 min linear gradient of 2 % to 4 % buffer B (0.2 % FoAc in ACN) at a flow rate of 300 nl/min with 1.8 kV spray voltage and 200 °C capillary temperature. Data-dependent acquisiton was performed using Xcalibur™ software v2.0 in positive ion mode. Full scan MS spectra (m/z 300 to 1700) were measured with a resolution of $M/\Delta M = 30,000$. The five peptide ions with with highest intensity were sequentially isolated for fragmentation by CID in the linear ion trap. The Orbitrap lock mass feature was applied to improve mass accuracy.

3.6.7 Data-processing and evaluation

Raw data acquired by MS analysis was processed using the SEQUEST algorithm in Proteome Discoverer software (v1.4, Thermo Scientific). Proteins were identified using following parameters: mass accuracy of 2 ppm; precursor ion mass tolerance of ±10 ppm; fragment ion mass tolerance of ±0.8 Da. Chosen variable modifications were: Carbamidomethylation (+57.021 Da), phosphorylation of serine (+79.966 Da) and the four SILAC labels K4 ($^2H_4$; +4.025 Da), K8 ($^{13}C_6$, $^{15}N_2$; +8.014 Da), R6 ($^{13}C_6$; +6.020 Da) and R10 ($^{13}C_6$,$^{15}N_4$; +10.008 Da). Trypsin was set as used proteolytic enzyme with a maximum allowance of two missed cleavage sites.

Only proteins identifed by at least one unique peptide were kept for further analysis. The false discovery rate (FDR) for peptides with high confidence was set to 1 % and of medium confidence to 5 %. Searches were performed against the *Homo Sapiens* data base of National Center for Biotechnology Information (NCBI) with 33286 entries as of 2013-12-15 [204].

In total, four SILAC experiments were conducted and a list with over 140 proteins bound to PKR after influenza A/PR/8 WT infection and more than 120 PKR binding proteins after influenza A/PR/8 ΔNS1 infection was retrieved. To systematically analyse this list and extract PKR interacting proteins with the utmost probability, identified proteins had to match the following criteria: The protein was found in two or more experiments, the average protein score was higher or equal to a value of 10 and the heavy to light (HL) or medium to light (ML) ratio in one or more experiments was higher than 1.5. Possible contaminants, for example proteins known to bind to GFP-Trap® matrix or sepharose, proteins from ribosomal subunits and heterogeneous ribonucleoprotein particle (hnRNP) proteins were excluded from the list [205].

4 Results

PKR is one of the key factors of the cellular innate antiviral immune response. Many viruses have evolved mechanisms to avoid PKR initiated effects [160]. Influenza viruses for example express the NS1 protein which inhibits PKR activation [206]. Despite profound investigation, the precise mechanism of PKR activation in the context of viral infection and the role of cellular and viral factors in regulating PKR activation are not fully understood.

Quantitative proteomics is currently one of the most powerful techniques to study whole cellular proteomes and to compare relative levels of proteins present in different samples. Hereby, SILAC experiments with affinity purification followed by MS provide a rapid, highly sensitive way to comprehensively map protein-protein interactions involving the discrimination between specific interaction partners and non-specifically binding proteins [207]. So far, only a few groups tried to identify PKR's interactome under different circumstances, but to date, there has been no study conducted to systematically analyse PKR protein-protein-interactions upon influenza virus infection using quantitative mass spectrometry.

To further elucidate the interplay of PKR and other host cell factors in the context of influenza virus infection, in this thesis a SILAC approach followed by MS/MS analysis was employed to identify immunoprecipitable interaction partners of PKR. Hereby, KSRP was identified as a novel PKR binding partner. The interaction of KSRP and PKR was validated and an effect of KSRP on viral replication caused by increasing PKR activity was determined.

4.1 Proteomic analysis of the PKR interactome

4.1.1 Experimental setup of SILAC experiments for MS analysis

To identify PKR interacting proteins in the context of influenza A virus infection, a triplex SILAC approach followed by high-resolution LC tandem mass spectrometric analysis was employed according to the protocol of Ong and Mann [201].

The PKR interactome was analysed at 16 h after infection with an influenza A/PR/8 WT or ΔNS1 virus. This time point was chosen according to tested PKR expression and activity levels. It can be seen in figure 4.1 that endogenous PKR was expressed ubiquitously in 293T cells and could be detected with similar levels at all time points regardless of influenza virus infection. Activation of PKR by infection with ΔNS1 virus led to phosphorylation of PKR. Hereby, 16 h p.i. was the earliest time point at which detection of phosphorylated PKR was possible in immunoblot analyses. To facilitate follow-up analyses of PKR and identified interaction partners with classical virological and cell biological techniques, the mass spectrometric PKR interactome analysis was conducted at 16 h p.i.

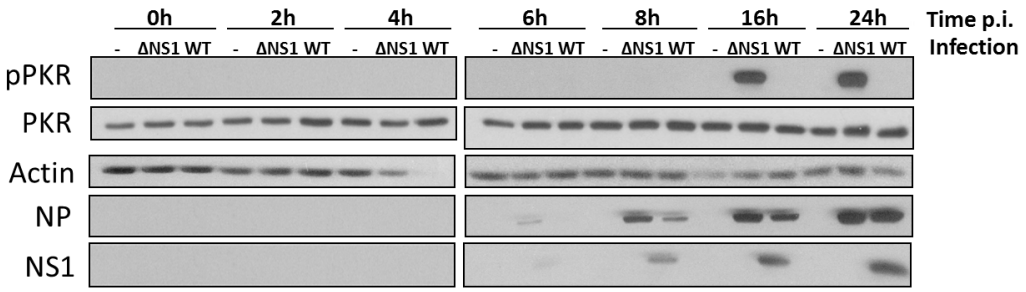

Figure 4.1. Time dependent expression of pPKR and PKR after influenza virus infection. 293T cells were either non-infected or infected with A/PR/8 WT or ΔNS1 virus at an MOI of 1.5. At 0 h, 2 h, 4 h, 6 h, 8 h, 16 h and 24 h p.i., cells were lysed and expression of proteins was analysed by SDS PAGE and immunoblotting with the indicated antibodies. Representative experiment of N = 3.

The complete workflow of the SILAC experiments is shown in figure 4.2.

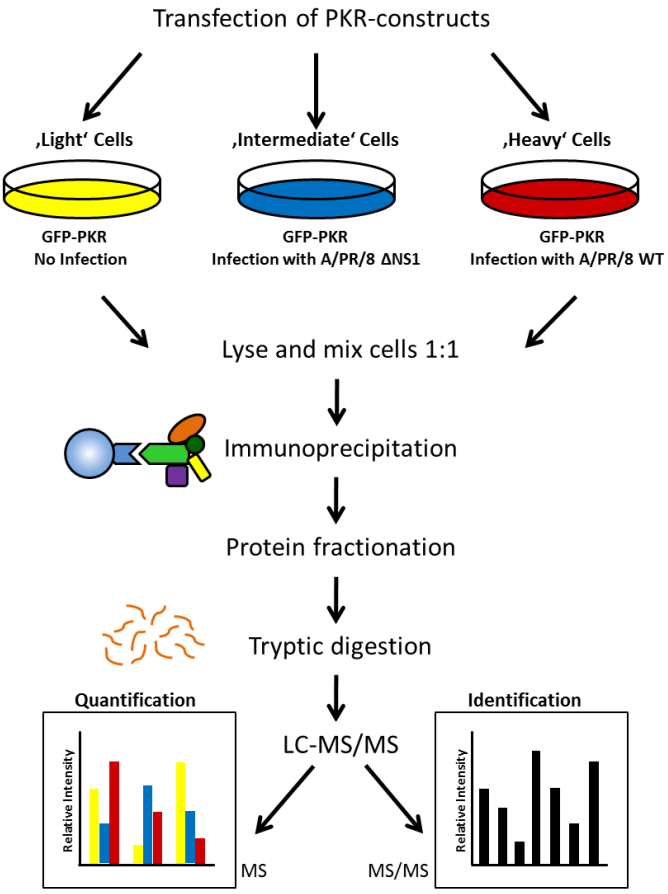

Figure 4.2. Workflow of SILAC experiments. 293T cells were labelled by cultivation in medium containing light (R0K0), intermediate (R6K4) or heavy (R10K8) amino acid isotopes of lysine and arginine. Cells were transfected with a GFP-PKR construct and either mock infected or infected with A/PR/8 WT or ΔNS1 virus. After cell lysis, same amounts of proteins were mixed and affinity-precipitated with GFP-Trap® matrix. The eluted proteins were fractionated and digested with trypsin. The resulting peptide solution was analysed using an LTQ-Orbitrap.

293T cells were cultured in medium containing light (R0K0), intermediate (R6K4) or heavy (R10K8) labelled amino acid isotopes of lysine and arginine. Cells were transfected with pEGFP-C1-PKR for 30 h and either mock infected (light state) or infected with influenza

A/PR/8 WT or ΔNS1 virus (intermediate or heavy state) at an MOI of 1.5. At 16 h p.i., cells were lysed and the protein concentration was determined by BCA assay. Equal amounts of protein lysates from light, intermediate and heavy cells were mixed and GFP-PKR was immunoprecipitated with GFP-Trap® matrix. Samples of whole cell lysates (WCL) from the three different states, non-bound (NB) and eluted proteins (IP) were analysed by SDS PAGE and immunoblotting to confirm specific precipitation of GFP-PKR, as can be examplarily seen in figure 4.3.

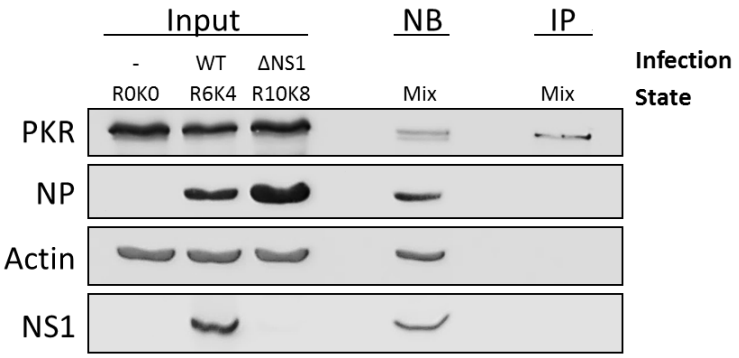

Figure 4.3. Precipitation of GFP-PKR for SILAC experiments. Cell lysates of light (R0K0), intermediate (R6K4) and heavy (R10K8) labelled 293T cells infected with A/PR/8 WT virus, ΔNS1 virus or mock infected were mixed before precipitating GFP-PKR and binding partners with GFP-Trap® matrix. Samples of cell lysates (Input), non bound (NB) and eluted proteins (IP) were analysed by SDS PAGE and immunoblotting to confirm specific precipitation of GFP-PKR. Representative experiment of N = 4.

Eluted proteins were concentrated by ultrafiltration, followed by reduction of disulfide bonds by β-mercaptoethanol (ME) treatment and alkylation with 2-iodoacetamide (IAA). Proteins were separated by one dimensional SDS PAGE and visualised by Coomassie staining. The resulting gel lane with the separated proteins was cut into ten slices, followed by in-gel-digestion with trypsin. Samples were separated by high pressure liquid chromatography (HPLC) and analysed with a LTQ Orbitrap Discovery™ mass spectrometer as described in section 3.6.6.

In total, four SILAC experiments were conducted. In two replicates the intermediate and heavy state were switched, meaning intermediate labelled cells were infected with A/PR/8 WT virus and heavy labelled cells were infected with /A/PR/8 ΔNS1 mutant virus. Changing of the states in replicate experiments is recommended to exclude systematical errors from different cell growth properties or introduction of protein contaminants from SILAC media.

4.1.2 Protein classification and network analysis

In four SILAC experiments, over 140 proteins bound to PKR after Influenza A/PR/8 WT infection and more than 120 proteins interacting with PKR after ΔNS1 mutant virus infection were detected. To extract the proteins with the highest biological relevance and to exclude contaminants, the obtained data was systematically analysed. Hereby, all PKR interacting

proteins were further classified and had to satisfy the following three criteria: The protein was found in two or more experiments, the average protein score was higher or equal to a value of 10 and the heavy to light (HL) or medium to light (ML) ratio in one or more experiments was higher than 1.5.

The protein score is a way to classify the quality of identified proteins from the input data. It is the sum of the scores of the individual peptides and represents the possibility of identifying a protein from the measured peptide ions. The HL and ML ratio refers to the proportion of identified peptides with heavy or intermediate labelling divided by the amount of light labelled peptides. It shows to which extent a PKR interacting protein is enriched in cells after viral infection. That means, a protein with a HL or ML ratio of 1 is equally bound to PKR in non-infected and infected cells. A HL or ML ratio of 2 defines that a protein was found bound to PKR twice as much in cells infected with WT or ΔNS1 mutant virus compared to non-infected cells. The maximum ratio of HL or ML peptide ions was set to 100 according to the manufacturer's instructions. Possible contaminants, for example proteins known to bind to GFP-Trap® matrix or sepharose, proteins from ribosomal subunits and hnRNP proteins were excluded from the list [205].

Gene name	**Description**	**Score**	**Ratio WT/ mock**	**Ratio ΔNS1/ mock**
CBS	Cystathionine beta-synthase	15.32	100.00	100.00
DDX5	Probable ATP-dependent RNA helicase DDX5	15.03	100.00	7.23
KPNA2	Importin subunit alpha-1	12.16	100.00	3.59
CD2BP2	CD2 antigen cytoplasmic tail-binding protein 2	10.91	100.00	2.05
SKIV2L2	Superkiller viralicidic activity 2-like 2	10.31	100.00	1.00
DDB1	DNA damage-binding protein 1	10.30	100.00	3.58
GRSF1	G-rich sequence factor 1	14.49	51.07	2.12
EIF6	Eukaryotic translation initiation factor 6	11.37	50.99	6.61
EXOSC2	Exosome complex component RRP4	40.61	50.92	6.49
EIF2S1	Eukaryotic translation initiation factor 2 subunit 1	27.03	50.90	2.64
EXOSC7	Exosome complex component RRP42	23.13	50.87	51.33
SRSF1	Serine/ arginine-rich splicing factor 1	11.98	50.87	8.59
SRSF7	Serine/ arginine-rich splicing factor 7	11.90	50.85	100.00

Gene name	Description	Score	Ratio WT/ Mock	Ratio ΔNS1/ Mock
SFPQ	Splicing factor, proline- and glutamine-rich	17.91	50.84	51.23
EXOSC6	Exosome complex component MTR3	18.36	50.81	6.03
GRWD1	Glutamate-rich WD repeat-containing protein 1	26.26	50.80	6.34
EXOSC5	Exosome complex component RRP46	12.48	48.32	4.68
HDAC6	Histone deacetylase 6	13.68	34.72	3.22
YWHAH	14-3-3 protein eta	62.97	10.35	9.92
PRKCSH	Glucosidase 2 subunit beta	21.19	7.61	7.73
MYBBP1A	Myb-binding protein 1A	20.46	5.48	1.00
PWP1	Periodic tryptophan protein 1 homolog	11.99	5.21	3.89
HSP90AA1	Heat shock protein HSP 90-alpha	39.25	3.85	5.06
SRSF5	Serine/ arginine-rich splicing factor 5	20.49	2.01	1.39
EZR	Ezrin	60.50	1.93	5.50
ACTB	Actin, cytoplasmic 1	40.84	1.86	2.62
ISOC2	Isochorismatase domain containing protein 2, mitochondrial	14.17	1.83	2.36
EEF1A1	Elongation factor 1-alpha 1	36.49	1.70	1.92
MSN	Moesin	35.80	1.69	6.39
TUBB	Tubulin beta chain	53.01	1.64	2.26
PRMT1	Protein arginine N-methyltransferase 1	18.99	1.64	2.74
RDX	Radixin	33.12	1.64	4.45
DECR1	2.4-dienoyl-CoA reductase, mitochondrial	37.97	1.54	0.49
EIF2AK2	Interferon-induced, double-stranded RNA-activated protein kinase	603.93	0.77	0.65
HSPA9	Stress-70 protein, mitochondrial	161.96	1.00	6.51
HSPA1A	Heat shock 70 kDa protein 1A/1B	148.94	1.00	6.45

Gene name	Description	Score	Ratio WT/ Mock	Ratio ΔNS1/ Mock
HSPA5	78 kDa glucose-regulated protein	130.76	1.50	3.82
DHX9	ATP-dependent RNA helicase A	47.08	1.00	4.70
HSP90AB1	Heat shock protein HSP 90-beta	45.98	1.00	100.00
CCT8	T-complex protein 1 subunit theta	20.86	1.00	10.60
PPP2R1A	Serine/ threonine protein phosphatase 2A 65 kDa regulatory subunit A alpha isoform	19.40	1.00	7.23
KSRP	Far upstream element-binding protein 2	17.04	1.00	4.84
IGF2BP1	Insulin-like growth factor 2 mRNA-binding protein 1	16.82	1.00	7.33
HPRT1	Hypoxanthine-guanine phosphoribosyltransferase	15.32	1.00	9.93
VIM	Vimentin	15.15	1.00	3.98
LRRC59	Leucine-rich repeat-containing protein 59	13.26	1.00	100.00
C7orf50	Uncharacterised protein C7orf50	12.37	0.95	2.23
C14orf166	UPF0568 protein C14orf166	10.89	0.87	52.77

Table 4.1. List of PKR binding partners after influenza A/PR/8 WT and ΔNS1 virus infection. List comprised of PKR interacting proteins from four individual SILAC experiments matching the following criteria: Protein found in two or more experiments, protein score ≥ 10, HL or ML ratio > 1.5. Table shows gene name of PKR binding partner, protein description, average score (of the experiments where protein was found) and average ratio of WT or ΔNS1 to mock (of the experiments where HL or ML ratio > 1.5; average ratio of other state from corresponding HL or ML ratios is shown in light grey, respectively). List is ordered by decreasing values of average ratio WT/ Mock. Average ratio for PKR (highlighted in yellow) was calculated from all four experiments. For detailed values of single experiments, see chapter 7.

After systematic analysis, a list of 47 proteins identified as specific PKR interaction partners after influenza A virus infection was obtained (table 4.1). By subjecting the proteins from table 4.1 to gene ontology (GO) term analysis with the "Protein Analysis Through Evolutionary Relationships (PANTHER)" classification system online tool, common features of the PKR binding proteins are revealed (figure 4.4) [208]. 60 % of all PKR interaction partners derived from influenza virus infected cells have catalytic or binding activity (figure 4.4 A). The binding function can further be subclassified, which reveals that especially proteins with RNA binding function were detected (data not shown). This is not surprising, since PKR is an RNA-binding protein itself and protein-protein-interactions could be mediated via binding of RNA. The classification of PKR binding partners according to biological processes shows that over 50 %

of the detected proteins belong to the categories cellular and metabolic process (figure 4.4 B). Interestingly, 6 % of the PKR interaction partners are involved in the regulation of immune system processes and 4 % play a role in apoptosis. These are also two main activities PKR contributes to after virus infection.

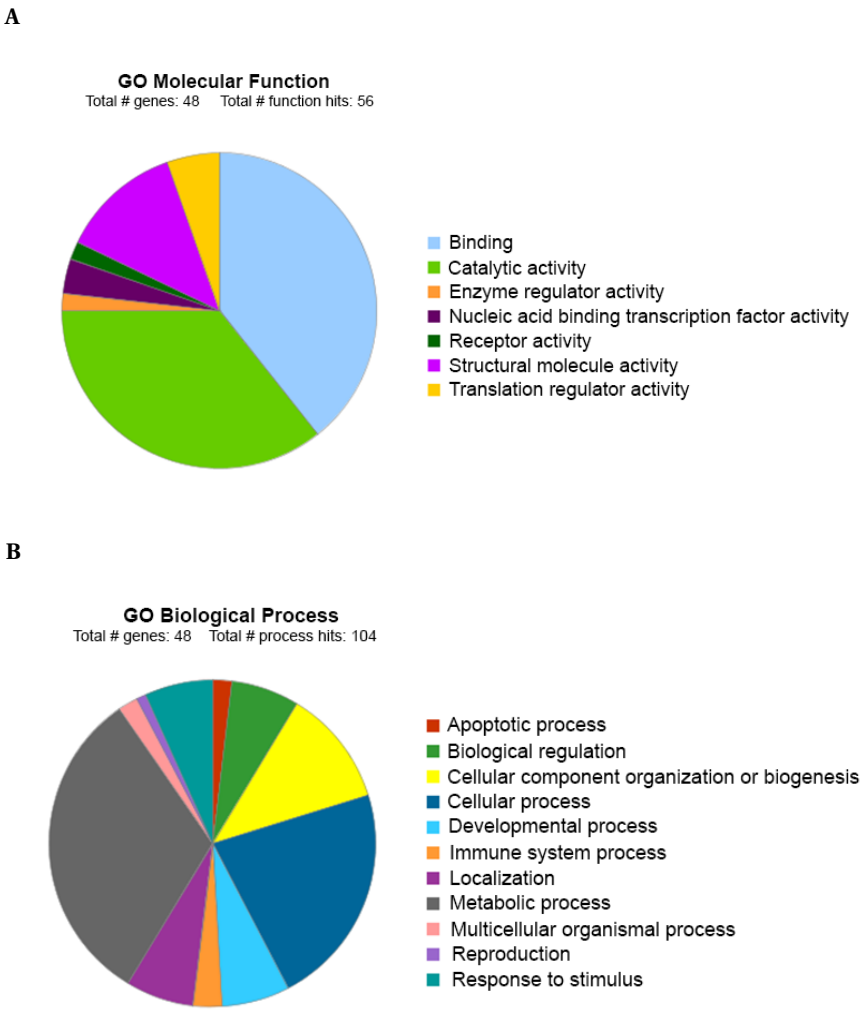

Figure 4.4. PANTHER GO term analysis of PKR bound proteins after virus infection. PANTHER gene list analysis of PKR interacting proteins from table 4.1 according to **A** their molecular functions, **B** the biological process they are involved in. Adapted from [208].

To visualise the relations between PKR and its interaction partners in greater detail, a "Search Tool for the Retrieval of Interacting Genes/ Proteins (STRING)" database network analysis was conducted and the generated network was clustered (Markov Cluster algorithm (MCL) = 2) for better visualisation of protein relations (figure 4.5). STRING is a biological meta-database of known and predicted protein-protein interactions. It contains information from numerous sources, e.g. Biological General Repository for Interaction Datasets (BioGRID), Kyoto Encyclopedia of Genes and Genomes (KEGG), Reactome, Molecular Interaction Database (MINT) or GO and combines experimental data, computational prediction methods and public text collections to create protein interaction networks [209].

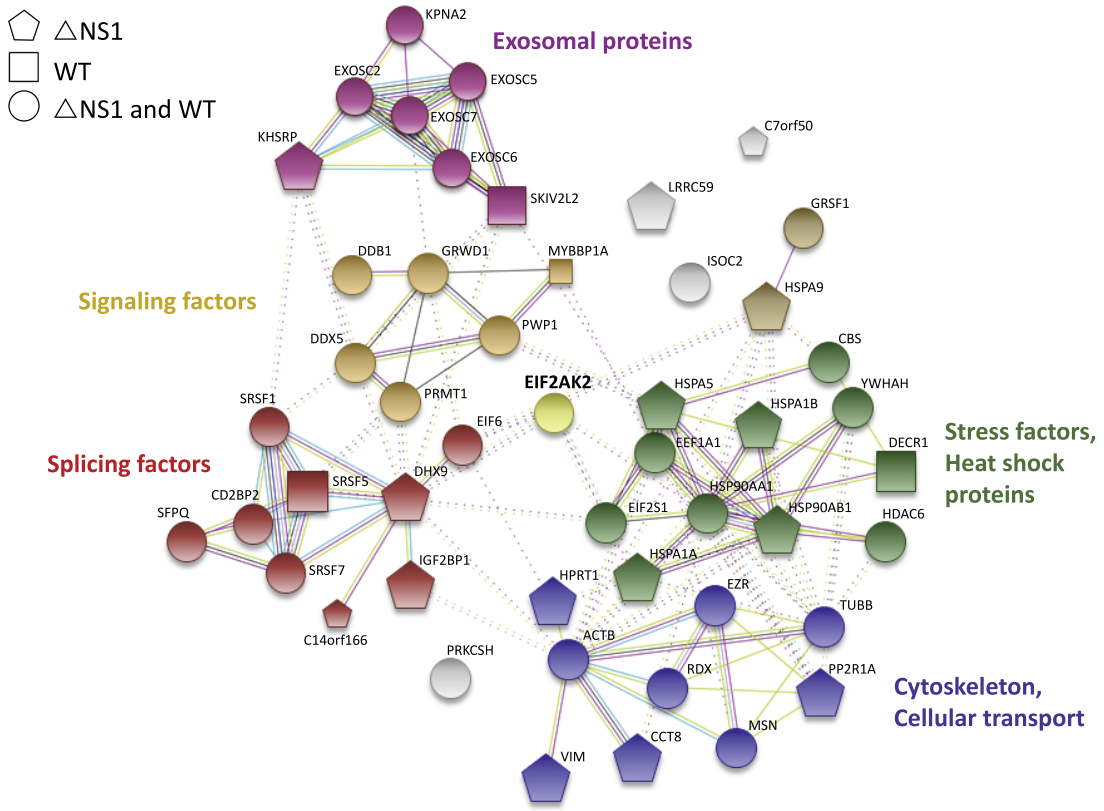

Figure 4.5. STRING network analysis of PKR interacting partners after influenza virus infection. STRING database analysis of GFP-PKR interacting proteins from table 4.1. STRING network was clustered (MCL = 2) to visualise protein relations. Line colours indicate: red = gene fusion evidence; green = neighbourhood evidence; blue = coocurrence evidence; purple = experimental evidence; yellow = textmining evidence; light blue = database evidence; black = coexpression evidence. Symbols indicate: Square = PKR binding partner only after influenza A WT infection; pentagon = PKR binding partner only after influenza A ΔNS1 infection; circle = PKR binding partner after influenza A WT and ΔNS1 infection. Adapted from [210].

The STRING network, generated with PKR interactors from table 4.1 and PKR ("EIF2AK2", yellow circle), consists of several protein clusters associated with different biological functions (figure 4.5). Protein clusters include signalling factors (orange) and cellular stress factors (green), which among others contain proteins that are known to play a role in cellular antiviral immunity, as for example heat shock protein 90 β (HSP90β) or DNA damage binding protein 1 (DDB1) [211–213]. Protein clusters of the STRING network are reflected in categories of the PANTHER analysis, for example signalling factors belong to the "response to stimulus"-category (figure 4.4 B). Please note that the identified proteins can contribute to multiple categories of the PANTHER analysis, e.g. cellular stress factors can be assigned to the "biological regulation", "cellular process" and "metabolic process"-category among others. Interestingly, the STRING network analysis also reveals a cluster with mRNA splicing factors (red) and exosomal proteins (purple). The exosomal protein cluster contains four specific exosome complex components and three associated proteins. So far, no correlation between PKR and the intracellular exosome complex has been observed, underlining the impact of MS based interactome studies to find novel interaction partners.

Most of the detected proteins from table 4.1 showed enriched binding to PKR after both WT

and ΔNS1 infection (circle symbol) whereas only a minority of detected proteins specifically interacted with PKR after either WT (square symbol) or ΔNS1 infection (pentagon symbol). This finding was rather unexpected, since the influence of the viral NS1 protein on the composition of the PKR interactome was thought to be bigger. Nevertheless, all factors are of great interest to deepen our understanding of cellular PKR regulatory processes.

4.1.3 Data validation

To support the relevance of factors identified to associate with PKR, exemplary candidates from the screen were validated by coprecipitation analyses of transfected GFP-PKR with the endogenous cellular proteins. Candidate proteins were chosen in a hypothesis driven process based on their molecular functions and reagents availability. Candidate proteins for analysis were HSP90β, insulin-like growth factor 2 mRNA-binding protein 1 (IGF2BP1), exosome complex component RRP42 (ExoSC7) and exosome complex component RRP46 (ExoSC5). HSP90β was chosen, because it is a known interactor of PKR [214]. IGF2BP1 was selected for coprecipitation assays as it has no described interaction with PKR, but both proteins share a set of common features, e.g. RNA-binding and recruitment to aSGs upon cellular stress [120, 215]. ExoSC5 and ExoSC7 are components of the catalytically inactive exosome core which has a pivotal role in binding and presentation of RNA. The exosomal core provides the scaffold for the association of the exosomal proteins with the catalytic subunits and other accessory proteins [216]. It is known that the nuclear exosome can associate with different RNA binding proteins, but so far, involvement of PKR in exosomal mRNA degration or interaction of PKR and exosomal proteins has not been shown [217].

For the coprecipitation analysis, 293T cells were transfected with pEGFP-C1-PKR and either mock-treated or infected with influenza A/PR/8 WT or ΔNS1 mutant virus, followed by precipitation of GFP-PKR with GFP-Trap® matrix. The experimental conditions were chosen according to the conditions of the mass spectrometric screen.

Coprecipitation analysis confirmed the interaction of PKR with HSP90β, IGF2BP1, ExoSC7 and ExoSC5 (figure 4.6). IGF2BP1 and the cellular exosome components ExoSC5 and ExoSC7 were evidently identified as novel binding partners of PKR in the SILAC based MS analysis.

On closer examination, quantitative differences of the PKR binding capacity between the mass spectrometric screen and the coprecipitation analysis occured. Whereas HSP90β and IGF2BP1 were distinctively detected as PKR interactors after influenza A ΔNS1 infection in the mass spectrometric screen, both proteins were found to coprecipitate with PKR also after WT infection. Moreover, the tested proteins, with the exception of HSP90β, coprecipitated with PKR in non-infected cells to comparable amounts as in infected cells, whereas the systematic analysis of the mass spectrometric results preferentially included factors with enriched binding to PKR after viral infection. These differences could result from table 4.1 depicting the average values of four independent mass spectrometry experiments. Comparison of values from each individual SILAC experiment shows variation for the interaction of PKR

and identified binding partners between the experimental replicates, which were reflected in the coprecipitation analysis shown in figure 4.6 (for comparison, see supplementary tables 7.2 to 7.5 with detailed results for all single mass spectrometric experiments).

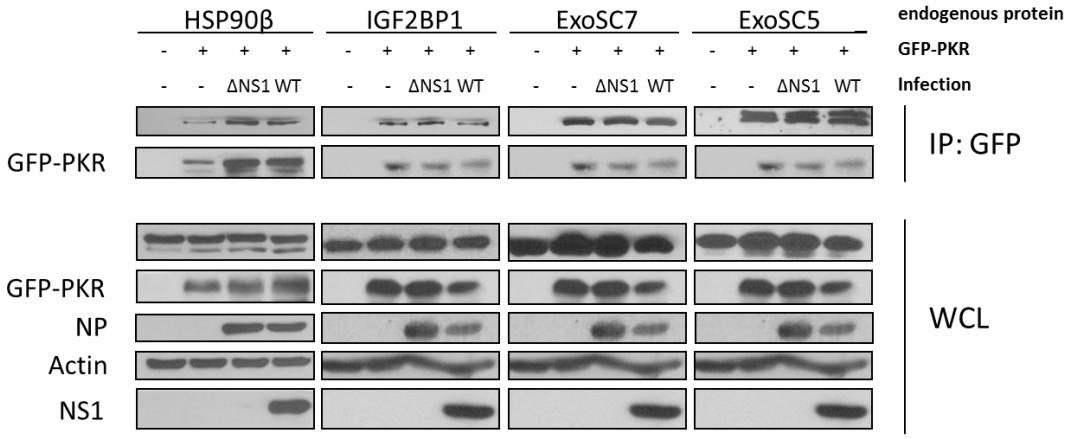

Figure 4.6. Validation of exemplary known and novel PKR binding partners. 293T cells were transfected with pEGFP-C1-PKR or plasmid vector pcDNA and infected with influenza A/PR/8 WT virus, ΔNS1 mutant virus or mock-treated. 16 h p.i., cells were lysed and GFP-PKR was precipitated using GFP-Trap® matrix. Bound proteins (IP) and cell lysates (WCL) were analysed by SDS PAGE and immunoblotting using the indicated antibodies. Representative experiment from $N \geq 3$.

Since the interaction between PKR and exemplary binding partners from table 4.1 could be confirmed in general, the biological impact of identified proteins on the catalytic activity of PKR was examined by testing their influence on PKR phosphorylation in non-infected and virus infected cells. Therefore, plasmids for overexpression of candidate proteins were transfected into 293T cells. Then, cells were mock-treated or infected with influenza A/PR/8 WT or ΔNS1 virus and levels of phosphorylated endogenous PKR were determined by SDS PAGE and immunoblot analysis. The amounts of pPKR were expected to reflect the activation status of PKR. Infection with influenza ΔNS1 virus provided an internal reference value, because the mutant virus is a potent activator of PKR and leads to expression of high pPKR levels independent of the transfected expression plasmid.

In total, 18 proteins from table 4.1 with different molecular functions were selected for the analysis in a hypothesis driven process. The pool of candidates was comprised of proteins from all clusters of the STRING network (figure 4.5) and included proteins bound to PKR after influenza A WT and ΔNS1 virus infection as well as interaction partners exclusively bound after either WT or ΔNS1 virus infection. Additionally, the empty pcDNA3.1 plasmid backbone was transfected as negative control and PACT overexpression was used as positve control. PACT is a known protein activator of PKR and is able to lead to PKR phosphorylation in absence of RNA binding [115].

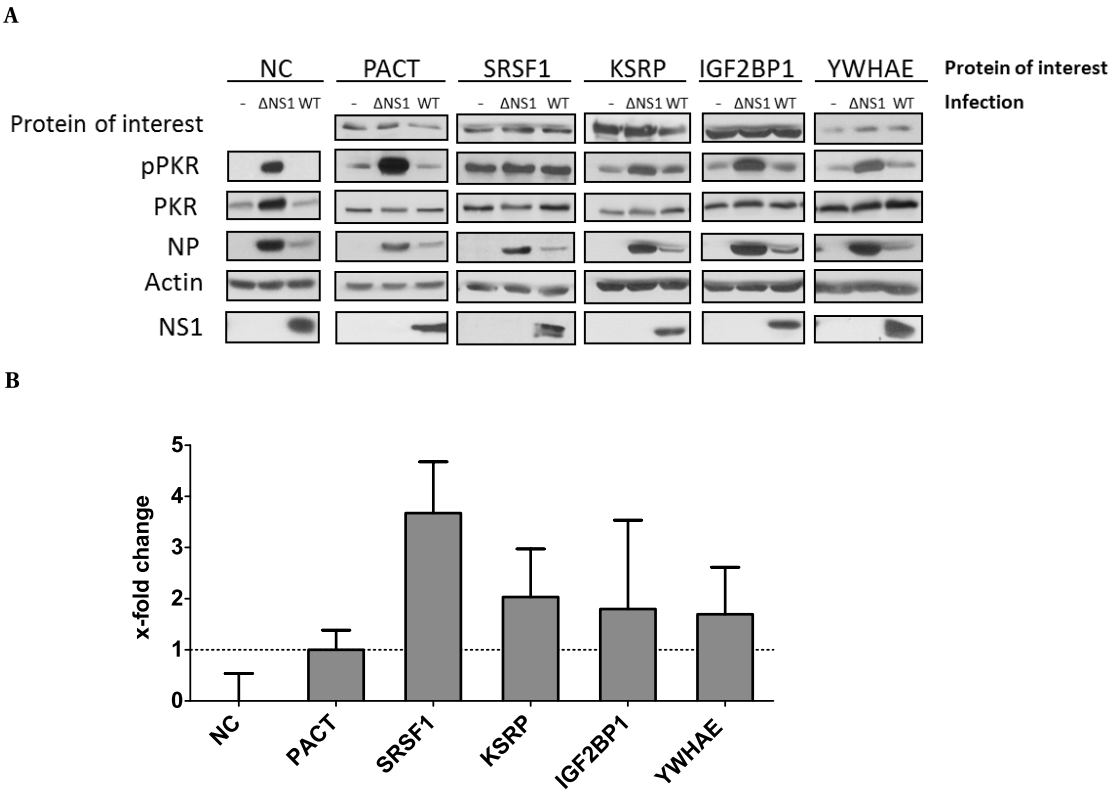

Figure 4.7. Overexpression of four identified PKR interaction partners induces phosphorylation of endogenous PKR. A 293T cells were transfected with pEGFP-SRSF1, pEGFP-KSRP, pcDNA-Flag-IGF2BP1, pcDNA-HA-YWHAE, pcDNA-Myc-PACT or pcDNA3.1 plasmid vector as negative control (NC) and infected with influenza A/PR/8 WT virus, ΔNS1 virus or mock-treated. 16 h p.i., cells were lysed and analysed by SDS PAGE and immunoblotting using tag-specific or the indicated antibodies. Representative experiment of N = 4. **B** pPKR bands of the non-infected state of two or more experiments were quantified using LabImage1D software and normalised on actin levels. Values represent mean x-fold change +SEM of band intensities compared to NC (corresponding empty vector) with x-fold change of positive control PACT set to 1.

It can be seen in figure 4.7 A that overexpression of the known PKR regulator PACT resulted in phosphorylation of PKR in unstimulated cells, which confirmed results shown before in the literature [115]. From the 18 tested proteins identified in the mass spectrometric analysis of this thesis, four candidates were able to induce phosphorylation of endogenous PKR in non-infected and influenza A WT virus infected cells: SRSF1, KSRP, IGF2BP1 and 14-3-3 protein epsilon (YWHAE) (figure 4.7 A) The other 14 tested proteins did not have a reproducible impact on PKR phosphorylation (see figure 7.1 in the appendix for detailed results). Quantification of results from two or more experiments revealed that SRSF1, KSRP, IGF2BP1 and YWHAE overexpression led to even stronger induction of pPKR in comparison to the known PKR activator PACT (figure 4.7 B). SRSF1 overexpression induced phosphorylation of PKR four times stronger than PACT transfection and KSRP, IGF2BP1 and YWHAE expression still caused a two-fold increase of PKR activation in non-infected cells compared to PACT (figure 4.7 B).

Taken together, a quantitative MS analysis was performed to investigate the interactome of PKR in influenza A virus infected cells. A triplex SILAC approach was employed to compare

the PKR interactome of non-infected cells, influenza A WT infected cells and cells infected with an NS1 deletion mutant virus. After systematic analysis of four individual replicates, a list of 47 proteins preferentially interacting with PKR after influenza virus infection was retrieved. The interaction between PKR and four exemplary binding partners was validated in coprecipitation assays. Biological impact of 18 candidate proteins on PKR activation was examined in non-infected and influenza virus infected cells in transfection-based assays. Hereby, overexpression of the four proteins SRSF1, KSRP, IGF2BP1and YWHAE strongly induced phosphorylation of PKR in non-infected and influenza WT infected cells. Since the phosphorylation status of PKR is thought to reflect its catalytic activity, these proteins could be novel regulators of PKR in the context of influenza virus infections.

4.2 Characterisation of the role of KSRP in regulating PKR activity

The SILAC-based MS approach resulted in the determination of the PKR interactome in influenza A virus infected cells. After validation of exemplary binding partners, a target interactor for further analysis was chosen according to the impact of the protein on PKR activity (figure 4.7). Please note that even if it had the strongest effect on PKR phosphorylation, SRSF1 was not considered for additional analyses, because previous studies in our group showed that SRSF1 knockdown had no effect on influenza A virus replication [218, p.115-119]. One of the most interesting proteins of all protein interactors was the KH type-splicing regulatory protein (KSRP). Mass spectrometric analysis found KSRP as PKR binding partner after ΔNS1 mutant virus infection (table 4.1) and KSRP overexpression had a strong influence on PKR activation in non-infected and influenza WT virus infected cells (figure 4.7).

KSRP is an RNA binding protein which is involved in gene expression, miRNA maturation and mRNA degradation [85]. It typically binds mRNAs with a short half-life, e.g. cytokine transcripts encoding for different forms of type I IFN, which then leads to the recruitment of the exosomal mRNA degradation machinery [77, 84]. This is reflected in KSRP being found in the exosomal protein cluster of the STRING network analysis (figure 4.5).

In this thesis, the effect of KSRP on PKR activity was further analysed. Binding of both proteins was confirmed for overexpessed and endogenous proteins and the interaction was examined more in detail by employing PKR mutants. Moreover the effects of KSRP knockdown on PKR activity and IFN expression in human cells after influenza A virus infection were analysed. Finally, an effect of KSRP knockdown on viral replication was confirmed.

4.2.1 KSRP overexpression facilitates activation of PKR in non-infected cells

It could be shown before that KSRP overexpression induced PKR phosphorylation (see figure 4.7 in section 4.1.3). This effect was reproduced in a dose-dependent manner in

non-stimulated cells by transfection of increasing amounts of either KSRP or PACT, which is a known regulator of PKR catalytic activity. In figure 4.8, it can be seen that both PACT and KSRP overexpression induced PKR phosphorylation in a dose-dependent manner in comparison to the negative controls transfected with similar amounts of empty vector.

For the experiment, plasmids for overexpression of PACT, KSRP or the empty plasmid vectors pcDNA or pEGFP as negative controls were transfected into 293T cells in different amounts, followed by detection of the pPKR levels by SDS PAGE and immunoblot analysis.

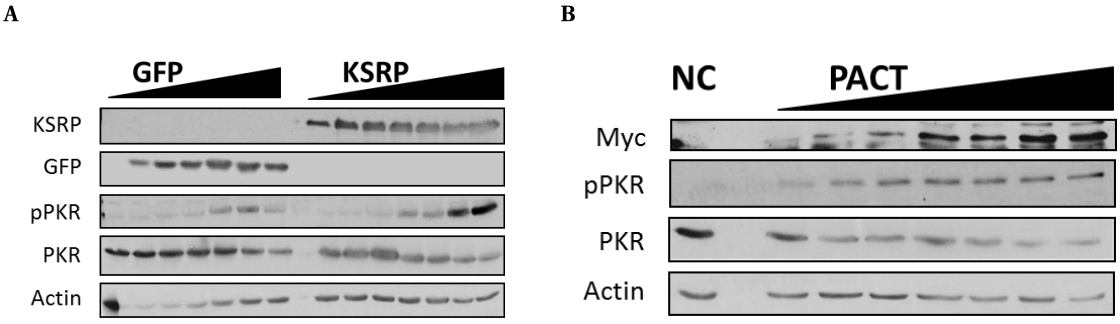

Figure 4.8. Overexpression of PACT or KSRP induces phosphorylation of endogenous PKR in a dose-dependent manner. A 293T cells were transfected with increasing amounts of pEGFP-KSRP or plasmid vector pEGFP as control. 46 h p.t., cells were lysed and levels of phosphorylated PKR were analysed by SDS PAGE and immunoblotting using the indicated antibodies. **B** 293T cells were transfected with increasing amounts of pcDNA-Myc-PACT or plasmid vector pcDNA3.1 as negative control (NC). 46 h p.t., cells were lysed and pPKR levels were analysed by SDS PAGE and immunoblotting using the indicated antibodies. Representative experiment of N = 5.

4.2.2 PKR and KSRP bind in a constitutive manner in non-infected and infected cells

To confirm the results from the MS analysis, binding of PKR and KSRP was examined in human embryonic kidney cells (293T) by coprecipitation analysis employing a pEGFP-C1-KSRP construct (figure 4.9 A) or precipitation of endogenous proteins in human lung epithelial cells (A549) respectively (figure 4.9 B). For the endogenous coprecipitation assay, PKR was immunoprecipitated with α-PKR antibody coupled to protein G agarose beads (see section 3.4.5). Beads coupled with α-Myc antibody were used as negative control to exclude non-specific interactions with the matrix. In this experiment, an influenza A/PR/8 derived mutant virus bearing an R46A mutation in the viral NS1 protein was employed in addition to WT and ΔNS1 virus infection. The NS1 protein of this mutant virus cannot bind dsRNA and is not able to inhibit PKR activation (see section 1.3.1 for detailed description). It was used as an additional control for a PKR-activating virus that, in contrast to the ΔNS1 virus, is able to express an NS1 protein.

Interaction of GFP-KSRP and PKR was confirmed in both experimental setups. Hereby, interaction of KSRP and PKR was found to be constitutive. This finding was inconsistent with the results of the mass spectrometric analysis shown in table 4.1, where KSRP seemed to bind to PKR preferentially after influenza ΔNS1 mutant virus infection. Close examination

of the results obtained in the single mass spectrometric experiments however showed that stronger binding of KSRP to PKR after influenza ΔNS1 infection was seen only in one replicate, whereas a constitutive interaction of KSRP and PKR was detected in another.

A distinctive feature of the precipitation analysis conducted by overexpression of GFP-KSRP in 293T cells was the reduced interaction of GFP-KSRP and PKR in influenza A WT infected cells. Additionally, with this experimental setup coprecipitation of the viral NP could be observed (figure 4.9 A).

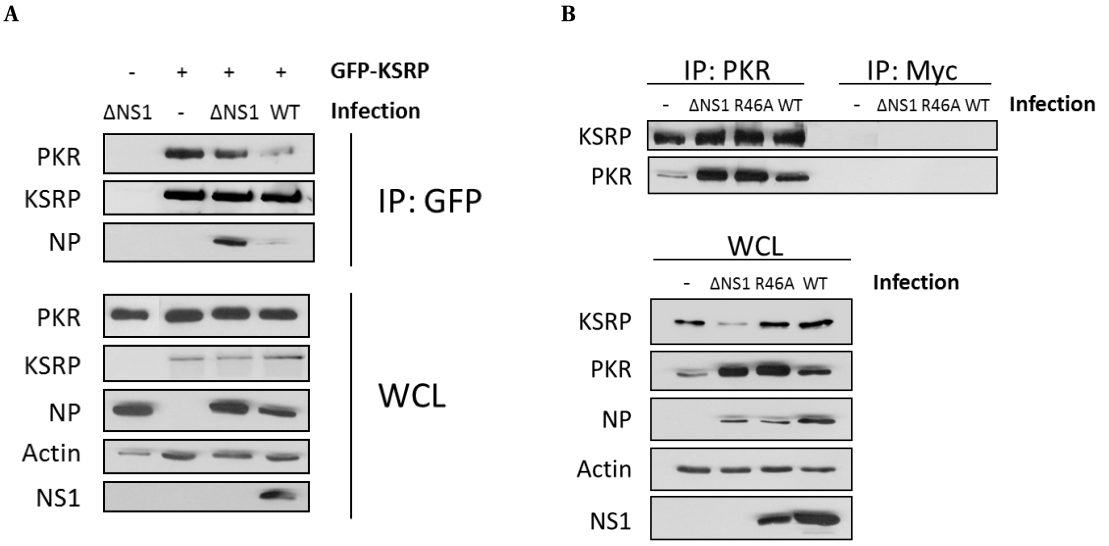

Figure 4.9. KSRP and PKR interact constitutively. A 293T cells were transfected with pEGFP-KSRP or pcDNA plasmid vector as negative control and infected with influenza A/PR/8 WT virus, ΔNS1 virus or non-infected. 16 h p.i., cells were lysed and GFP-KSRP was precipitated using GFP-Trap® matrix. Bound proteins (IP) and cell lysates (WCL) were analysed by SDS PAGE and immunoblotting using the indicated antibodies. Representative experiment of N = 2. **B** A549 cells were infected with influenza A/PR/8 WT virus, R46A mutant virus, ΔNS1 mutant virus or non-infected. 16 h p.i., cells were lysed and PKR was immunoprecipitated using α-PKR antibody. α-Myc antibody was used as negative control. Bound proteins (IP) and cell lysates (WCL) were analysed by SDS PAGE and immunoblotting using the indicated antibodies. Representative experiment of N = 5.

4.2.3 Binding of PKR and KSRP requires PKR N-terminal domain but not PKR kinase or dsRNA-binding activity

To determine the protein domains of PKR involved in the interaction with KSRP, coprecipitation experiments with PKR mutants were conducted. PKR consists of two major functional domains: The RBD consisting of two RBMs (aa 9-77 and 100-167) and the kinase domain with the serine/ threonine kinase (aa 267-538), which are seperated by an interdomain-linker (aa 168-266) [100]. In addition to domain deletion mutants, two PKR loss-of-function mutants with single point mutations were employed. A mutation at position 296 from lysine to arginine results in the loss of kinase activity as ATP cannot be bound and phosphotransfer to downstream proteins is inhibited [105]. Mutation of the lysine at position 60 in the dsRNA binding domain to an alanine leads to loss of dsRNA binding function, hereby preventing PKR activation by RNA but retaining the ability to be activated by artificial stimuli like heparin

[109]. By employing the WT PKR protein and the four PKR mutants, which are schematically shown in figure 4.10 A, the binding of PKR and KSRP was characterised in non-infected and infected cells. Therefore, GFP-KSRP and V5-PKR WT or mutants were co-expressed in 293T cells, followed by infection with influenza A WT or ΔNS1 virus and coprecipitation of GFP-KSRP with GFP-Trap® matrix (figure 4.10 B).

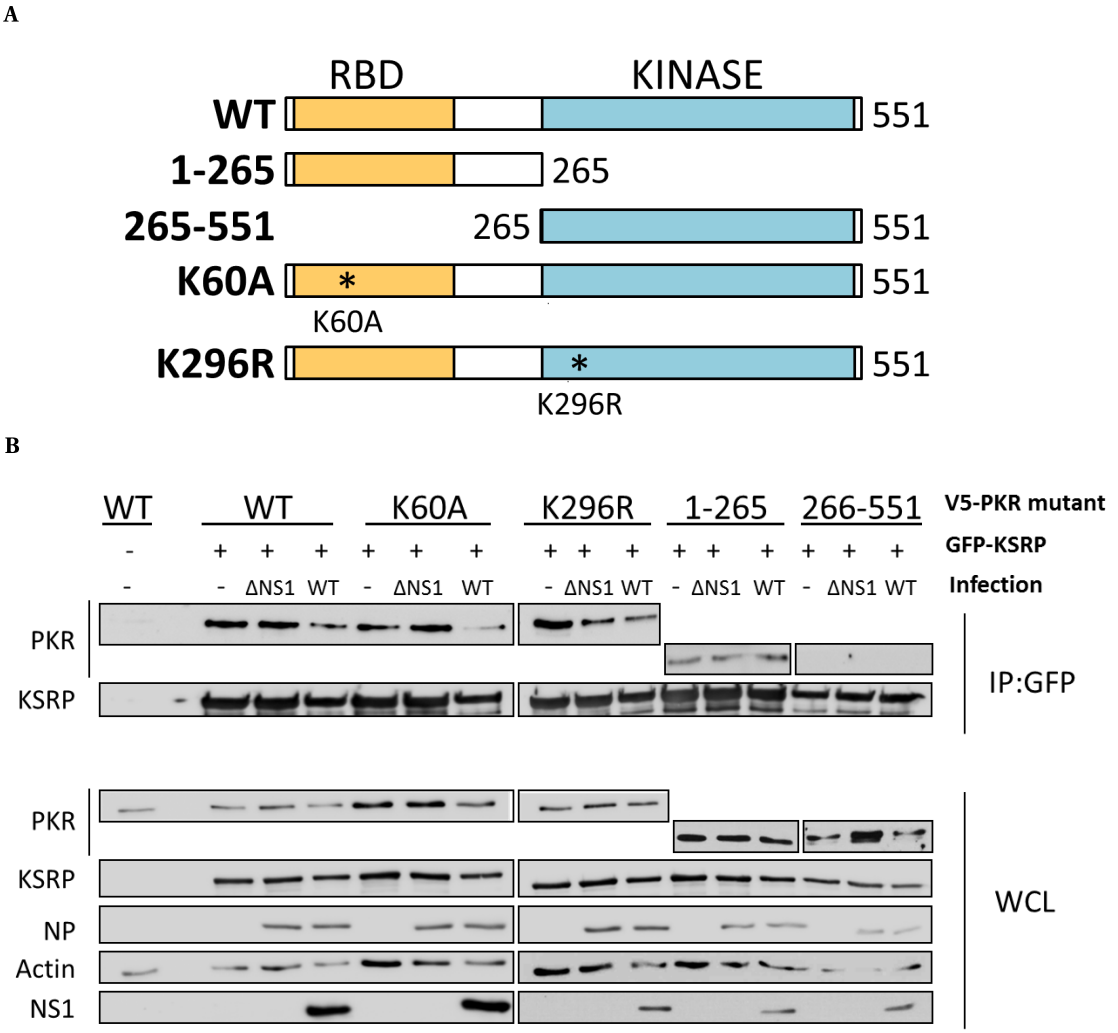

Figure 4.10. Binding of PKR and KSRP requires PKR N-terminal domain but not PKR kinase or dsRNA-binding activity. A Schematic representation of PKR WT and mutants missing either the kinase domain (1-265), the RBD (266-551) or carrying point mutations to abolish dsRNA binding function (K60A) or kinase activity (K296R). **B** 293T cells were transfected with pEGFP-KSRP or pcDNA empty vector as negative control and pcDNA-V5-PKR WT or mutants and infected with influenza A/PR/8 WT virus, ΔNS1 virus or non-infected. 16 h p.i., cells were lysed and GFP-KSRP was precipitated. Bound proteins (IP) and cell lysates (WCL) were analysed by SDS PAGE and immunoblotting with the indicated antibodies. Representative experiment of N = 3.

As seen in previous overexpression experiments, KSRP and PKR bind constitutively in non-infected and infected cells with decreased interaction of both proteins after influenza WT infection (compare figure 4.9 A). PKR mutants K60A and K296R were able to interact with KSRP at comparable levels as the WT protein, indicating that the interaction of PKR and KSRP is independent from dsRNA-binding and PKR kinase activity. Interaction could also be observed between KSRP and the PKR 1-265 mutant. The only mutant incapable of binding

to KSRP was the PKR 266-551 mutant that only consists of the C-terminal domain. This indicates, that binding of PKR and KSRP requires the PKR N-terminal domain but not PKR kinase or dsRNA-binding activity.

4.2.4 PKR and KSRP colocalise in cytoplasmatic granules in ΔNS1 mutant virus infected cells

In the next step, cellular localisation of KSRP and PKR was analysed by confocal microscopy. In the experiments of this thesis, KSRP mainly showed nuclear distribution in non-infected and infected cells (figure 4.11 A). Infection with influenza A/PR/8 ΔNS1 virus led to formation of aSGs that were visualised by staining the SG marker G3BP1. In ΔNS1 virus infected cells, KSRP was found in cytoplasmatic stress granules (SGs) as shown by colocalisation of KSRP and G3BP1 (see intensity profile of enlarged excerpts in figure 4.11 A). Infection with the influenza WT virus did not detectably influence KSRP distribution.

PKR showed diffuse staining throughout the cytosol in non-infected and influenza A WT virus infected cells with a small fraction of PKR localised in the nucleus (figure 4.11 B). Upon infection with influenza A/PR/8 ΔNS1 virus, cytoplasmatic PKR accumulated in aSGs (see intensity profiles of G3BP1 and PKR in figure 4.11 B). Infection with the influenza WT virus, which is able to inhibit PKR activation, did not have a noticeable effect on PKR localisation compared to non-infected cells.

Comparison of figure 4.11 A and B reveals that KSRP and PKR differ in their cellular distribution. Whereas KSRP was detected nearly exclusively in the nucleus in non-infected and WT infected cells, PKR was detected in the cytoplasm and to a smaller part in the nucleus of non-infected and WT infected cells. The nuclear fraction of PKR hereby would be in close proximity to the nuclear KSRP, which could facilitate the interaction of both proteins. In ΔNS1 infected cells, KSRP and PKR were additionally detected in newly formed SGs. Aggregation of both proteins in aSGs could further support their interaction, but does not seem to be the exclusive determining factor, since interaction of KSRP and PKR could also be seen in non-infected and influenza WT virus infected cells in coprecipitation assays (compare figure 4.9).

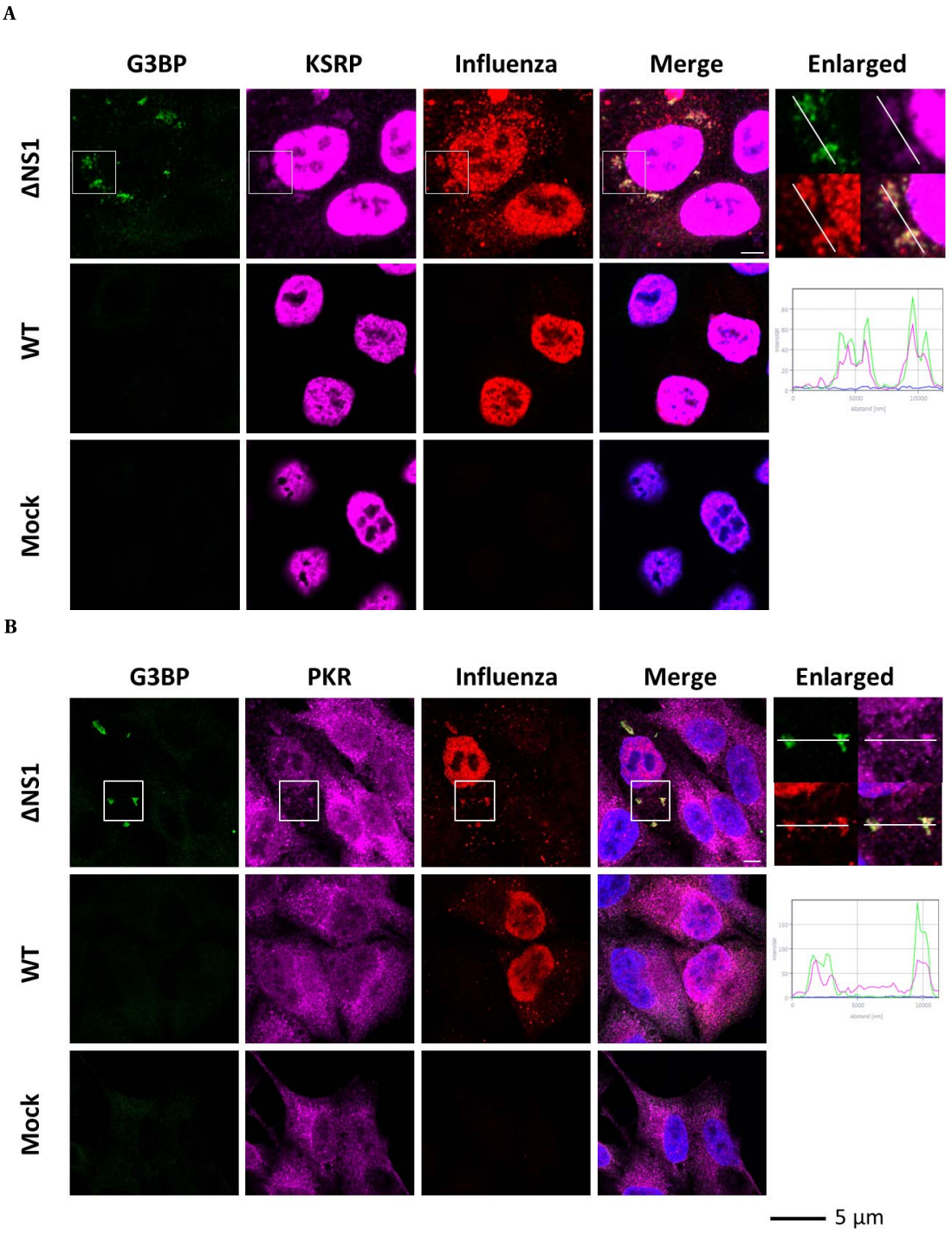

Figure 4.11. Cellular distribution of endogenous KSRP and PKR in human cells. HeLa cells were seeded on glass cover slips and infected with influenza A/PR/8 WT virus, ΔNS1 virus or mock-treated. 16 h p.i., cells were fixed, blocked, permeabilised and stained with antibodies against **A** KSRP, G3BP and influenza virion or **B** PKR, G3BP and influenza virion. Cell nuclei were visualised by DAPI staining. Samples were analysed by spectral confocal microscopy with a LSM 780 laser scanning microscope (Zeiss; objective 63). The indicated excerpts in ΔNS1 infected samples are digitally magnified (Enlarged) and the corresponding intensity profiles of the green (G3BP1) and pink (KSRP/ PKR) channel are shown. Scale bar shown in ΔNS1 pictures is equivalent to 5 µm.

4.2.5 Knockdown of KSRP impairs PKR activation and expression of ISGs

As described in section 1.2.1, KSRP can affect viral replication of different viruses in a positive or negative manner. It was shown to interfere with the viral protein translation of Enterovirus 71 by interacting with the viral internal ribosomal entry site (IRES) [93]. In contrast, it was shown to destabilise cellular antiviral cytokine transcripts which supported viral replication of HSV type 1 and VSV [86]. To further elucidate the role of KSRP in PKR mediated signalling and to determine its influence on replication of influenza A viruses, experiments with KSRP siRNA for transient knockdown (KD) of the protein were performed. Hereby two different results could be expected to occur: KSRP expression could either negatively influence viral replication of influenza A NS1 mutant viruses by supporting PKR activation (compare figures 4.7 and 4.8) or could enhance viral replication of IFN sensitive influenza mutant viruses by reducing type I IFN levels as described before in the literature [86].

First, suitable conditions for siRNA experiments had to be determined. Since the endogenous levels of PKR in human embryonic kidney cells (293T) are quite low, human lung epithelial cells (A549) with higher endogenous PKR levels were used for all following experiments. A549 cells were transfected with different amounts of KSRP-siRNA or scrambled siRNA (NT) as negative control for 24 h to 72 h. Two different species of KSRP-siRNA were tested, a single KSRP directed siRNA "#2" and an siRNA Mix consisting of four different KSRP-siRNA. It can be seen in figure 4.12 A that both tested siRNA solutions were able to diminish endogenous KSRP expression. Hereby, the siRNA Mix seemed to have a slightly stronger effect at all tested concentrations . Quantification of KSRP band intensities of three independent experiments followed by normalisation on actin levels indicated that the most prominent effect was achieved for transfection of 100 pM Mix KSRP-siRNA after 48 h, which was accordingly used for the following experiments (data not shown).

To rule out effects of the KSRP-siRNA on cell proliferation, cell viability of A549 cells transfected with KSRP-siRNA was determined with an MTT assay. KSRP-siRNA Mix and NT siRNA were compared against non-treated cells as negative control and cells treated with cytotoxic DMSO in different concentrations as positive control (figure 4.12 B). Neither KSRP-siRNA Mix nor NT siRNA had cytotoxic effects on cell viability compared to non-treated control cells at the tested experimental conditions.

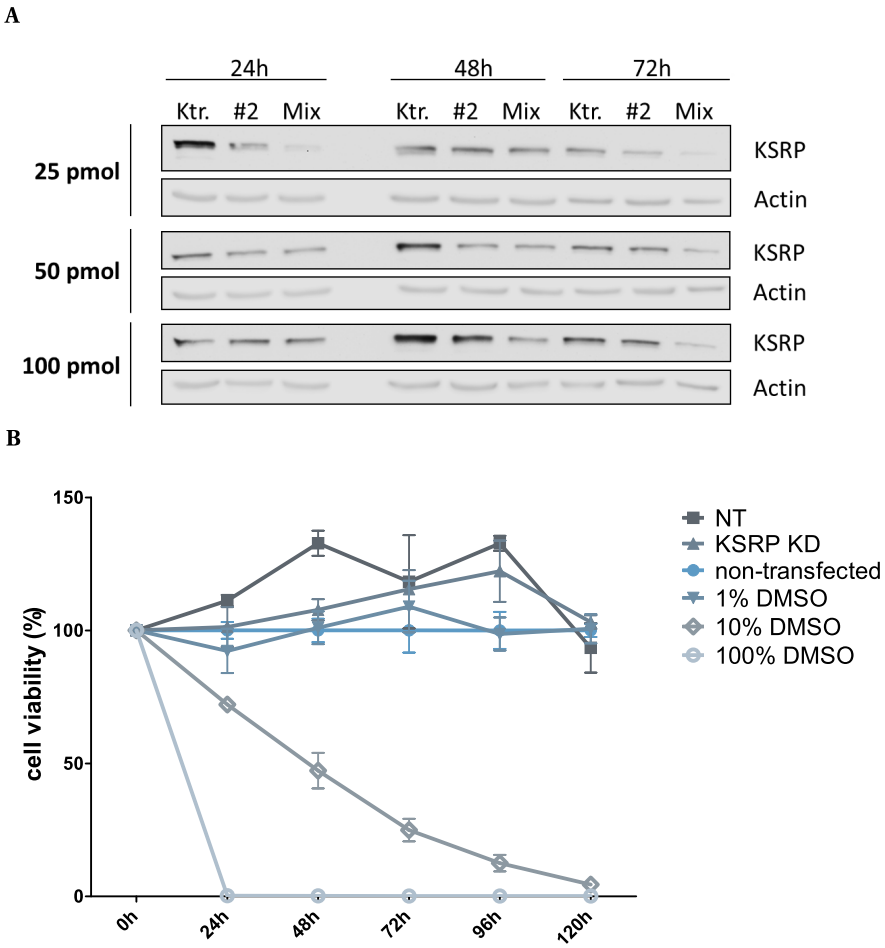

Figure 4.12. Establishment of KSRP siRNA knockdown in A549 cells. A A549 cells were transfected with 25 pM, 50 pM and 100 pM of KSRP siRNA #2, KSRP siRNA Mix or scrambled siRNA (NT) as negative control. 24 h, 48 h and 72 h p.t., cells were lysed and knockdown of endogenous KSRP was analysed by SDS PAGE and immunoblotting using the indicated antibodies. Representative result from N = 3. **B** A549 cells were transfected with 100 pM of KSRP siRNA Mix or scrambled siRNA (NT) as control or treated with DMSO in different concentrations. Cell viability was measured by MTT test at indicated time points. Values represent mean ±SEM of two independent experiments conducted in duplicates.

After establishment of conditions for KSRP-siRNA experiments, the effect of KSRP KD on PKR activity and ISG expression was tested in non-infected and infected cells. As expected from previous overexpression experiments, PKR activation seemed to be reduced in cells with KSRP KD (figure 4.13) after infection with the influenza A ΔNS1 and NS1 R46A mutant viruses. This would further support an involvement of KSRP in regulation of PKR activity. Interestingly, also the expression of tested ISGs (ubiquitin-like protein ISG15 (ISG15)) and proteins involved in type I IFN signalling (STAT2) was reduced in KSRP KD cells.

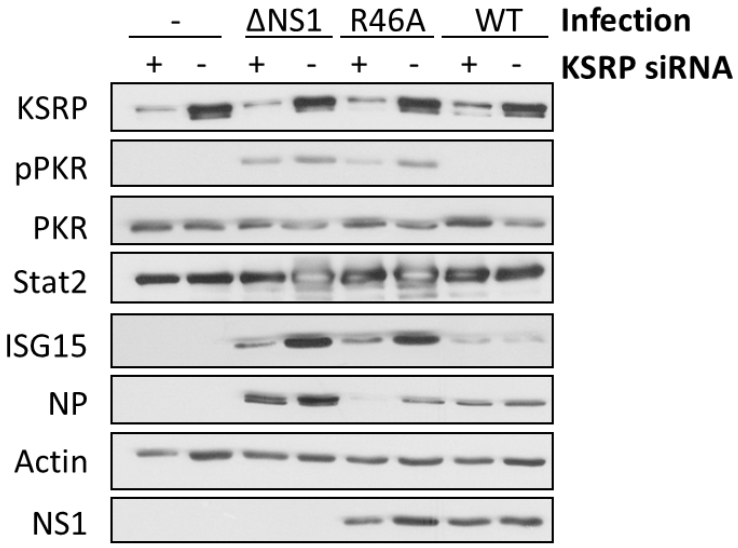

Figure 4.13. Knockdown of KSRP leads to decrease of PKR phosphorylation and expression of ISGs in influenza mutant virus infected cells. A549 cells were transfected with 100 pM of KSRP-siRNA Mix (+) or NT siRNA (-) for 48 h and infected with influenza A/PR/8 WT virus, R46A virus, ΔNS1 virus or non-infected. At 16 h p.i., cells were lysed and protein expression was analysed by SDS PAGE and immunoblotting using the indicated antibodies.

4.2.6 KSRP knockdown negatively influences NS1 mutant influenza virus replication due to slightly increased IFNβ levels

To investigate the previous findings in more detail, the effect of KSRP KD on viral replication was examined for influenza A/PR/8 WT, ΔNS1 and R46A virus infections (figure 4.14 A-D). The influenza R46A mutant virus was employed as an additional control, since it expresses an NS1 protein which is not able to inhibit PKR activation. Immunoblot analysis confirmed that expression of KSRP was still efficiently reduced 72 h p.i. (figure 4.14 E).

The results depicted in figure 4.14 show that KSRP KD had no effect on influenza WT infection, which is able to inhibit PKR activation and IFN induction. However, in influenza R46A and ΔNS1 mutant virus infected cells, KSRP KD reduced viral replication. The effect of the KSRP KD on the replication of both NS1 mutant viruses did not prove to be statistically significant, but followed a distinctive negative trend. This finding was difficult to explain with the previous results obtained in KSRP KD immunoblot experiments, in which KSRP KD led to decreased activation of PKR (compare figure 4.13), since it was shown before in the literature that decreased cellular levels of PKR can support viral replication of viruses that are unable to inhibit PKR [206].

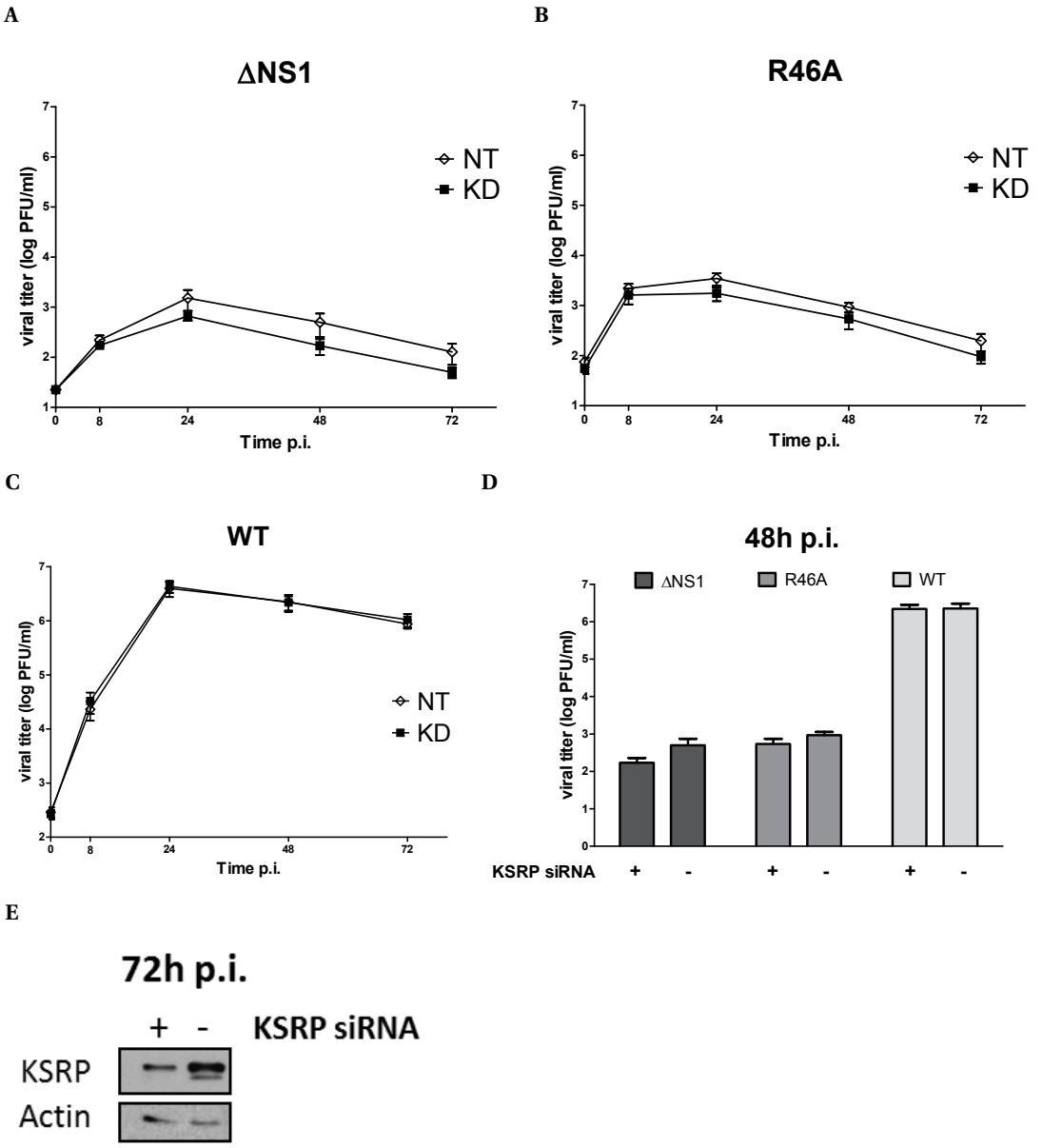

Figure 4.14. Knockdown of KSRP leads to slightly decreased viral replication of IFN inducing influenza virus mutants. A549 cells were transfected with 100 pM of KSRP-siRNA Mix (KD, +) or scrambled siRNA (NT, -) as negative control. 48 h p.t., cells were infected with A/PR/8 WT, ΔNS1 or R46A virus or mock infected. **A-C** At 0 h, 8 h, 24 h, 48 h and 72 h p.i., supernatants of infected cells were harvested and viral titers were determined by standard plaque titration assay. Values are mean +SEM of four independent experiments conducted in duplicates. **D** Viral titers at 48 h p.i., determined by plaque titration, were visualised in a bar chart for better comparison. **E** 72 h p.i., cells were lysed and lysates were analysed for KSRP KD by SDS PAGE and immunoblotting with the indicated antibodies.

However, the negative effect of KSRP KD on viral replication could be explained with the destabilising impact of KSRP on type I IFN transcripts such as IFNβ mRNA, which was shown before in the literature [84, 86]. Influenza viruses, among other viruses, react very sensitive to high levels of IFN [70]. Therefore, they have evolved mechanisms to inhibit the antiviral IFN response. The influenza NS1 mutant viruses are not able to efficiently inhibit the cellular IFN expression, which is also indicated by their lower replication rates compared to WT virus replication (figure 4.14). Because of this, it was hypothesised that the decreased viral

replication of the NS1 mutant viruses in KSRP KD cells could be attributed to elevated levels of IFN. This was tested by measuring the IFNβ protein concentration 16 h after influenza virus infection (figure 4.15). It can be seen that the influenza A ΔNS1 virus induced high levels of IFNβ that were further elevated in cells transfected with KSRP siRNA. The same trend could also be observed in cells infected with the influenza A NS1 R46A mutant virus, even if this virus induced lower levels of IFNβ. As expected, the influenza A WT virus did not induce IFNβ expression, which would explain the absence of an effect of KSRP KD on influenza WT virus replication seen in figure 4.14.

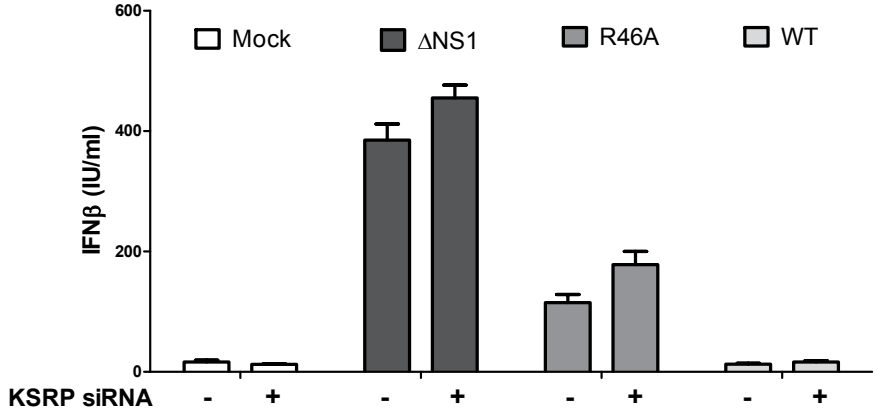

Figure 4.15. Knockdown of KSRP leads to slightly increased expression of IFNβ. A549 cells were transfected with 100 pM of KSRP-siRNA Mix (+) or NT siRNA as negative control (-). 48 h p.t., cells were infected with A/PR/8 WT, ΔNS1 or R46A virus or mock-treated. 16 h p.i., supernatants of infected cells were harvested and IFNβ levels were measured using the "Fujirebio® Inc. IFNβ ELISA Kit". Values represent mean +SEM of four independent experiments.

4.2.7 Knockdown of KSRP leads to significantly enhanced viral replication in cells with impaired IFNβ expression

So far, different effects of KSRP KD on PKR regulation and influenza virus replication were observed. KSRP KD reduced the catalytic activity of PKR, which was concluded from pPKR levels in immunoblot analyses and resulted in decreased viral replication of NS1 mutant viruses, which could be explained by elevated levels of IFNβ in KSRP KD cells. To further elucidate the correlation between KSRP and PKR in the context of viral infection, IFNβ-mediated effects were excluded by employment of the NFκB inhibitor BAY 11-7085. As shown before in our group, inhibition of NFκB results in strongly decreased IFNβ expression, so that the influence of IFN expression on virus replication can be disregarded [219, p.78-81].

For influenza growth curve analysis, A549 cells were transfected with KSRP-siRNA or scrambled NT siRNA for 48 h. Cells were pretreated with 50 µM BAY 11-7085 for 1 h followed by influenza virus infection and replication analysis. The negative impact of BAY-7085 on IFNβ expression was confirmed by measuring IFNβ levels with an IFNβ ELISA (figure 4.16 A). In addition, KSRP KD following siRNA transfection was tested by immunoblotting (figure 4.16 B). KSRP levels were still efficiently reduced at 72 h p.i.

A

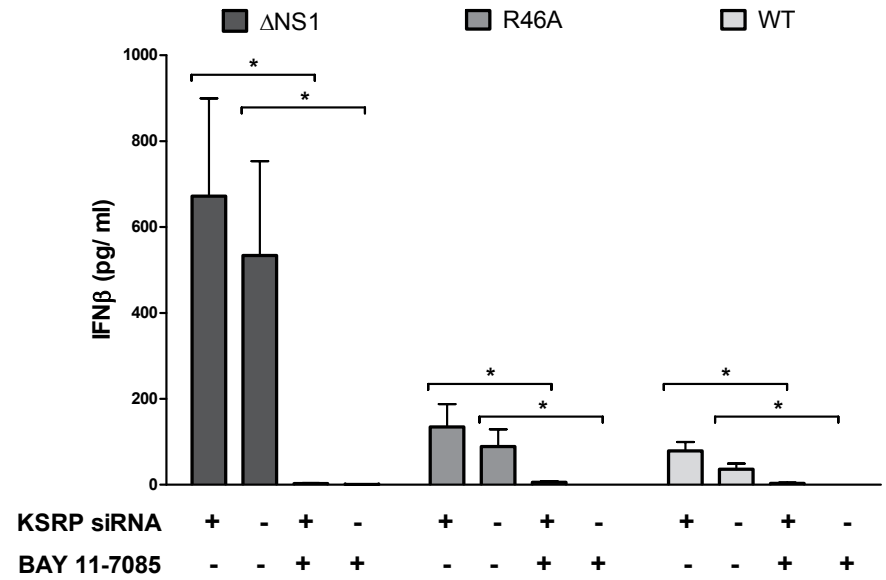

B

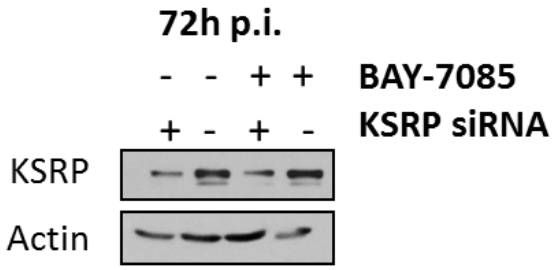

Figure 4.16. Validation of KSRP KD and BAY-7085 mediated effects on IFN production for influenza virus replication analysis. A549 cells were transfected with 100 pM of KSRP-siRNA Mix (+) or NT siRNA as negative control (-). 48 h p.t., cells were pretreated with 50 µM of BAY 11-7085 for 1 h, followed by infection with A/PR/8 WT, ΔNS1 or R46A virus or mock infection. **A** 24 h p.i., supernatants of infected cells were harvested and IFNβ levels were measured using the "VeriKine™ Human IFNβ ELISA Kit". Values represent mean +SEM of four independent experiments. ($*$ $p \leq 0.05$, Mann-Whitney U test). **B** 72 h p.i., cells were lysed and lysates were analysed for KSRP KD by SDS PAGE and immunoblotting with the indicated antibodies.

By excluding the stimulatory effect of KSRP KD on IFNβ expression, the influence of KSRP on PKR activation clearly became evident (figure 4.17). In IFNβ suppressed cells, the replication efficiency of both influenza mutant viruses was rescued by one order of magnitude in KSRP KD cells beginning at 24 h p.i. This could be attributed to the fact that both influenza mutant viruses lack the ability to inhibit PKR activation and therefore react sensitive to PKR mediated antiviral effects. As seen in previous analyses, KSRP was able to support PKR phosphorylation (figure 4.8). Here, KSRP KD possibly interfered with PKR activation, resulting in reduced pPKR levels which supported viral replication of ΔNS1 and R46A viruses (see figures 4.13 and 4.17). Compared to the mutant viruses, the effect of the KSRP KD on influenza WT virus replication was not as prominent. Only at 24 h p.i., KSRP KD led to enhanced viral replication. An effect of the KSRP KD on influenza WT virus replication was not expected since the influenza WT virus is able to inhibit PKR activation by expression of the viral NS1 protein. Despite this function, KSRP KD seemed to support viral replication of the WT virus

particularly at earlier time points of infection.

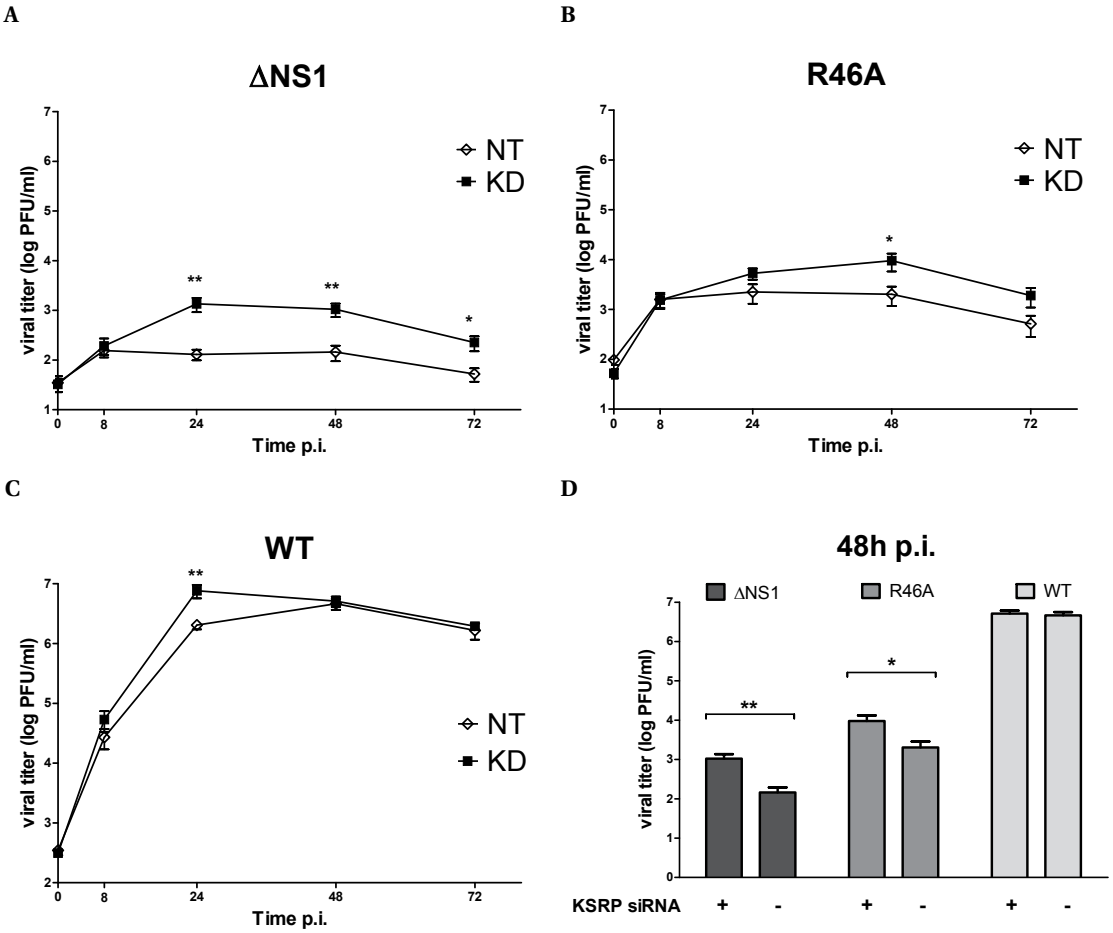

Figure 4.17. Knockdown of KSRP leads to enhanced viral replication in BAY-7085 treated cells. A549 cells were transfected with 100 pM of KSRP-siRNA Mix (KD, +) or scrambled siRNA (NT, -) as negative control. 48 h p.t., cells were pretreated with 50 µM of BAY 11-7085 for 1 h, followed by infection with A/PR/8 WT, ΔNS1 or R46A virus or mock infection. **A-C** At 0 h, 8 h, 24 h, 48 h and 72 h p.i., supernatants of infected cells were harvested and viral titers were determined by standard plaque titration assay. Values are mean +SEM of four independent experiments conducted in duplicates. (∗ p≤0.05, ∗∗ p≤0.01, Mann-Whitney U test). **D** Viral titers at 48 h p.i., determined by plaque titration, were visualised in a bar chart for better comparison (∗ p≤0.05, ∗∗ p≤0.01, Mann-Whitney U test).

To conclude, it is possible to envision a scenario, in which KSRP affects the viral replication by regulating the expression of IFNβ and by supporting the catalytic activity of PKR. This could be especially interesting for viruses that are not able to inhibit PKR activation.

5 Discussion

5.1 Mass spectrometric analysis revealed the PKR interactome in influenza virus infected cells

The IFN system is one of the most important innate defense mechanisms in vertebrate cells. One of its key factors is the RNA-dependent protein kinase (PKR). It is not only a sensor for multiple harmful conditions, such as cellular stress, bacterial PAMPs and viral RNA, but also a multifunctional effector protein. Its activation can result in wide-ranging processes, as translational stop and apoptosis, but also leads to upregulation of transcription factors for the expression of antiviral IFNs and ISGs and on a cellular level to accumulation of aSGs as antiviral signalling platforms. Since its discovery, many factors that contribute to the cellular antiviral defense and stress regulation could be linked to PKR activation, but the network of PKR interacting proteins is not yet complete.

Most proteins interact with other proteins to fulfil their biological tasks. Hence, the determination of protein interactomes can provide insights into specific protein functions. The biological impact of protein-protein-interactions was impressively illustrated in a recent study by Sahni and colleagues [220]. According to their estimations, about 60 % of disease-causing mutations in proteins affect their association with other proteins by either completely abrogating protein binding or perturbing a particular subset of interactions. Due to the central role for biological processes, different experimental methods were developed to systematically map protein interactions. Technologies like protein microarrays, yeast two-hybrid systems and affinity-purification mass spectrometry (AP-MS) enable high-throughput screens for protein interactions. Hereby, recent advances in the field of mass spectrometry provided great advantages for the systematic analysis of interactomes of proteins under different conditions [221]. Mass spectrometric interactome analyses are highly sensitive and allow the detection of protein interactions under physiological conditions in relevant biological contexts such as mammalian cell lines or tissues [221]. In contrast to yeast two-hybrid screens, AP-MS allows the detection of interactions that require post-translational modifications by specific cellular factors and it is able to determine indirect protein interactions [222]. That means, by employing AP-MS all components of large protein complexes can be determined, even if they not necessarily all directly interact with another. Moreover, AP-MS enables the detection of protein interactions that are mediated by DNA- or RNA-binding. However, most high-throughput-screening- methods used to determine protein interactions only provide qualitative data. This limitation can be overcome in AP-MS analyses by using quantitative techniques, such as stable isotopic labelling by amino acids in cell culture (SILAC). This method allows the quantitative comparison of two or more cell populations and the elimination of false positives and external protein contaminations, which greatly increases the confidence in detected interaction partners [221]. Therefore,

quantitative AP-MS is one of the most suitable techniques to study protein interactomes and the consequences of perturbations by pathogens on cellular protein interactions.

In this study, protein interactions of PKR in the context of influenza A/PR/8 virus infection were examined by SILAC-based quantitative AP-MS of precipitated PKR binding partners. Four experimental replicates and systematic evaluation of the data according to self-imposed criteria resulted in a list of 47 proteins that were identified as specific PKR binding partners after influenza A/PR/8 WT and/ or ΔNS1 virus infection (table 4.1). Of these, four were exclusively bound to PKR after WT virus infection, whereas 14 were identified as PKR interaction partners in particular after ΔNS1 virus infection. Herein, proteins bound to PKR after ΔNS1 virus infection seem to belong mostly to protein clusters of heat shock proteins and proteins involved in cellular stress defense, whereas no clear pattern could be seen for the PKR binding partners in WT infected cells (figure 4.5). This is not unexpected, since ΔNS1 virus infection leads to activation of PKR, resulting in the participation of PKR in the cellular stress response. Seven of the 47 proteins have been previously shown to interact with PKR. These factors include EIF2S1 among others, which is a different identifier for the well known PKR substrate eIF2α. Identification of eIF2α in the mass spectrometric interactome analysis conducted in this thesis is an indication for the validity and robustness of the SILAC based AP-MS screen.

GO-term analysis of PKR binding partners revealed that most PKR interacting proteins after influenza virus infection have catalytic activity or binding functions, such as RNA-binding and binding of transcription factors. PKR interacting proteins are by the majority involved in metabolic processes, cellular component organisation and biogenesis, for example ribosome biogenesis, but some of the identified proteins were directly linked to apoptotic processes and immune system functions (figure 4.4). Interestingly, GO-term analysis of proteins bound to PKR after WT or ΔNS1 virus infection showed a similar distribution pattern according to their molecular functions and the biological process they are involved in (data not shown).

The results of the GO-term analysis are in line with other proteomic studies of PKR. Blalock and colleagues determined binding partners of the active and inactive form of nuclear PKR in an acute T-cell leukemia cell line. They were able to identify 138 proteins, that were associated with PKR in the nucleus, including several novel binding partners with roles in ribosome biogenesis, mRNA processing and cell division [223]. However, this study completely disregarded cytoplasmatic PKR, which represents the main part of cellular PKR. Moreover, Li *et al.* performed a systematic proteomic analysis of the human innate immunity interactome for type I IFN to explore the signal transduction pathways responsible for regulating cellular antiviral defense and IFN production [224]. They analysed different affinity-tagged bait proteins with known or suspected involvement in transcriptional regulation of type I IFN production, including a FLAG-PKR construct, in cell lines that were artificially stimulated with poly(rI:rC), poly(dA:dT), LPS or CpG. They succeeded in expanding the protein network of innate immunity and were able to detect 36 high confidence known or novel PKR binding partners. Please note, that both studies did not provide any information about the role of PKR in viral infections. Therefore, detecting binding partners of nuclear and cytoplasmatic

PKR after influenza virus infection, as presented in this thesis, is of great importance to add additional data to the network of PKR protein interactors.

Comparison of the results of PKR interactome studies conducted by Blalock *et al.*, Li *et al.* or in this thesis showed only little overlap between the lists of identified PKR binding partners (figure 5.1), which underlines the complexity of mass spectrometric experiments. However, two proteins were identified in all three PKR interactome studies, namely eukaryotic translation initiation factor 6 (eIF6) and ATP-dependent RNA helicase A (DHX9). eIF6 is involved in ribosome biogenesis, translational control and tumor progression [225]. It is known to bind to the 60S ribosomal subunit, hereby preventing its association with the 40S subunit, resulting in inhibition of translation initiation [226]. An interacton with PKR has not been mechanistically described yet, but eIF6 binding to PKR was validated by Li *et al.* in coprecipitation assays [224]. However, since all studies analysing the PKR interactome were conducted in tumor derived immortalised cells, the detection of eIF6, which is highly abundant in transformed tissues, could be a side effect with unclear biological meaning.

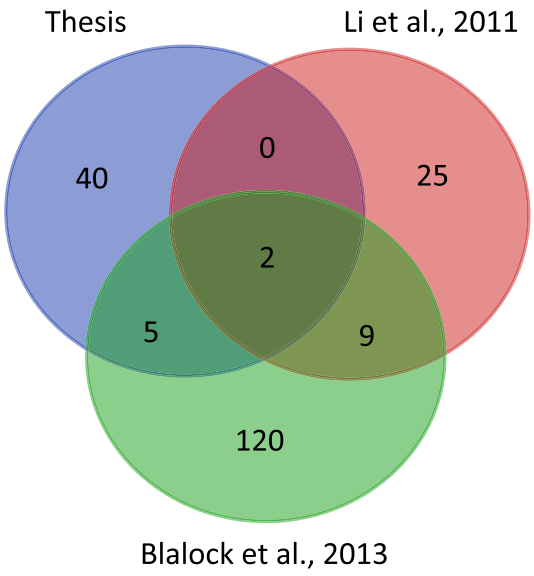

Figure 5.1. Comparison of PKR interactome studies. Lists of 137 PKR binding proteins from Blalock *et al.* and 36 high confidence candidate proteins (HCIP) for Flag-PKR from Li *et al.* were compared to 47 PKR interacting proteins from this thesis [223, 224]. Resulting overlaps of results are visualised in a Venn diagram [227]. For detailed results, see table 7.1.

The second factor, which was found in all PKR interactome studies, is DHX9. DHX9 is a dsDNA and RNA helicase with functions in transcription activation [228]. More recently, it was shown to contribute to antiviral processes, for example it is able to detect viral nucleic acids and can bind to the mitochondrial adapter protein IPS-1 which links it to the RIG-I mediated antiviral signalling pathway [229]. Moreover, DHX9 was shown to be a substrate for PKR phosphorylation and is involved in regulating transcription of ISGs or subsequent processing of ISG mRNAs [230, 231]. In parallel to its role in antiviral signalling, DHX9 is actively recruited by many different viruses as it is required for their replication [232]. For influenza viruses an RNA-mediated interaction of DHX9 and the viral NS1 protein was demonstrated, which is needed for efficient viral replication [233]. These findings could be reflected by the results

obtained in this study, where DHX9 was found as a PKR binding partner in particular after influenza A ΔNS1 virus infection. It is possible that in cells infected with the WT virus, the viral NS1 protein inhibits DHX9-PKR binding by sequestration, hereby supporting viral replication and inhibiting antiviral signalling. On the contrary, DHX9 could bind to PKR in ΔNS1 infected cells to contribute to the antiviral IFN response. These hypothesised interactions need to be validated in future experiments.

As seen for DHX9, some of the identified PKR binding partners have been previously reported to interact with PKR. This is also the case for HSP90. HSP90 is a highly conserved member of the eukaryotic chaperone family. It is constitutively expressed at high levels and is essential for cell viability. Its major task is to prevent unfolding and aggregation of cellular proteins, such as signalling factors, kinases and transcription factors [214]. Two forms of HSP90 can be found in cells, the stress-induced HSP90α and the constitutive HSP90β [234]. In the interactome screen conducted in this thesis, both forms were identified as PKR binding partners (table 4.1). The interaction of PKR and HSP90 was first described by Donzé *et al.* [214]. They showed that a complex of HSP90, PKR and the co-chaperone p23 is essential for folding, maturation and stabilisation of PKR. Upon recognition of dsRNA by PKR, the complex dissociates and PKR is activated.

Since the interaction of PKR and HSP90 is well characterised, HSP90 was chosen among other factors for in vitro validation of results from the mass spectrometric screen. Interaction of PKR and the tested proteins could be confirmed, but quantitative differences between the interaction patterns determined by mass spectrometry and coprecipitation assays occured. In the presented study, quantitative mass spectrometry was employed to determine PKR interaction partners that were bound to PKR particularly after influenza virus infection (figure 4.5). The results of the coprecipitation experiments showed constitutive binding of PKR to all tested proteins in non-infected and infected cells (figure 4.6). This can be explained by the fact that the systematic analysis depicts the numerical mean of four independent experiments. The experimental replicates have a certain variance, which can be illustrated at the example of the IGF2BP1 protein. In table 4.1, which shows the results for the PKR interaction partners after systematic analysis, IGF2BP1 is listed as a specific PKR binding partner after influenza ΔNS1 virus infection. However, IGF2BP1 was found in the single mass spectrometric experiments as a PKR interacting proteins in non-infected and infected cells in replicate 2, showed increased binding to PKR after ΔNS1 infection in replicate 3 and slightly decreased binding after virus infection in replicate 4. Hence, the results obtained by systematic analysis of the mass spectrometric experiments only provide a hint and have to be validated by independent biochemical assays such as coprecipitation analyses.

Reproducibility of mass spectrometric experimental replicates was also described to be a problem in other studies, because the analysis of complex protein mixtures is dependent on many factors and underlies sample preparation-related variations like the passage of used cells as well as subtle differences in mass spectrometry configurations such as sample temperature and duration of the measurement [235]. If the reproducibility of experimental replicates is rather small, low stringent criteria have to be used for data evaluation, which

facilitates the detection of false positives. It is therefore desirable to standardise and optimise all workflow conditions to achieve high sensitivity, reliability and robustness of the assay. In this thesis, it was tried to keep the experimental conditions as constant as possible, e.g. by employing cells with subsequent passages and using the same virus and plasmid stocks for all replicates. However, taking into account the AP-MS results presented in this thesis, it would be worthwhile to repeat the mass spectrometric experiments with further optimised conditions for sample preparation and measurement. For example, different methods for the protein fractionation or different enzymes for the proteolytic cleavage of proteins could be tested. Also the amount of cells used for the coprecipitation analysis could be further optimised. In the mass spectrometric measurement itself, different gradients could be tested to enhance the yield of detected proteins.

Nevertheless, despite the limited reproducibility of the results obtained in different experimental replicates, the SILAC based mass spectrometric screening of affinity purified complexes described in this thesis proved to be a suitable method for the detection of PKR interactors, which is shown by the identification and validation of KSRP as a novel PKR regulator.

5.2 KSRP is a novel regulator of PKR

To identify proteins that affect PKR mediated antiviral signalling, 18 candidate proteins were chosen in a hypothesis driven process from the list of PKR binding partners (table 4.1). Their influence on the catalytic PKR activity, represented by phosphorylation of endogenous PKR, was tested in overexpression experiments. From the tested proteins, four were able to directly induce phosphorylation of PKR without exogenous, activating stimuli (figure 4.7). These were SRSF1, KSRP, IGF2BP1 and YWHAE. The proteins supported PKR activation not only in mock-treated samples, but also in cells infected with influenza A/PR/8 WT virus, in which the viral PKR antagonist NS1 is expressed in high amounts. PKR activation hereby even exceeded the levels determined in cells overexpressing the established PKR activating protein PACT, which was used as a positive control (see figure 4.7 B) [115]. In ΔNS1 virus infected cells, overexpression of the proteins had no cumulative effect on PKR phosphorylation, which is possibly due to the limited levels of endogenous PKR in the human embryonic kidney cells (293T) used for the analysis. Due to time constraints, only the role of KSRP in PKR mediated antiviral signalling was analysed in detail by independent biochemical assays.

KSRP is an ARE-binding protein (ABP) that is involved in control of the cellular antiviral IFN response. It regulates expression levels of different forms of type I IFNs and other cytokines by transcription repression, translational silencing and especially ARE-mediated decay (AMD) involving the intracellular exosome complex (see section 1.2.1 for detailed description) [84, 86]. One of the best described functions of KSRP is its ability to destabilise ARE-containing mRNA transcripts in order to retain basal levels of type I IFNs, which are constantly expressed at low concentrations in non-stimulated cells [85, 236]. Detection of

bacterial or viral infections by PRRs triggers the translation of type I IFNs, which consequently results in the upregulated expression of several hundred genes that in combination specify the antiviral state. Hereby, a wide range of mechanisms such as apoptosis, autophagy and cell cycle arrest are executed and the adaptive immune system is activated to support pathogen clearance (see section 1.2.1). Since the expression of type I IFNs induces extreme proinflammatory and cytotoxic action, the IFN concentration in healthy cells has to be rigorously restricted. Enduring, excessive IFN production is detrimental for cells and is described to play a role in the pathogenesis of different autoimmune diseases [237].

In this study, it could be shown for the first time, that KSRP not only regulates type I IFN expression on transcriptional and post-transcriptional levels as described before in the literature, but also directly supports antiviral signalling by enhancing PKR activation in a process that appears to involve direct protein-protein-interaction.

5.2.1 Interaction of KSRP and PKR

KSRP was identified as a PKR binding partner in two of four replicates of the mass spectrometric analysis. Data evaluation according to systematic criteria described in section 4.1.2 suggested that interaction of KSRP and PKR occured predominantly after influenza A/PR/8 ΔNS1 virus infection (table 4.1). To confirm these results, cellular localisation of KSRP and PKR proteins was analysed in immunofluorescence experiments. Hereby, KSRP was detected predominantly in the nucleus, whereas PKR was distributed throughout the cytoplasm and to a smaller extent in the nucleus in influenza A WT virus infected and non-infected cells. In influenza A ΔNS1 virus infected cells, both proteins accumulated in cytoplasmatic aSGs (figure 4.11). Similar to the results obtained in the immunofluorescence experiments of this thesis, KSRP and PKR were both described as SG components before in the literature [92, 141, 144]. This could hint at a possible steric proximity of both proteins in aSGs that could support protein-protein interaction. Moreover, it could be a reason for the decreased binding of PKR and KSRP after influenza WT virus infection, seen in different coprecipitation assays (figures 4.9 and 4.10), because here the NS1 protein that is expressed after influenza WT but not ΔNS1 infection actively inhibits SG formation [180]. This assumption is supported by similar observations made for other SG components. G3BP1, a resident SG protein crucial for their formation, was shown to directly interact with inactive PKR, thereby facilitating recruitment of PKR to aSGs and enhancing PKR activation [144, 238, 239]. IPS-1 was initially described as the adaptor protein of RIG-I that transduces transcription activation of type I IFN genes and ISGs. Recently, Zhang *et al.* could show that IPS-1 has an essential role in dsRNA induced SG formation by interaction with PKR [143]. Unfortunately, direct colocalisation of KSRP and PKR could not be examined in this thesis due to technical problems regarding antibody quality and availability. For further analyses, experimental conditions of the colocalisation studies would need to be optimised.

Interestingly, other biochemical assays suggested that formation of SGs was not mandatory for the interaction of KSRP and PKR, since the interaction of both proteins was detected in

a constitutive manner in coprecipitation analyses (figure 4.9). In fact, the coprecipitation results point out limitations of the immunofluorescence analysis concerning the detection of protein-protein-interactions, because the latter only showed little overlap of the intracellular distribution of KSRP and PKR in non-infected and influenza WT virus infected cells at steady state (figure 4.11). Thus, the spatiotemporal dynamics of the KSRP-PKR-interaction remain to be elucidated in future experiments. Herein, time course experiments could facilitate the detection of transient colocalisation of both proteins. Moreover, bimolecular fluorescence complementation assays could be employed to further validate the protein interaction and its intracellular localisation. In this context, it would also be interesting to conduct coprecipitation analyses with separated nuclear and cytoplasmic cell extracts.

Even though KSRP was predominantly detected in the nucleus in the presented thesis and other studies, Winzen *et al.* were able to show binding of KSRP and cellular ARE-mRNAs in cytoplasmic extracts of human cells, which suggests that KSRP functions also in the cytoplasm [84]. In a different study, Gerecht and colleagues were able to detect and quantify endo- and exogenous cytoplasmatic KSRP by Förster resonance energy transfer (FRET) analysis [79]. These findings support the conclusion that KSRP can bind to PKR in the cytoplasm. Another possibility to explain the constitutive binding of KSRP and PKR could be the interaction of nuclear KSRP and PKR. For a long time, PKR was thought to be localised exclusively in the cytosol, but recent studies have attributed pathological significance to nuclear PKR, for example phosphorylated nuclear forms of PKR were found in neuronal cells retrieved from patients with Alzheimer's and Huntington's disease [240, 241]. Please note that active, nuclear PKR has only been observed in diseased tissue or cell lines so far [223]. Since all cell lines used in this thesis are immortalised or tumor-derived, the detection of nuclear PKR could be of minor biological relevance. Thus, it would be interesting to use other cell lines or primary cells to further analyse the role of nuclear PKR, especially in the context of viral infection.

To examine the binding of KSRP and PKR more in detail, coprecipitation assays of KSRP and a set of PKR mutant proteins were conducted (figure 4.10). The obtained results show that the interaction of KSRP and PKR is mediated by the N-terminal domain of PKR, but does not seem to be dependent on binding of viral RNA, since all tested PKR mutants with the exception of the C-terminal-domain mutant "PKR 266-551" were coprecipitated by KSRP (figure 4.10). Therefore, binding of both proteins is likely to be mediated by direct protein-protein interaction. To completely exclude the possibility of RNA mediated interaction of KSRP and PKR, in follow-up experiments cell lysates could be treated with different ribonuclease enzymes prior to coprecipitation assays. Comparison of the results of this thesis to findings obtained for other protein regulators of PKR reveals similarities. For example, binding of PKR to PACT also involves the N-terminal domain and was described to be dsRNA-independent [115]. Comparable observations were reported for binding of PKR and IPS-1. Their interaction involves the N-terminal domain of PKR and promotes PKR activation [143]. These findings suggest a general role of the PKR N-terminal domain in mediating protein-protein-interactions. The conformation of PKR does not seem to be crucial for the

interaction of PKR and KSRP, since both the active form of PKR in ΔNS1 infected cells and the inactive form (in non-infected cells or represented by the K296R mutant) showed binding to KSRP. To describe the interaction of PKR and KSRP mechanistically, future coprecipitation experiments should also include different KSRP mutants. It would be interesting to see, if binding of KSRP to PKR is mediated by the N-terminal domain, one of its KH-domains or the C-terminal region that contains sites for other protein interactions [87].

5.2.2 Role of KSRP in PKR mediated antiviral signalling

In addition to the interaction of KSRP and PKR, the influence of KSRP on the activation of PKR was examined. Expression of KSRP induced phosphorylation of PKR in a dose-dependent manner (figures 4.7 and 4.8). This result was confirmed for the endogenous proteins in KSRP KD studies. KSRP KD resulted in slightly decreased PKR phosphorylation upon infection with the PKR activating influenza A ΔNS1 or R46A viruses without affecting overall PKR levels or cell viability (figures 4.12 and 4.13 B). In addition to reduced PKR activation, KSRP KD led to decreased expression of different ISGs and proteins involved in ISG expression, such as ISG15 and STAT2 in cells infected with the influenza NS1 mutant viruses (figure 4.13). KSRP KD also negatively influenced viral replication of influenza NS1 mutant viruses, which coincided with slightly higher protein levels of IFNβ (figures 4.14 and 4.15). Interestingly, treatment of cells with the NFκB inhibitor BAY-7085, which diminished IFNβ expression, reversed these effects. Herein, viral replication of influenza A ΔNS1 and NS1 R46A mutant viruses was rescued upon KSRP KD by one order of magnitude in cells with reduced IFNβ accumulation (figure 4.17). This highlights the supportive effect of KSRP on PKR activation, which was detected before in phosphorylation assays (compare figures 4.8 and 4.13). Please note, that all described effects were not as prominent in cells infected with influenza A WT virus. This can most likely be assigned to the expression of the viral NS1 protein, which inhibits PKR activation.

The findings of this study can be summarised with the following model of PKR-KSRP interplay (figure 5.2 A): Infection of a cell with influenza A ΔNS1 mutant virus is detected by the PRRs PKR and RIG-I [60, 160]. Activation of PKR by binding of viral RNA induces a translation stop via phosphorylation of the translation initiation factor eIF2α, which is also the prerequisite for the formation of aSGs [118, 140]. Accordingly, PKR can accumulate in aSGs. Another effect of PKR signalling is the activation of p38, which results not only in the transcription of type I IFNs and other cytokines, but was also shown to regulate KSRP dependent degradation of mRNA [80, 125]. Active p38 is able to phosphorylate KSRP at serine 692 of the C-terminal domain [80]. This could lead to nucleocytoplasmic shuttling of the protein in a similar way as shown for KSRP phosphorylation by AKT or phosphorylation of the ABP TTP by p38 MAPK [81, 91].

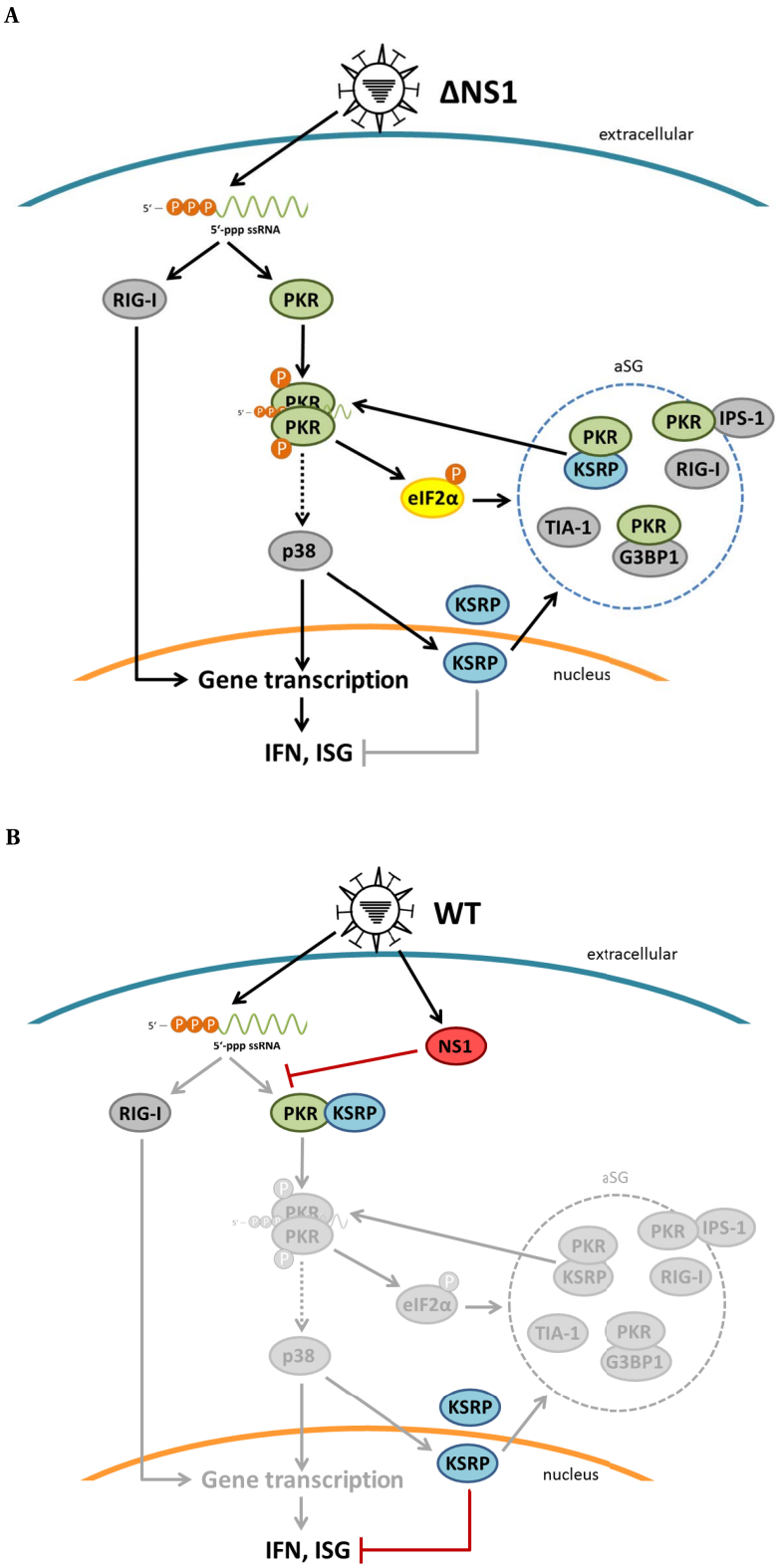

Figure 5.2. Proposed model for regulation of PKR activity by KSRP. A Infection with A/PR/8 ΔNS1 virus leads to activation of RIG-I and PKR. RIG-I mediated signalling results in transcription of type I IFN and ISGs. PKR activation involves dimerisation and autophosphorylation and leads to a translation stop by phosphorylation of eIF2α. Phosphorylated eIF2α induces aSG formation. Active PKR additionally activates p38 MAPK, which results in transcription of proinflammatory cytokines and nucleo-cytoplasmic shuttling of KSRP. Thus, KSRP mediated mRNA degradation is suppressed and KSRP aggregates in aSGs, where it interacts with PKR to enhance PKR activity. **B** RIG-I and PKR mediated antiviral signalling upon Influenza A WT infection is blocked by the viral NS1 protein. Active KSRP facilitates degradation of ARE-mRNA to maintain basal levels of type I IFN.

Cytoplasmatic KSRP can then relocalise to aSGs [79, 92]. This would bring KSRP and PKR in close proximity, which could support the formation of direct protein-protein-interaction. Binding of KSRP to PKR could subsequently enhance PKR activation, hereby further augmenting PKR downstream effects for complete clearance of the pathogen. In addition, accumulation of KSRP in aSGs would block KSRP's ability to destabilise ARE-containing mRNA transcripts, so that degradation of ARE-mRNAs would be inhibited. This is of importance, since KSRP was shown to be involved in degradation of different IFN-transcripts such as IFNβ or IFNα4, but upon infection the expression of IFN is crucial for subsequent antiviral counteractions and establishment of the cellular antiviral state [70, 84, 86]. Hence, relocalisation of KSRP to aSGs could stabilise type I IFN-transcripts that are produced in high amounts as a result of RIG-I as well as PKR activation [63, 64]. This hypothesis is supported by the finding that SGs were described to store translationally stalled mRNAs and formation of aSGs was shown to induce alternative translation of stress dependent mRNAs to support pathogen clearance [139, 242]. Moreover, also PKR was described to be involved in preserving ARE-mRNAs by increasing their stability [243].
In influenza WT virus infected cells, PKR and KSRP can also interact, but in contrast to the mechanisms described above for influenza ΔNS1 virus infected cells, PKR activation and following downstream processes are blocked by the viral PKR antagonist NS1 (figure 5.2 B) [161, 167]. Taken together, the results of this study hint at a novel antiviral effector pathway that is inhibited by the viral NS1 protein via its PKR antagonistic function.

The experiments conducted in cells with reduced IFNβ production clearly demonstrate the supportive effect of KSRP on PKR activation and underline the role of PKR in antiviral signalling, since KSRP KD here significantly enhanced viral replication of influenza A NS1 mutant viruses by one order of magnitude (figure 4.17). However, in normal cells KSRP KD resulted in slightly decreased replication of mutant viruses, which could be attributed to increased levels of IFNβ (figures 4.14 and 4.15). These findings support the observations made by Lin and colleagues [86]. The group detected elevated amounts of IFNα4 and IFNβ on mRNA and protein level in cells derived from KSRP knockout mice upon infection with HSV1 or VSV and explained these findings by impaired mRNA degradation upon KSRP knockout. In contrast to Lin *et al.*, the KSRP KD effects observed in this study were not as prominent. This could be explained by the inhibition of KSRP mediated IFN-mRNA degradation activity as a result of PKR activation upon influenza NS1 mutant virus infection, as depicted in the model above (figure 5.2 A). To confirm the inhibitory effect of catalytically active PKR on the destabilising activity of KSRP, the replication experiments and the measurement of IFNβ levels could be repeated with the inactive PKR K296R mutant. The PKR K296R mutant was able to bind to KSRP as seen in coprecipitation experiments (figure 4.10), but should not be able to inhibit KSRP's mRNA destabilising activity, since the mutant is not able to activate p38 MAPK or SG formation. The slightly decreased IFNβ levels in non-treated cells in comparison to KSRP KD cells are assumed to originate from initial effects of KSRP on IFN mRNA degradation before its inactivation. Another reason could be the tight regulation and timed coordination of the microbial stress response. Upon viral infection, the cytosolic PRR RIG-I induces type I IFN expression, which subsequently leads to transcription activation

of several ISGs, including PKR in an auto- and paracrine fashion. Elevated cytosolic PKR levels can then induce SG formation. SG formation however is only transient, meaning infected cells can oscillate between type I IFN production following RIG-I activation and translation inhibition mediated by PKR activation [244]. KSRP activity could consequently switch between both cellular states, leading to a minor effect on overall IFNβ protein levels as determined in this work.

Another way for KSRP to influence influenza virus replication, which could be independent of its role in supporting PKR activation, could be the destabilisation of viral RNA species during infection. In one of the coprecipitation analyses performed in this thesis, a coprecipitation of GFP-KSRP and the viral NP protein was detected (figure 4.9). The viral NP protein is one of the components of the viral RNP complexes and is associated with the viral RNA genome segments. Interaction of KSRP and NP could hint at an involvement of KSRP in degradation of viral RNA. Comparable observations regarding the interaction of KSRP and influenza virus proteins were reported by Watanabe *et al.* The group performed a comprehensive screen to determine host factors required for viral replication, in which they used Flag-tagged influenza virus proteins for coimmunoprecipitation and mass spectrometric analyses [245]. They were able to identify 1292 host proteins that coprecipitated with one or more viral proteins. Among these 1292 proteins, they detected KSRP as a binding partner of the viral NP, NA and M2 protein. Based upon these findings, it would be interesting to test if KSRP is able to bind viral RNA. This could be done by precipitating KSRP from influenza virus infected cells and analysing the complete set of bound cellular and viral RNA by deep-sequencing.

5.3 Outlook

The results presented in this study demonstrate the suitability of SILAC based mass spectrometric screening of affinity purified protein complexes to determine the interactome of host cell factors involved in antiviral defense mechanisms. The experimental setup described in this thesis enabled the detection of known and novel PKR interacting proteins and identified KSRP as a new protein regulator of PKR. The effect of KSRP on PKR activity and antiviral signalling was examined and a correlation between KSRP activity and influenza virus replication could be validated.

Despite the great effort to analyse the mechanism of KSRP mediated PKR activation in all its aspects, some questions still remain unanswered. In the model presented in figure 5.2, it was hypothesised that the inhibitory effect of PKR activation on KSRP's mRNA destabilisation activity is mediated by p38 MAPK. This hypothesis needs to be validated in future experiments, for example by employing inhibitors to suppress PKR or p38 downstream effects. Interestingly, a link between p38 MAPK activity and expression of IFNβ levels in the context of influenza virus infection was described before by Börgeling *et al.* [246]. The group could show that in cells infected with highly pathogenic avian influenza viruses the inhibition of p38 resulted in reduction of IFNβ production. By applying the model stated in this thesis,

this could be explained with the regulation of KSRP degradation activity by p38, meaning that reduced levels of p38 could enhance KSRP activity and thereby lower IFNβ mRNA stability.

In this thesis, the effect of KSRP was analysed according to its effect on PKR activation, viral replication and expression of IFNβ. However, KSRP was shown to bind various mRNA transcripts, including mRNAs linked to cellular transcription factors, such as NFκB inhibitor ζ transcripts [84]. PKR is able to regulate cellular gene expression via NFκB in a process that is independent of PKR's catalytic activity [128, 247]. It would be of interest to analyse the impact of KSRP on noncatalytic PKR signalling and corresponding downstream effects in this regard.

The results in this study point to a previously unknown function of KSRP as a protein regulator of PKR. In addition, different studies suggest indirect ways for KSRP to regulate PKR functionality. It was shown that KSRP negatively influences the expression of nucleophosmin (NPM) via AMD of NPM mRNA [248]. NPM was described to interact with PKR, thereby inhibiting eIF2α phosphorylation and PKR-mediated apoptosis [249]. This suggests that KSRP could also enhance PKR activity by controlling the mRNA stability of PKR regulatory factors such as NPM. However, there is no experimental proof for this hypothesis yet, so that additional experiments, as e.g. PKR activity assays in cells with parallel KD of KSRP and NPM, would be required for its validation.

Moreover, the contribution of other ABPs to regulation of PKR catalytic activity and IFNβ production should be analysed further. Lin and colleagues described before that in cells derived from KSRP knockout mice treated with poly(rI:rC), the half-lives of IFNα4 and IFNβ mRNAs were increased two- to four-fold, but the type I IFN levels returned to basal amounts at later time points [86]. They speculate that this is due to the shutoff of IFN transcription and IFN mRNA decay mediated by other destabilising ABPs. Hence, it would be interesting to analyse the effects of other ABPs such as TTP on PKR activation and viral replication.

Influenza viruses are well adapted to their host and evade the cellular immune response in manifold ways. The results of this study suggest that influenza viruses are not affected by KSRP mediated increase of PKR activity due to the inhibition of PKR by the viral NS1 protein. Because of this, future studies could also analyse the effect of KSRP on replication of viruses that lack a potent viral PKR antagonist, such as VSV. Nevertheless, it is likely that influenza viruses also employ other methods to control KSRP mediated actions. Herein, different studies suggest a participation of KSRP in pro- or antiviral processes based on up- or downregulation of its levels upon viral infection. For influenza virus infection, enhanced KSRP mRNA levels were reported for low pathogenic avian H9N2 virus in chicken cells [250]. In contrast to these findings, Coombs *et al.* observed downregulation of KSRP at protein level upon influenza A H1N1 infection in human A549 cells [251]. An impact of influenza A/PR/8 WT, ΔNS1 or R46A virus infection on cellular KSRP levels could not be detected in this study, but systematic analysis of KSRP expression at mRNA and protein level upon virus infection would be an interesting point for future analyses to expand our knowledge of antiviral signalling mechanisms and corresponding viral countermeasures.

To conclude, the underlying mechanisms of KSRP mediated PKR activation are highly complex and seem to be tightly regulated by direct and indirect protein interactions. Expanding our knowledge about antiviral signalling pathways and their modulation by viral proteins is crucial for our understanding of pathogenesis and the identification of new antiviral targets for drug development. Hereby, the list of PKR interacting partners created by mass spectrometry provides a useful tool for future analyses.

6 Bibliography

[1] van Riel, D., Munster, V., de Wit, E., Rimmelzwaan, G., Fouchier, R., Osterhaus, A. and Kuiken, T. "Human and avian influenza viruses target different cells in the lower respiratory tract of humans and other mammals". *The American Journal of Pathology* (2007); 171:1215–1223

[2] WHO. "Influenza (seasonal), fact sheet n°211" (2014). `http://www.who.int/mediacentre/factsheets/fs211/en/` [accessed: 2016-03-25]

[3] Fiore, A., Shay, D., Broder, K., Iskander, J., Uyeki, T., Mootrey, G., Bresee, J. and Cox, N. "Prevention and control of influenza: Recommendations of the advisory committee on immunization practices (ACIP), 2008." *Morbidity and mortality weekly report. Centers for Disease Control* (2008); 57:1–60

[4] Hause, B., Collin, E., Liu, R., Huang, B., Sheng, Z., Lu, W., Wang, D., Nelson, E. and Li, F. "Characterization of a novel influenza virus in cattle and swine: Proposal for a new genus in the orthomyxoviridae family". *mBio* (2014); 5:1–10

[5] Webster, R., Bean, W., Gorman, O., Chambers, T. and Kawaoka, Y. "Evolution and ecology of influenza A viruses." *Microbiological Reviews* (1992); 56:152–179

[6] Tong, S., Zhu, X., Li, Y., Shi, M., Zhang, J., Bourgeois, M., Yang, H., Chen, X., Recuenco, S., Gomez, J., Chen, L., Johnson, A., Tao, Y., Dreyfus, C., Yu, W., McBride, R., Carney, P., Gilbert, A., Chang, J., Guo, Z., Davis, C., Paulson, J., Stevens, J., Rupprecht, C., Holmes, E., Wilson, I. and Donis, R. "New world bats harbor diverse influenza A viruses". *PLoS Pathogens* (2013); 9:1–12

[7] Kates, M., Allison, A., Tyrell, D. and James, A. "Origin of lipids in influenza virus". *Cold Spring Harbor Symposia on Quantitative Biology* (1962); 27:293–301

[8] Compans, R., Content, J. and Duesberg, P. "Structure of the ribonucleoprotein of influenza virus". *Journal of Virology* (1972); 10:795–800

[9] Murti, K., Webster, R. and Jones, I. "Localization of RNA polymerases on influenza viral ribonucleoproteins by immunogold labeling". *Virology* (1988); 164:562–566

[10] Desselberger, U., Racaniello, V., Zazra, J. and Palese, P. "The 3' and 5'-terminal sequences of influenza A, B, and C virus RNA segments are highly conserved and show partial inverted complementarity". *Gene* (1980); 8:315 – 328

[11] Flick, R., Neumann, G., Hoffmann, E., Neumeier, E. and Hobom, G. "Promoter elements in the influenza vRNA terminal structure." *RNA* (1996); 2:1046–1057

[12] Hsu, M., Parvin, J., Gupta, S., Krystal, M. and Palese, P. "Genomic RNAs of influenza viruses are held in a circular conformation in virions and in infected cells by a terminal panhandle." *Proc Natl Acad Sci USA* (1987); 84:8140–8144

[13] Fodor, E., Pritlove, D. and Brownlee, G. "The influenza virus panhandle is involved in the initiation of transcription." *Journal of Virology* (1994); 68:4092–4096

[14] Crescenzo-Chaigne, B., Barbezange, C. and van der Werf, S. "Non coding extremities of the seven influenza virus type C vRNA segments: Effect on transcription and replication by the type C and type A polymerase complexes". *Virology Journal* (2008); 5:1–11

[15] Yamayoshi, S., Watanabe, M., Goto, H. and Kawaoka, Y. "Identification of a novel viral protein expressed from the PB2 segment of influenza A virus". *Journal of Virology* (2016); 90:444–456

[16] Hutchinson, E., Charles, P., Hester, S., Thomas, B., Trudgian, D., Martínez-Alonso, M. and Fodor, E. "Conserved and host-specific features of influenza virion architecture". *Nature Communications* (2014); 5:1–10

[17] Wise, H., Foeglein, A., Sun, J., Dalton, R., Patel, S., Howard, W., Anderson, E., Barclay, W. and Digard, P. "A complicated message: Identification of a novel PB1-related protein translated from influenza A virus segment 2 mRNA". *Journal of Virology* (2009); 83:8021–8031

[18] Chen, W., Calvo, P., Malide, D., Gibbs, J., Schubert, U., Bacik, I., Basta, S., O'Neill, R., Schickli, J., Palese, P., Henklein, P., Bennink, J. and Yewdell, J. "A novel influenza A virus mitochondrial protein that induces cell death". *Nature Medicine* (2001); 7:1306–1312

[19] Jagger, B., Wise, H., Kash, J., Walters, K., Wills, N., Xiao, Y., Dunfee, R., Schwartzman, L., Ozinsky, A., Bell, G., Dalton, R., Lo, A., Efstathiou, S., Atkins, J., Firth, A., Taubenberger, J. and Digard, P. "An overlapping protein-coding region in influenza a virus segment 3 modulates the host response". *Science* (2012); 337:199–204

[20] Vasin, A., Temkina, O., Egorov, V., Klotchenko, S., Plotnikova, M. and Kiselev, O. "Molecular mechanisms enhancing the proteome of influenza A viruses: An overview of recently discovered proteins". *Virus Research* (2014); 185:53–63

[21] Nagayama, K. and Danev, R. "Phase contrast electron microscopy: development of thin-film phase plates and biological applications". *Philosophical Transactions of the Royal Society of London B: Biological Sciences* (2008); 363:2153–2162

[22] Horimoto, T. and Kawaoka, Y. "Influenza: lessons from past pandemics, warnings from current incidents". *Nature Reviews Microbiology* (2005); 3:591–600

[23] Matlin, K., Reggio, H., Helenius, A. and Simons, K. "Infectious entry pathway of influenza virus in a canine kidney cell line." *The Journal of Cell Biology* (1981); 91:601–13

[24] Bullough, P., Hughson, F., Skehel, J. and Wiley, D. "Structure of influenza haemagglutinin at the pH of membrane fusion". *Nature* (1994); 371:37–43

[25] Palese, P., Tobita, K., Ueda, M. and Compans, R. "Characterization of temperature sensitive influenza virus mutants defective in neuraminidase". *Virology* (1974); 61:397–410

[26] Sugrue, R. and Hay, A. "Structural characteristics of the M2 protein of influenza A viruses: Evidence that it forms a tetrameric channel". *Virology* (1991); 180:617–624

[27] Noton, S., Medcalf, E., Fisher, D., Mullin, A., Elton, D. and Digard, P. "Identification of the domains of the influenza A virus M1 matrix protein required for NP binding, oligomerization and incorporation into virions." *The Journal of General Virology* (2007); 88:2280–2290

[28] Das, K., Aramini, J., Ma, L., Krug, R. and Arnold, E. "Structures of influenza A proteins and insights into antiviral drug targets". *Nat Struct Mol Biol* (2010); 17:530–538

[29] Couceiro, J., Paulson, J. and Baum, L. "Influenza virus strains selectively recognize sialyloligosaccharides on human respiratory epithelium; the role of the host cell in selection of hemagglutinin receptor specificity". *Virus Research* (1993); 29:155–165

[30] Connor, R., Kawaoka, Y., Webster, R. and Paulson, J. "Receptor specificity in human, avian, and equine H2 and H3 influenza virus isolates". *Virology* (1994); 205:17–23

[31] Matlin, K., Reggio, H., Helenius, A. and Simons, K. "Infectious entry pathway of influenza virus in a canine kidney cell line." *The Journal of Cell Biology* (1981); 91:601–13

[32] Skehel, J. and Wiley, D. "Receptor binding and membrane fusion in virus entry: The influenza hemagglutinin". *Annual Review of Biochemistry* (2000); 69:531–569

[33] Tsurudome, M., Glück, R., Graf, R., Falchetto, R., Schaller, U. and Brunner, J. "Lipid interactions of the hemagglutinin HA2 NH2-terminal segment during influenza virus-induced membrane fusion". *Journal of Biological Chemistry* (1992); 267:20225–20232

[34] Helenius, A. "Unpacking the incoming influenza virus". *Cell* (1992); 69:577–578

[35] Cros, J., García-Sastre, A. and Palese, P. "An unconventional NLS is critical for the nuclear import of the influenza A virus nucleoprotein and ribonucleoprotein". *Traffic* (2005); 6:205–213

[36] Wu, W. and Panté, N. "The directionality of the nuclear transport of the influenza A genome is driven by selective exposure of nuclear localization sequences on nucleoprotein". *Virology Journal* (2009); 6:1–12

[37] Ulmanen, I., Broni, B. and Krug, R. "Role of two of the influenza virus core P proteins in recognizing cap 1 structures (m7GpppNm) on RNAs and in initiating viral RNA transcription." *PNAS* (1981); 78:7355–7359

[38] Plotch, S., Bouloy, M., Ulmanen, I. and Krug, R. "A unique cap(m7gpppxm)-dependent influenza virion endonuclease cleaves capped RNAs to generate the primers that initiate viral RNA transcription." *Cell* (1981); 23:847–858

[39] Neumann, G., Brownlee, G., Fodor, E. and Kawaoka, Y. "Orthomyxovirus replication, transcription, and polyadenylation". *Current topics in microbiology and immunology* (2004); 283:121–143

[40] Luo, G., Luytjes, W., Enami, M. and Palese, P. "The polyadenylation signal of influenza virus RNA involves a stretch of uridines followed by the RNA duplex of the panhandle structure." *Journal of Virology* (1991); 65:2861–2867

[41] Poon, L., Pritlove, D., Fodor, E. and Brownlee, G. "Direct evidence that the poly(A) tail of influenza A virus mRNA is synthesized by reiterative copying of a U track in the virion RNA template". *Journal of Virology* (1999); 73:3473–3476

[42] Nemeroff, M., Barabino, S., Li, Y., Keller, W. and Krug, R. "Influenza virus NS1 protein interacts with the cellular 30 kDa subunit of CPSF and inhibits 3' end formation of cellular pre-mRNAs". *Molecular Cell* (1998); 1:991–1000

[43] Shimizu, K., Iguchi, A., Gomyou, R. and Ono, Y. "Influenza virus inhibits cleavage of the HSP70 pre-mRNAs at the polyadenylation site". *Virology* (1999); 254:213–219

[44] Smith, G., Levin, J., Palese, P. and Moss, B. "Synthesis and cellular location of the ten influenza polypeptides individually expressed by recombinant vaccinia viruses". *Virology* (1987); 160:336–345

[45] Bouvier, N. and Palese, P. "The biology of influenza viruses." *Vaccine* (2008); 26:49–53

[46] Leser, G. and Lamb, R. "Influenza virus assembly and budding in raft-derived microdomains: A quantitative analysis of the surface distribution of HA, NA and M2 proteins". *Virology* (2005); 342:215–227

[47] Perez, J., Varble, A., Sachidanandam, R., Zlatev, I., Manoharan, M., García-Sastre, A. and tenOever, B. "Influenza A virus-generated small RNAs regulate the switch from transcription to replication". *Proceedings of the National Academy of Sciences* (2010); 107:11525–11530

[48] Robb, N., Smith, M., Vreede, F. and Fodor, E. "NS2/NEP protein regulates transcription and replication of the influenza virus RNA genome". *Journal of General Virology* (2009); 90:1398–1407

[49] Vreede, F., Jung, T. and Brownlee, G. "Model suggesting that replication of influenza virus is regulated by stabilization of replicative intermediates". *Journal of Virology* (2004); 78:9568–9572

[50] Neumann, G., Hughes, M. and Kawaoka, Y. “Influenza a virus NS2 protein mediates vRNP nuclear export through NES-independent interaction with hCRM1”. *The EMBO Journal* (2000); 19:6751–6758

[51] Brunotte, L., Flies, J., Bolte, H., Reuther, P., Vreede, F. and Schwemmle, M. “The nuclear export protein of H5N1 influenza A viruses recruits matrix 1 (M1) protein to the viral ribonucleoprotein to mediate nuclear export”. *Journal of Biological Chemistry* (2014); 289:20067–20077

[52] Nayak, D., Hui, E. and Barman, S. “Assembly and budding of influenza virus.” *Virus Research* (2004); 106:147–165

[53] Rossman, J. and Lamb, R. “Influenza virus assembly and budding.” *Virology* (2011); 411:2280–2290

[54] Medzhitov, R. and Janeway, C. “Innate immunity: The virtues of a nonclonal system of recognition”. *Cell* (1997); 91:295–298

[55] Riera Romo, M., Pérez-Martínez, D. and Castillo Ferrer, C. “Innate immunity in vertebrates: an overview”. *Immunology* (2016); pp. 125–39

[56] Medzhitov, R. “Recognition of microorganisms and activation of the immune response”. *Nature* (2007); 449:819–826

[57] Pestka, S. “The interferons: 50 years after their discovery, there is much more to learn”. *Journal of Biological Chemistry* (2007); 282:20047–20051

[58] Onoguchi, K., Yoneyama, M., Takemura, A., Akira, S., Taniguchi, T., Namiki, H. and Fujita, T. “Viral infections activate types I and III interferon genes through a common mechanism”. *Journal of Biological Chemistry* (2007); 282:7576–7581

[59] Takeuchi, O. and Akira, S. “Pattern recognition receptors and inflammation”. *Cell* (2010); 140:805–820

[60] Weber, F. “The catcher in the RIG-I”. *Cytokine* (2015); 76:38–41

[61] Gack, M., Shin, Y., Joo, C., Urano, T., Liang, C., Sun, L., Takeuchi, O., Akira, S., Chen, Z., Inoue, S. and Jung, J. “TRIM25 RING-finger E3 ubiquitin ligase is essential for RIG-I-mediated antiviral activity”. *Nature* (2007); 446:916–920

[62] Hou, F., Sun, L., Zheng, H., Skaug, B., Jiang, Q. and Chen, Z. “MAVS forms functional prion-like aggregates to activate and propagate antiviral innate immune response”. *Cell* (2011); 146:448–461

[63] Kell, A. and Gale, M. “RIG-I in RNA virus recognition”. *Virology* (2015); 479-480:110–121

[64] Chan, Y. and Gack, M. “RIG-I-like receptor regulation in virus infection and immunity”. *Current Opinion in Virology* (2015); 12:7–14

[65] van Kempen, T., Wenink, M., Leijten, E., Radstake, T. and Boes, M. "Perception of self: distinguishing autoimmunity from autoinflammation". *Nat Rev Rheumatol* (2015); 11:483–492

[66] Kumar, H., Kawai, T. and Akira, S. "Toll-like receptors and innate immunity". *Biochemical and Biophysical Research Communications* (2009); 388:621–625

[67] Lund, J., Alexopoulou, L., Sato, A., Karow, M., Adams, N., Gale, N., Iwasaki, A. and Flavell, R. "Recognition of single-stranded RNA viruses by Toll-like receptor 7". *PNAS* (2004); 101:5598–5603

[68] Blasius, A. and Beutler, B. "Intracellular toll-like receptors". *Immunity* (2010); 32:305–315

[69] Mogensen, T. "Pathogen recognition and inflammatory signaling in innate immune defenses". *Clinical Microbiology Reviews* (2009); 22:240–273

[70] Randall, R. and Goodbourn, S. "Interferons and viruses: an interplay between induction, signalling, antiviral responses and virus countermeasures". *Journal of General Virology* (2008); 89:1–47

[71] Ivashkiv, L. and Donlin, L. "Regulation of type I interferon responses". *Nat Rev Immunol* (2014); 14:36–49

[72] Haller, O., Kochs, G. and Weber, F. "The interferon response circuit: Induction and suppression by pathogenic viruses". *Virology* (2006); 344:119–130

[73] Whittemore, L. and Maniatis, T. "Postinduction turnoff of beta-interferon gene expression." *Molecular and Cellular Biology* (1990); 10:1329–1337

[74] Shaw, G. and Kamen, R. "A conserved AU sequence from the 3' untranslated region of GM-CSF mRNA mediates selective mRNA degradation". *Cell* (1986); 46:659–667

[75] Barreau, C., Paillard, L. and Osborne, H. "AU-rich elements and associated factors: are there unifying principles?" *Nucleic Acids Research* (2005); 33:7138–7150

[76] Khabar, K. and Young, H. "Post-transcriptional control of the interferon system". *Biochimie* (2007); 89:761–769

[77] Chen, C., Gherzi, R., Ong, S., Chan, E., Raijmakers, R., Pruijn, G., Stoecklin, G., Moroni, C., Mann, M. and Karin, M. "AU binding proteins recruit the exosome to degrade ARE-containing mRNAs". *Cell* (2001); 107:451–464

[78] Houseley, J., LaCava, J. and Tollervey, D. "RNA-quality control by the exosome". *Nature Reviews Molecular Cell Biology* (2006); 7:529–539

[79] David Gerecht, P., Taylor, M. and Port, J. "Intracellular localization and interaction of mRNA binding proteins as detected by FRET". *BMC Cell Biology* (2010); 11:1–18

[80] Briata, P., Forcales, S., Ponassi, M., Corte, G., Chen, C., Karin, M., Puri, P. and Gherzi, R. "p38-dependent phosphorylation of the mRNA decay-promoting factor KSRP controls the stability of select myogenic transcripts". *Molecular Cell* (2005); 20:891–903

[81] Díaz-Moreno, I., Hollingworth, D., Frenkiel, T., Kelly, G., Martin, S., Howell, S., García-Mayoral, M., Gherzi, R., Briata, P. and Ramos, A. "Phosphorylation-mediated unfolding of a KH domain regulates KSRP localisation via 14-3-3 binding". *Nature structural and molecular biology* (2009); 16:238–246

[82] Sandler, H. and Stoecklin, G. "Control of mRNA decay by phosphorylation of tristetraprolin". *Biochemical Society Transactions* (2008); 36:491–496

[83] Brook, M., Tchen, C., Santalucia, T., McIlrath, J., Arthur, J., Saklatvala, J. and Clark, A. "Posttranslational regulation of tristetraprolin subcellular localization and protein stability by p38 mitogen-activated protein kinase and extracellular signal-regulated kinase pathways". *Molecular and Cellular Biology* (2006); 26:2408–2418

[84] Winzen, R., Thakur, B., Dittrich-Breiholz, O., Shah, M., Redich, N., Dhamija, S., Kracht, M. and Holtmann, H. "Functional analysis of KSRP interaction with the AU-rich element of interleukin-8 and identification of inflammatory mRNA targets". *Molecular and Cellular Biology* (2007); 27:8388–8400

[85] King, P. and Chen, C. "Role of KSRP in control of type I interferon and cytokine expression". *Journal of Interferon and Cytokine Research* (2014); 34:267–274

[86] Lin, W., Zheng, X., Lin, C., Tsao, J., Zhu, X., Cody, J., Coleman, J., Gherzi, R., Luo, M., Townes, T., Parker, J. and Chen, C. "Posttranscriptional control of type I interferon genes by KSRP in the innate immune response against viral infection". *Molecular and Cellular Biology* (2011); 31:3196–3207

[87] Briata, P., Chen, C., Ramos, A. and Gherzi, R. "Functional and molecular insights into KSRP function in mRNA decay". *Biochimica et Biophysica Acta - Gene Regulatory Mechanisms* (2013); 1829:689–694

[88] Dhamija, S., Kuehne, N., Winzen, R., Doerrie, A., Dittrich-Breiholz, O., Thakur, B., Kracht, M. and Holtmann, H. "Interleukin-1 activates synthesis of interleukin-6 by interfering with a KH-type splicing regulatory protein (KSRP)-dependent translational silencing mechanism". *Journal of Biological Chemistry* (2011); 286:33279–33288

[89] Trabucchi, M., Briata, P., Garcia-Mayoral, M., Haase, A., Filipowicz, W., Ramos, A., Gherzi, R. and Rosenfeld, M. "The RNA-binding protein KSRP promotes the biogenesis of a subset of microRNAs". *Nature* (2009); 459:1010–1014

[90] Briata, P., Chen, C., Giovarelli, M., Pasero, M., Trabucchi, M., Ramos, A. and Gherzi, R. "KSRP, many functions for a single protein." *Frontiers in Bioscience (Landmark Ed)*. (2011); 16:1787–1796

[91] Tiedje, C., Holtmann, H. and Gaestel, M. "The role of mammalian MAPK signaling in regulation of cytokine mRNA stability and translation". *Journal of Interferon & Cytokine Research* (2014); 34:220–232

[92] Rothé, F., Gueydan, C., Bellefroid, E., Huez, G. and Kruys, V. "Identification of FUSE-binding proteins as interacting partners of TIA proteins". *Biochemical and Biophysical Research Communications* (2006); 343:57–68

[93] Lin, J., Li, M. and Shih, S. "Far upstream element binding protein 2 interacts with enterovirus 71 internal ribosomal entry site and negatively regulates viral translation". *Nucleic Acids Research* (2009); 37:47–59

[94] Proud, C. "eIF2 and the control of cell physiology". *Seminars in Cell & Developmental Biology* (2005); 16:3–12

[95] Haines, G., Becker, S., Ghadge, G., Kies, M., Pelzer, H. and Radosevich, J. "Expression of the double-stranded RNA-dependent protein kinase (p68) in squamous cell carcinoma of the head and neck region". *Archives of Otolaryngology: Head & Neck Surgery* (1993); 119:1142–1147

[96] Zhu, S., Romano, P. and Wek, R. "Ribosome targeting of PKR is mediated by two double-stranded RNA-binding domains and facilitates in vivo phosphorylation of eukaryotic initiation factor-2". *Journal of Biological Chemistry* (1997); 272:14434–14441

[97] Jeffrey, I., Kadereit, S., Meurs, E., Metzger, T., Bachmann, M., Schwemmle, M., Hovanessian, A. and Clemens, M. "Nuclear localization of the interferon-inducible protein kinase PKR in human cells and transfected mouse cells". *Experimental Cell Research* (1995); 218:17–27

[98] Kuhen, K. and Samuel, C. "Mechanism of interferon action: Functional characterization of positive and negative regulatory domains that modulate transcriptional activation of the human RNA-dependent protein kinase PKR promoter". *Virology* (1999); 254:182–195

[99] Cole, J. "Activation of PKR: an open and shut case?" *Trends in Biochemical Sciences* (2007); 32:57–62

[100] Meurs, E., Chong, K., Galabru, J., Thomas, N., Kerr, I., Williams, B. and Hovanessian, A. "Molecular cloning and characterization of the human double-stranded RNA-activated protein kinase induced by interferon". *Cell* (1990); 62:379–390

[101] Dey, M., Mann, B., Anshu, A. and Mannan, M. "Activation of protein kinase PKR requires dimerization-induced cis-phosphorylation within the activation loop". *Journal of Biological Chemistry* (2014); 289:5747–5757

[102] Zhang, F., Romano, P., Nagamura-Inoue, T., Tian, B., Dever, T., Mathews, M., Ozato, K. and Hinnebusch, A. "Binding of double-stranded RNA to protein kinase PKR is required for dimerization and promotes critical autophosphorylation events in the activation loop". *Journal of Biological Chemistry* (2001); 276:24946–24958

[103] Lemaire, P., Lary, J. and Cole, J. "Mechanism of PKR activation: Dimerization and kinase activation in the absence of double-stranded RNA". *Journal of Molecular Biology* (2005); 345:81–90

[104] de Haro, C., Méndez, R. and Santoyo, J. "The eIF2αkinases and the control of protein synthesis." *The FASEB Journal* (1996); 10:1378–87

[105] Hanks, S., Quinn, A. and Hunter, T. "The protein kinase family: conserved features and deduced phylogeny of the catalytic domains". *Science* (1988); 241:42–52

[106] Thomis, D. and Samuel, C. "Mechanism of interferon action: characterization of the intermolecular autophosphorylation of PKR, the interferon-inducible, RNA-dependent protein kinase." *Journal of Virology* (1995); 69:5195–5198

[107] Hatada, E., Saito, S. and Fukuda, R. "Mutant influenza viruses with a defective NS1 protein cannot block the activation of PKR in infected cells". *Journal of Virology* (1999); 73:2425–2433

[108] Nallagatla, S., Hwang, J., Toroney, R., Zheng, X., Cameron, C. and Bevilacqua, P. "5'-Triphosphate-dependent activation of PKR by RNAs with short stem-loops". *Science* (2007); 318:1455–1458

[109] Dauber, B., Martínez-Sobrido, L., Schneider, J., Hai, R., Waibler, Z., Kalinke, U., García-Sastre, A. and Wolff, T. "Influenza B virus ribonucleoprotein is a potent activator of the antiviral kinase PKR". *PLoS Pathogens* (2009); 5:1–12

[110] Lemaire, P., Anderson, E., Lary, J. and Cole, J. "Mechanism of PKR activation by dsRNA". *Journal of Molecular Biology* (2008); 381:351–360

[111] McMillan, N., Carpick, B., Hollis, B., Toone, W., Zamanian-Daryoush, M. and Williams, B. "Mutational analysis of the double-stranded RNA (dsRNA) binding domain of the dsRNA-activated protein kinase, PKR". *Journal of Biological Chemistry* (1995); 270:2601–2606

[112] García, M., Meurs, E. and Esteban, M. "The dsRNA protein kinase PKR: Virus and cell control". *Biochimie* (2007); 89:799–811

[113] Hovanessian, A. and Galabru, J. "The double-stranded RNA-dependent protein kinase is also activated by heparin". *European Journal of Biochemistry* (1987); 167:467–473

[114] Saelens, X., Kalai, M. and Vandenabeele, P. "Translation inhibition in apoptosis: Caspase-dependent PKR activation and eIF2α phosphorylation". *Journal of Biological Chemistry* (2001); 276:41620–41628

[115] Patel, R. and Sen, G. "PACT, a protein activator of the interferon-induced protein kinase, PKR". *The EMBO Journal* (1998); 17:4379–4390

[116] Pataer, A., Vorburger, S., Barber, G., Chada, S., Mhashilkar, A., Zou-Yang, H., Stewart, A., Balachandran, S., Roth, J., Hunt, K. and Swisher, S. "Adenoviral transfer of the melanoma differentiation-associated gene 7 (mda7) induces apoptosis of lung cancer cells via up-regulation of the double-stranded RNA-dependent protein kinase (PKR)". *Cancer Research* (2002); 62:2239–2243

[117] Kirkegaard, K., Taylor, M. and Jackson, W. "Cellular autophagy: Surrender, avoidance and subversion by microorganisms". *Nature Reviews Microbiology* (2004); 2:301–314

[118] Pindel, A. and Sadler, A. "The role of protein kinase R in the interferon response". *Journal of Interferon & Cytokine Research* (2011); 31:59–70

[119] Hershey, J. "Translational control in mammalian cells". *Annual Review of Biochemistry* (1991); 60:717–755

[120] Onomoto, K., Jogi, M., Yoo, J., Narita, R., Morimoto, S., Takemura, A., Sambhara, S., Kawaguchi, A., Osari, S., Nagata, K., Matsumiya, T., Namiki, H., Yoneyama, M. and Fujita, T. "Critical role of an antiviral stress granule containing RIG-I and PKR in viral detection and innate immunity". *PLoS ONE* (2012); 7:1–15

[121] Guerra, S., López-Fernández, L., García, M., Zaballos, A. and Esteban, M. "Human gene profiling in response to the active protein kinase, interferon-induced serine/threonine protein kinase (PKR), in infected cells: Involvement of the transcription factor ATF-3 in PKR-induced apoptosis". *Journal of Biological Chemistry* (2006); 281:18734–18745

[122] Lee, E., Yoon, C., Kim, Y. and Bae, Y. "The double-strand RNA-dependent protein kinase PKR plays a significant role in a sustained ER stress-induced apoptosis". *FEBS Letters* (2007); 581:4325–4332

[123] Harding, H., Zhang, Y., Zeng, H., Novoa, I., Lu, P., Calfon, M., Sadri, N., Yun, C., Popko, B., Paules, R. Stojdl, D., Bell, J., Hettmann, T., Leiden, J. and Ron, D. "An integrated stress response regulates amino acid metabolism and resistance to oxidative stress". *Molecular Cell* (2003); 11:619–633

[124] Harding, H., Novoa, I., Zhang, Y., Zeng, H., Wek, R., Schapira, M. and Ron, D. "Regulated translation initiation controls stress-induced gene expression in mammalian cells". *Molecular Cell* (2000); 6:1099–1108

[125] Goh, K., deVeer, M. and Williams, B. "The protein kinase PKR is required for p38 MAPK activation and the innate immune response to bacterial endotoxin". *The EMBO Journal* (2000); 19:4292–4297

[126] Chu, W., Ostertag, D., Li, Z., Chang, L., Chen, Y., Hu, Y., Williams, B., Perrault, J. and Karin, M. "JNK2 and IKKβare required for activating the innate response to viral infection". *Immunity* (1999); 11:721–731

[127] Williams, B. "Signal integration via PKR". *Science Signaling* (2001); 2001:re2

[128] Zamanian-Daryoush, M., Mogensen, T., DiDonato, J. and Williams, B. "NF-κB activation by double-stranded-RNA-activated protein kinase (PKR) is mediated through NF-κB-inducing kinase and IκB kinase". *Molecular and Cellular Biology* (2000); 20:1278–1290

[129] García, M., Gil, J., Ventoso, I., Guerra, S., Domingo, E., Rivas, C. and Esteban, M. "Impact of protein kinase PKR in cell biology: from antiviral to antiproliferative action". *Microbiology and Molecular Biology Reviews* (2006); 70:1032–1060

[130] Cuddihy, A., Wong, A., Tam, N., Li, S. and Koromilas, A. "The double-stranded RNA activated protein kinase PKR physically associates with the tumor suppressor p53 protein and phosphorylates human p53 on serine 392 in vitro". *Oncogene* (1999); 18:2690–2702

[131] Yeung, M., Liu, J. and Lau, A. "An essential role for the interferon-inducible, double-stranded RNA-activated protein kinase PKR in the tumor necrosis factor-induced apoptosis in U937 cells." *PNAS* (1996); 93:12451–12455

[132] Toth, A., Zhang, P., Das, S., George, C. and Samuel, C. "Interferon action and the double-stranded RNA-dependent enzymes ADAR1 adenosine deaminase and PKR protein kinase". *Progress in Nucleic Acid Research and Molecular Biology* (2006); 81:369–434

[133] Li, Z., Wolff, K. and Samuel, C. "RNA adenosine deaminase ADAR1 deficiency leads to increased activation of protein kinase PKR and reduced vesicular stomatitis virus growth following interferon treatment". *Virology* (2010); 396:316–322

[134] Xu, Z. and Williams, B. "The B56α regulatory subunit of protein phosphatase 2A is a target for regulation by double-stranded RNA-dependent protein kinase PKR". *Molecular and Cellular Biology* (2000); 20:5285–5299

[135] Ruvolo, V., Kurinna, S., Karanjeet, K., Schuster, T., Martelli, A., McCubrey, J. and Ruvolo, P. "PKR regulates B56α-mediated BCL2 phosphatase activity in acute lymphoblastic leukemia-derived REH cells". *Journal of Biological Chemistry* (2008); 283:35474–35485

[136] Lee, S. and Esteban, M. "The interferon-induced double-stranded RNA-activated protein kinase induces apoptosis." *Virology* (1994); 199:491–496

[137] Gil, J. and Esteban, M. "Induction of apoptosis by the dsRNA-dependent protein kinase (PKR): Mechanism of action". *Apoptosis* (2000); 5:107–114

[138] Nover, L., Scharf, K. and Neumann, D. "Formation of cytoplasmic heat shock granules in tomato cell cultures and leaves." *Molecular and Cellular Biology* (1983); 3:1648–1655

[139] Kedersha, N., Gupta, M., Li, W., Miller, I. and Anderson, P. "RNA-binding proteins Tia-1 and Tiar link the phosphorylation of eIF2α to the assembly of mammalian stress granules". *The Journal of Cell Biology* (1999); 147:1431–1442

[140] Anderson, P. and Kedersha, N. “Stressful initiations”. *Journal of Cell Science* (2002); 115:3227–3234

[141] Anderson, P. and Kedersha, N. “RNA granules”. *The Journal of Cell Biology* (2006); 172:803–808

[142] Kedersha, N. and Anderson, P. “Chapter 4: Regulation of translation by stress granules and processing bodies”. In *Translational Control in Health and Disease*, vol. 90 of *Progress in Molecular Biology and Translational Science*, pp. 155–185. Academic Press (2009);

[143] Zhang, P., Li, Y., Xia, J., He, J., Pu, J., Xie, J., Wu, S., Feng, L., Huang, X. and Zhang, P. “IPS-1 plays an essential role in dsRNA-induced stress granule formation by interacting with PKR and promoting its activation”. *Journal of Cell Science* (2014); 127:2471–2482

[144] Reineke, L. and Lloyd, R. “The stress granule protein G3BP1 recruits protein kinase R to promote multiple innate immune antiviral responses”. *Journal of Virology* (2015); 89:2575–2589

[145] den Boon, J. and Ahlquist, P. “Organelle-like membrane compartmentalization of positive-strand RNA virus replication factories”. *Annual Review of Microbiology* (2010); 64:241–256

[146] Ning, Y., Wang, M., Deng, M., Shen, S., Liu, W., Cao, W., Deng, F., Wang, Y., Hu, Z. and Wang, H. “Viral suppression of innate immunity via spatial isolation of TBK1/IKKε from mitochondrial antiviral platform”. *Journal of Molecular Cell Biology* (2014); 6:324–337

[147] Santiago, F., Covaleda, L., Sanchez-Aparicio, M., Silvas, J., Diaz-Vizarreta, A., Patel, J., Popov, V., Yu, X., García-Sastre, A. and Aguilar, P. “Hijacking of RIG-I signaling proteins into virus-induced cytoplasmic structures correlates with the inhibition of type I interferon responses”. *Journal of Virology* (2014); 88:4572–4585

[148] Graef, K., Vreede, F., Lau, Y., McCall, A., Carr, S., Subbarao, K. and Fodor, E. “The PB2 subunit of the influenza virus RNA polymerase affects virulence by interacting with the mitochondrial antiviral signaling protein and inhibiting expression of beta interferon”. *Journal of Virology* (2010); 84:8433–8445

[149] Varga, Z., Grant, A., Manicassamy, B. and Palese, P. “Influenza virus protein PB1-F2 inhibits the induction of type I interferon by binding to MAVS and decreasing mitochondrial membrane potential”. *Journal of Virology* (2012); 86:8359–8366

[150] Prins, K., Cárdenas, W. and Basler, C. “Ebola virus protein VP35 impairs the function of interferon regulatory factor-activating kinases IKKε and TBK-1”. *Journal of Virology* (2009); 83:3069–3077

[151] Gao, S., Song, L., Li, J., Zhang, Z., Peng, H., Jiang, W., Wang, Q., Kang, T., Chen, S. and Huang, W. “Influenza A virus-encoded NS1 virulence factor protein inhibits innate immune response by targeting IKK”. *Cellular Microbiology* (2012); 14:1849–1866

[152] Fang, X., Gao, J., Zheng, H., Li, B., Kong, L., Zhang, Y., Wang, W., Zeng, Y. and Ye, L. "The membrane protein of SARS-CoV suppresses NF-κB activation". *Journal of Medical Virology* (2007); 79:1431–1439

[153] Guo, J., Hayashi, J. and Seeger, C. "West Nile virus inhibits the signal transduction pathway of alpha interferon". *Journal of Virology* (2005); 79:1343–1350

[154] Okumura, A., Pitha, P., Yoshimura, A. and Harty, R. "Interaction between Ebola virus glycoprotein and host Toll-like receptor 4 leads to induction of proinflammatory cytokines and SOCS1". *Journal of Virology* (2010); 84:27–33

[155] Pauli, E., Schmolke, M., Wolff, T., Viemann, D., Roth, J., Bode, J. and Ludwig, S. "Influenza A virus inhibits type I IFN signaling via NF-κB-dependent induction of SOCS-3 expression". *PLoS Pathogens* (2008); 4:1–15

[156] Jia, D., Rahbar, R., Chan, R., Lee, S., Chan, M., Wang, B., Baker, D., Sun, B., Peiris, J., Nicholls, J. and Fish, E. "Influenza virus non-structural protein 1 (NS1) disrupts interferon signaling". *PLoS ONE* (2010); 5:1–13

[157] Mazzon, M., Jones, M., Davidson, A., Chain, B. and Jacobs, M. "Dengue virus NS5 inhibits interferon-α signaling by blocking signal transducer and activator of transcription 2 phosphorylation". *Journal of Infectious Diseases* (2009); 200:1261–1270

[158] Muñoz Jordán, J., Laurent-Rolle, M., Ashour, J., Martínez-Sobrido, L., Ashok, M., Lipkin, W. and García-Sastre, A. "Inhibition of alpha/beta interferon signaling by the NS4B protein of flaviviruses". *Journal of Virology* (2005); 79:8004–8013

[159] Ma, D. and Suthar, M. "Mechanisms of innate immune evasion in re-emerging RNA viruses". *Current Opinion in Virology* (2015); 12:26–37

[160] Dauber, B. and Wolff, T. "Activation of the antiviral kinase PKR and viral countermeasures." *Viruses* (2009); 1:523–544

[161] Min, J., Li, S., Sen, G. and Krug, R. "A site on the influenza a virus NS1 protein mediates both inhibition of PKR activation and temporal regulation of viral RNA synthesis". *Virology* (2007); 363:236–243

[162] Cassady, K. and Gross, M. "The herpes simplex virus type 1 US11 protein interacts with protein kinase R in infected cells and requires a 30-amino-acid sequence adjacent to a kinase substrate domain". *Journal of Virology* (2002); 76:2029–2035

[163] Romano, P., Zhang, F., Tan, S., Garcia-Barrio, M., Katze, M., Dever, T. and Hinnebusch, A. "Inhibition of double-stranded RNA-dependent protein kinase PKR by Vaccinia virus E3: Role of complex formation and the E3 N-terminal domain". *Molecular and Cellular Biology* (1998); 18:7304–7316

[164] Chang, H., Watson, J. and Jacobs, B. "The E3L gene of vaccinia virus encodes an inhibitor of the interferon-induced, double-stranded RNA-dependent protein kinase". *Proceedings of the National Academy of Sciences* (1992); 89:4825–4829

[165] Perdiguero, B. and Esteban, M. "The interferon system and vaccinia virus evasion mechanisms". *Journal of Interferon & Cytokine research* (2009); 29:581–598

[166] Bierle, C., Semmens, K. and Geballe, A. "Double-stranded RNA binding by the human cytomegalovirus PKR antagonist TRS1". *Virology* (2013); 442:28–37

[167] Li, S., Min, J., Krug, R. and Sen, G. "Binding of the influenza A virus NS1 protein to PKR mediates the inhibition of its activation by either PACT or double-stranded RNA". *Virology* (2006); 349:13–21

[168] Tawaratsumida, K., Phan, V., Hrincius, E., High, A., Webby, R., Redecke, V. and Häcker, H. "Quantitative proteomic analysis of the influenza A virus nonstructural proteins NS1 and NS2 during natural cell infection identifies PACT as an NS1 target protein and antiviral host factor". *Journal of Virology* (2014); 88:9038–9048

[169] Luthra, P., Ramanan, P., Mire, C., Weisend, C., Tsuda, Y., Yen, B., Liu, G., Leung, D., Geisbert, T., Ebihara, H., Amarasinghe, G. and Basler, C. "Mutual antagonism between the ebola virus VP35 protein and the RIG-I activator PACT determines infection outcome". *Cell Host & Microbe* (2013); 14:74–84

[170] Brand, S., Kobayashi, R. and Mathews, M. "The Tat protein of human immunodeficiency virus type 1 is a substrate and inhibitor of the interferon-induced, virally activated protein kinase, PKR". *Journal of Biological Chemistry* (1997); 272:8388–8395

[171] He, B., Gross, M. and Roizman, B. "The γ134.5 protein of herpes simplex virus 1 has the structural and functional attributes of a protein phosphatase 1 regulatory subunit and is present in a high molecular weight complex with the enzyme in infected cells". *Journal of Biological Chemistry* (1998); 273:20737–20743

[172] Habjan, M., Pichlmair, A., Elliott, R., Överby, A., Glatter, T., Gstaiger, M., Superti-Furga, G., Unger, H. and Weber, F. "NSs protein of rift valley fever virus induces the specific degradation of the double-stranded RNA-dependent protein kinase". *Journal of Virology* (2009); 83:4365–4375

[173] García-Sastre, A., Egorov, A., Matassov, D., Brandt, S., Levy, D., Durbin, J., Palese, P. and Muster, T. "Influenza a virus lacking the NS1 gene replicates in interferon-deficient systems". *Virology* (1998); 252:324–330

[174] Hatada, E. and Fukuda, R. "Binding of influenza A virus NS1 protein to dsRNA in vitro". *Journal of General Virology* (1992); 73:3325–3329

[175] Egorov, A., Brandt, S., Sereinig, S., Romanova, J., Ferko, B., Katinger, D., Grassauer, A., Alexandrova, G., Katinger, H. and Muster, T. "Transfectant influenza A viruses with long deletions in the NS1 protein grow efficiently in Vero cells". *Journal of Virology* (1998); 72:6437–6441

[176] Marc, D., Barbachou, S. and Soubieux, D. "The RNA-binding domain of influenzavirus non-structural protein-1 cooperatively binds to virus-specific RNA sequences in a structure-dependent manner". *Nucleic Acids Research* (2013); 41:434–449

[177] Mibayashi, M., Martínez-Sobrido, L., Loo, Y., Cárdenas, W., Gale, M. and García-Sastre, A. "Inhibition of retinoic acid-inducible gene I-mediated induction of beta interferon by the NS1 protein of influenza A virus". *Journal of Virology* (2007); 81:514–524

[178] Gack, M., Albrecht, R., Urano, T., Inn, K., Huang, I., Carnero, E., Farzan, M., Inoue, S., Jung, J. and García-Sastre, A. "Influenza A virus NS1 targets the ubiquitin ligase TRIM25 to evade recognition by the host viral RNA sensor RIG-I". *Cell Host & Microbe* (2009); 5:439–449

[179] Hale, B., Randall, R., Ortín, J. and Jackson, D. "The multifunctional NS1 protein of influenza A viruses". *Journal of General Virology* (2008); 89:2359–2376

[180] Khaperskyy, D., Hatchette, T. and McCormick, C. "Influenza A virus inhibits cytoplasmic stress granule formation". *The FASEB Journal* (2012); 26:1629–1639

[181] Qian, X., Alonso-Caplen, F. and Krug, R. "Two functional domains of the influenza virus NS1 protein are required for regulation of nuclear export of mRNA". *Journal of Virology* (1994); 68:2433–2441

[182] Burgui, I., Aragón, T., Ortín, J. and Nieto, A. "PABP1 and eIF4GI associate with influenza virus NS1 protein in viral mRNA translation initiation complexes". *Journal of General Virology* (2003); 84:3263–3274

[183] Hale, B., Jackson, D., Chen, Y., Lamb, R. and Randall, R. "Influenza A virus NS1 protein binds p85β and activates phosphatidylinositol-3-kinase signaling". *Proc Natl Acad Sci USA* (2006); 103:14194–14199

[184] Hale, B.G., Kerry, P.S., Jackson, D., Precious, B.L., Gray, A., Killip, M.J., Randall, R.E. and Russell, R.J. "Structural insights into phosphoinositide 3-kinase activation by the influenza a virus ns1 protein". *Proceedings of the National Academy of Sciences* (2010); 107:1954–1959

[185] Forbes, N., Ping, J., Dankar, S., Jia, J., Selman, M., Keleta, L., Zhou, Y. and Brown, E. "Multifunctional adaptive NS1 mutations are selected upon human influenza virus evolution in the mouse". *PLoS ONE* (2012); 7:1–20

[186] Cheng, A., Wong, S. and Yuan, Y. "Structural basis for dsRNA recognition by NS1 protein of influenza A virus". *Cell Research* (2009); 19:187–195

[187] Schierhorn, K. “Mutational analysis of the NS1 protein of influenza A virus and its impact on PKR inhibition and TRAIL regulation”. Ph.D. thesis, Humboldt University Berlin (2015)

[188] Aebersold, R. and Mann, M. “Mass spectrometry-based proteomics”. *Nature* (2003); 422:198–207

[189] Gooley, A., Hughes, G., Humphery-Smith, I., Williams, K. and Hochstrasser, D. “From proteins to proteomes: Large scale protein identification by two-dimensional electrophoresis and amino acid analysis”. *Biotechnology* (1996); 14:1

[190] El-Aneed, A., Cohen, A. and Banoub, J. “Mass spectrometry, review of the basics: Electrospray, MALDI, and commonly used mass analyzers”. *Applied Spectroscopy Reviews* (2009); 44:210–230

[191] Domon, B. and Aebersold, R. “Mass spectrometry and protein analysis”. *Science* (2006); 312:212–217

[192] Kelleher, N. “Peer reviewed: Top-down proteomics”. *Analytical chemistry* (2004); 76:196–203

[193] Chait, B. “Mass spectrometry: Bottom-up or top-down?” *Science* (2006); 314:65–66

[194] Hu, Q., Noll, R., Li, H., Makarov, A., Hardman, M. and Graham Cooks, R. “The Orbitrap: a new mass spectrometer”. *Journal of mass spectrometry* (2005); 40:430–443

[195] Eng, J., McCormack, A. and Yates, J. “An approach to correlate tandem mass spectral data of peptides with amino acid sequences in a protein database”. *Journal of the American Society for Mass Spectrometry* (1994); 5:976–989

[196] Elias, J. and Gygi, S. “Target-decoy search strategy for increased confidence in large-scale protein identifications by mass spectrometry”. *Nature methods* (2007); 4:207–214

[197] Chen, X., Wei, S., Ji, Y., Guo, X. and Yang, F. “Quantitative proteomics using SILAC: Principles, applications, and developments”. *Proteomics* (2015); 15:3175–3192

[198] Zhu, H., Pan, S., Gu, S., Bradbury, E. and Chen, X. “Amino acid residue specific stable isotope labeling for quantitative proteomics”. *Rapid Communications in Mass Spectrometry* (2002); 16:2115–2123

[199] Ong, S., Blagoev, B., Kratchmarova, I., Kristensen, D., Steen, H., Pandey, A. and Mann, M. “Stable isotope labeling by amino acids in cell culture, SILAC, as a simple and accurate approach to expression proteomics”. *Molecular & Cellular Proteomics* (2002); 1:376–386

[200] Mann, M. “Functional and quantitative proteomics using SILAC”. *Nat Rev Mol Cell Biol* (2006); 7:952–958

[201] Ong, S. and Mann, M. "A practical recipe for stable isotope labeling by amino acids in cell culture (SILAC)". *Nature Protocols* (2007); 1:2650–2660

[202] Daviña Nuñez, R. "Mass spectrometric analysis of RIG-I interaction partners during influenza B virus infection". Ph.D. thesis, Humboldt University Berlin (2015)

[203] Graham, F. and van der Eb, A. "A new technique for the assay of infectivity of human adenovirus 5 DNA." *Virology* (1973); 52:456–467

[204] NCBI. "Ncbi gene database". `http://www.ncbi.nlm.nih.gov/gene/` [accessed: 2013-12-15]

[205] Trinkle-Mulcahy, L., Boulon, S., Lam, Y., Urcia, R., Boisvert, F., Vandermoere, F., Morrice, N., Swift, S., Rothbauer, U., Leonhardt, H. and Lamond, A. "Identifying specific protein interaction partners using quantitative mass spectrometry and bead proteomes". *The Journal of Cell Biology* (2008); 183:223–239

[206] Bergmann, M., García-Sastre, A., Carnero, E., Pehamberger, H., Wolff, K., Palese, P. and Muster, T. "Influenza virus NS1 protein counteracts PKR-mediated inhibition of replication". *Journal of Virology* (2000); 74:6203–6206

[207] Paul, F., Hosp, F. and Selbach, M. "Analyzing protein-protein interactions by quantitative mass spectrometry". *Methods* (2011); 54:387–395

[208] Thomas, P. "Panther classification system" (2006). `http://pantherdb.org/` [accessed: 2015-09-15]

[209] Jensen, L., Kuhn, M., Stark, M., Chaffron, S., Creevey, C., Muller, J., Doerks, T., Julien, P., Roth, A., Simonovic, M., Bork, P. and von Mering, C. "STRING 8 - a global view on proteins and their functional interactions in 630 organisms". *Nucleic Acids Research* (2009); 37:D412–D416

[210] Jensen, L., Kuhn, M., Stark, M., Chaffron, S., Creevey, C., Muller, J., Doerks, T., Julien, P., Roth, A., Simonovic, M., Bork, P. and von Mering, C. "String database network analysis tool". `http://string-db.org` [accessed: 2016-02-10]

[211] Chase, G., Deng, T., Fodor, E., Leung, B., Mayer, D., Schwemmle, M. and Brownlee, G. "HSP90 inhibitors reduce influenza virus replication in cell culture." *Virology* (2008); 377:431–439

[212] Momose, F., Naito, T., Yano, K., Sugimoto, S., Morikawa, Y. and Nagata, K. "Identification of HSP90 as a stimulatory host factor involved in influenza virus RNA synthesis". *Journal of Biological Chemistry* (2002); 277:45306–45314

[213] Bortz, E., Westera, L., Maamary, J., Steel, J., Albrecht, R., Manicassamy, B., Chase, G., Martínez-Sobrido, L., Schwemmle, M. and García-Sastre, A. "Host- and strain-specific regulation of influenza virus polymerase activity by interacting cellular proteins". *mBio* (2011); 2:00151–11

[214] Donzé, O., Abbas-Terki, T. and Picard, D. "The HSP90 chaperone complex is both a facilitator and a repressor of the dsRNA-dependent kinase PKR". *The EMBO Journal* (2001); 20:3771–3780

[215] Stöhr, N., Lederer, M., Reinke, C., Meyer, S., Hatzfeld, M., Singer, R. and Hüttelmaier, S. "ZBP1 regulates mRNA stability during cellular stress". *The Journal of Cell Biology* (2006); 175:527–534

[216] Shen, V. and Kiledjian, M. "A view to a kill: Structure of the RNA exosome". *Cell* (2006); 127:1093–1095

[217] Büttner, K., Wenig, K. and Hopfner, K. "The exosome: a macromolecular cage for controlled RNA degradation". *Molecular Microbiology* (2006); 61:1372–1379

[218] Franz, M. "Charakterisierung einer potentiellen rolle des nicht-strukturproteins (NS) 1 der influenza A viren im viralen mRNA export". Ph.D. thesis, Free University Berlin (2012)

[219] von Recum-Knepper, J. "Single cell analysis of interferon-stimulated gene induction in response to influenza A virus infection". Ph.D. thesis, Humboldt University Berlin (2014)

[220] Sahni, N., Yi, S., Taipale, M., Fuxman Bass, J., Coulombe-Huntington, J., Yang, F., Peng, J., Weile, J., Karras, G., Wang, Y., Kovács, I., Kamburov, A., Krykbaeva, I., Lam, M., Tucker, G., Khurana, V., Sharma, A., Liu, Y., Yachie, N., Zhong, Q., Shen, Y., Palagi, A., San-Miguel, A., Fan, C., Balcha, D., Dricot, A., Jordan, D., Walsh, J., Shah, A., Yang, X., Stoyanova, A., Leighton, A., Calderwood, M., Jacob, Y., Cusick, M., Salehi-Ashtiani, K., Whitesell, L., Sunyaev, S., Berger, B., Barabási, A., Charloteaux, B., Hill, D., Hao, T., Roth, F., Xia, Y., Walhout, A., Lindquist, S. and Vidal, M. "Widespread macromolecular interaction perturbations in human genetic disorders". *Cell* (2015); 161:647–660

[221] Meyer, K. and Selbach, M. "Quantitative affinity purification mass spectrometry: a versatile technology to study protein-protein interactions". *Frontiers in Genetics* (2015); 6:1–7

[222] Brückner, A., Polge, C., Lentze, N., Auerbach, D. and Schlattner, U. "Yeast two-hybrid, a powerful tool for systems biology". *International journal of molecular sciences* (2009); 10:2763–2788

[223] Blalock, W., Piazzi, M., Bavelloni, A., Raffini, M., Faenza, I., D'Angelo, A. and Cocco, L. "Identification of the PKR nuclear interactome reveals roles in ribosome biogenesis, mRNA processing and cell division". *Journal of Cellular Physiology* (2014); 229:1047–1060

[224] Li, S., Wang, L., Berman, M., Kong, Y. and Dorf, M. "Mapping a dynamic innate immunity protein interaction network regulating type I interferon production". *Immunity* (2011); 35:1074–7613

[225] Brina, D., Miluzio, A., Ricciardi, S. and Biffo, S. “eIF6 anti-association activity is required for ribosome biogenesis, translational control and tumor progression”. *Biochimica et Biophysica Acta - Gene Regulatory Mechanisms* (2015); 1849:830–835

[226] Miluzio, A., Beugnet, A., Volta, V. and Biffo, S. “Eukaryotic initiation factor 6 mediates a continuum between 60s ribosome biogenesis and translation”. *EMBO reports* (2009); 10:459–465

[227] VIB/ UGent, B..E.G. “Venn diagram calculation tool”. `http://bioinformatics.psb.ugent.be/webtools/Venn/` [accessed: 2016-04-16]

[228] Fuller-Pace, F. “DExD/H box RNA helicases: multifunctional proteins with important roles in transcriptional regulation”. *Nucleic Acids Research* (2006); 34:4206–4215

[229] Zhang, Z., Yuan, B., Lu, N., Facchinetti, V. and Liu, Y. “DHX9 pairs with IPS-1 to sense double-stranded RNA in myeloid dendritic cells”. *The Journal of Immunology* (2011); 187:4501–4508

[230] Sadler, A., Latchoumanin, O., Hawkes, D., Mak, J. and Williams, B. “An antiviral response directed by PKR phosphorylation of the RNA helicase A”. *PLoS Pathogens* (2009); 5:1–11

[231] Fuchsová, B., Novák, P., Kafková, J. and Hozák, P. “Nuclear DNA helicase II is recruited to IFN-α-activated transcription sites at PML nuclear bodies”. *The Journal of Cell Biology* (2002); 158:463–473

[232] Fullam, A. and Schroeder, M. “DExD/H-box RNA helicases as mediators of antiviral innate immunity and essential host factors for viral replication”. *Biochimica et Biophysica Acta - Gene Regulatory Mechanisms* (2013); 1829:854–865

[233] Lin, L., Li, Y., Pyo, H., Lu, X., Thulasi Raman, S., Liu, Q., Brown, E. and Zhou, Y. “Identification of RNA helicase A as a cellular factor that interacts with influenza A virus NS1 protein and its role in the virus life cycle”. *Journal of Virology* (2012); 86:1942–1954

[234] Chen, B., Piel, W., Gui, L., Bruford, E. and Monteiro, A. “The HSP90 family of genes in the human genome: Insights into their divergence and evolution”. *Genomics* (2005); 86:627–637

[235] Varjosalo, M., Sacco, R., Stukalov, A., van Drogen, A., Planyavsky, M., Hauri, S., Aebersold, R., Bennett, K., Colinge, J., Gstaiger, M. and Superti-Furga, G. “Interlaboratory reproducibility of large-scale human protein-complex analysis by standardized AP-MS”. *Nature methods* (2013); 10:307–314

[236] Gough, D., Messina, N., Clarke, C., Johnstone, R. and Levy, D. “Constitutive type I interferon modulates homeostatic balance through tonic signaling”. *Immunity* (2012); 36:166–174

[237] Banchereau, J. and Pascual, V. “Type I interferon in systemic lupus erythematosus and other autoimmune diseases”. *Immunity* (2006); 25:383–392

[238] Reineke, L., Kedersha, N., Langereis, M., van Kuppeveld, F. and Lloyd, R. “Stress granules regulate double-stranded RNA-dependent protein kinase activation through a complex containing G3BP1 and Caprin1”. *MBio* (2015); 6:1–12

[239] Reineke, L., Dougherty, J., Pierre, P. and Lloyd, R. “Large G3BP-induced granules trigger eIF2α phosphorylation”. *Molecular Biology of the Cell* (2012); 23:3499–3510

[240] Onuki, R., Bando, Y., Suyama, E., Katayama, T., Kawasaki, H., Baba, T., Tohyama, M. and Taira, K. “An RNA-dependent protein kinase is involved in tunicamycin-induced apoptosis and Alzheimer’s disease”. *The EMBO Journal* (2004); 23:959–968

[241] Bando, Y., Onuki, R., Katayama, T., Manabe, T., Kudo, T., Taira, K. and Tohyama, M. “Double-strand RNA dependent protein kinase (PKR) is involved in the extrastriatal degeneration in Parkinson’s disease and Huntington’s disease”. *Neurochemistry International* (2005); 46:11–18

[242] Yamasaki, S. and Anderson, P. “Reprogramming mRNA translation during stress”. *Current Opinion in Cell Biology* (2008); 20:222–226

[243] Zhao, M., Tang, D., Lechpammer, S., Hoffman, A., Asea, A., Stevenson, M. and Calderwood, S. “Double-stranded RNA-dependent protein kinase (PKR) is essential for thermotolerance, accumulation of HSP70, and stabilization of ARE-containing HSP70 mRNA during stress”. *Journal of Biological Chemistry* (2002); 277:44539–44547

[244] Dalet, A., Gatti, E. and Pierre, P. “Integration of PKR-dependent translation inhibition with innate immunity is required for a coordinated anti-viral response”. *FEBS Letters* (2015); 589:1539–1545

[245] Watanabe, T., Kawakami, E., Shoemaker, J., Lopes, T., Matsuoka, Y., Tomita, Y., Kozuka-Hata, H., Gorai, T., Kuwahara, T., Takeda, E., Nagata, A., Takano, R., Kiso, M., Yamashita, M., Sakai-Tagawa, Y., Katsura, H., Nonaka, N., Fujii, H., Fujii, K., Sugita, Y., Noda, T., Goto, H., Fukuyama, S., Watanabe, S., Neumann, G., Oyama, M., Kitano, H. and Kawaoka, Y. “Influenza virus-host interactome screen as a platform for antiviral drug development”. *Cell host & microbe* (2014); 16:795–805

[246] Börgeling, Y., Schmolke, M., Viemann, D., Nordhoff, C., Roth, J. and Ludwig, S. “Inhibition of p38 mitogen-activated protein kinase impairs influenza virus-induced primary and secondary host gene responses and protects mice from lethal H5N1 infection”. *Journal of Biological Chemistry* (2014); 289:13–27

[247] Gil, J. and Esteban, M. “Activation of NF-κB by the dsRNA-dependent protein kinase, PKR involves the iκB kinase complex”. *Oncogene* (2000); 19:1369–1378

[248] Cammas, A., Sanchez, B., Lian, X., Dormoy-Raclet, V., van der Giessen, K., de Silanes, I., Ma, J., Wilusz, C., Richardson, J., Gorospe, M., Millevoi, S., Giovarelli, M., Gherzi, R., Di Marco, S. and Gallouzi, I. "Destabilization of nucleophosmin mRNA by the HuR/KSRP complex is required for muscle fibre formation". *Nature Communications* (2014); 5:1–16

[249] Pang, Q., Christianson, T., Koretsky, T., Carlson, H., David, L., Keeble, W., Faulkner, G., Speckhart, A. and Bagby, G. "Nucleophosmin interacts with and inhibits the catalytic function of eukaryotic initiation factor 2 kinase PKR". *Journal of Biological Chemistry* (2003); 278:41709–41717

[250] Liu, A., Li, Y., Qi, W., Ma, X., Yu, K., Huang, B., Liao, M., Li, F., Pan, J. and Song, M. "Comparative analysis of selected innate immune-related genes following infection of immortal DF-1 cells with highly pathogenic (H5N1) and low pathogenic (H9N2) avian influenza viruses". *Virus Genes* (2015); 50:189–199

[251] Coombs, K., Berard, A., Xu, W., Krokhin, O., Meng, X., Cortens, J., Kobasa, D., Wilkins, J. and Brown, E. "Quantitative proteomic analyses of influenza virus-infected cultured human lung cells". *Journal of Virology* (2010); 84:10888–10906

7 Appendix

One and three letter code of amino acids

A	Ala	Alanine	M	Met	Methionine
C	Cys	Cysteine	N	Asn	Asparagine
D	Asp	Aspartic acid	P	Pro	Proline
E	Glu	Glutamic acid	Q	Gln	Glutamine
F	Phe	Phenylalanine	R	Arg	Arginine
G	Gly	Glycine	S	Ser	Serine
H	His	Histidine	T	Thr	Threonine
I	Ile	Isoleucine	V	Val	Valine
K	Lys	Lysine	W	Trp	Tryptophan
L	Leu	Leucine	Y	Tyr	Tyrosine

Supplementary figures

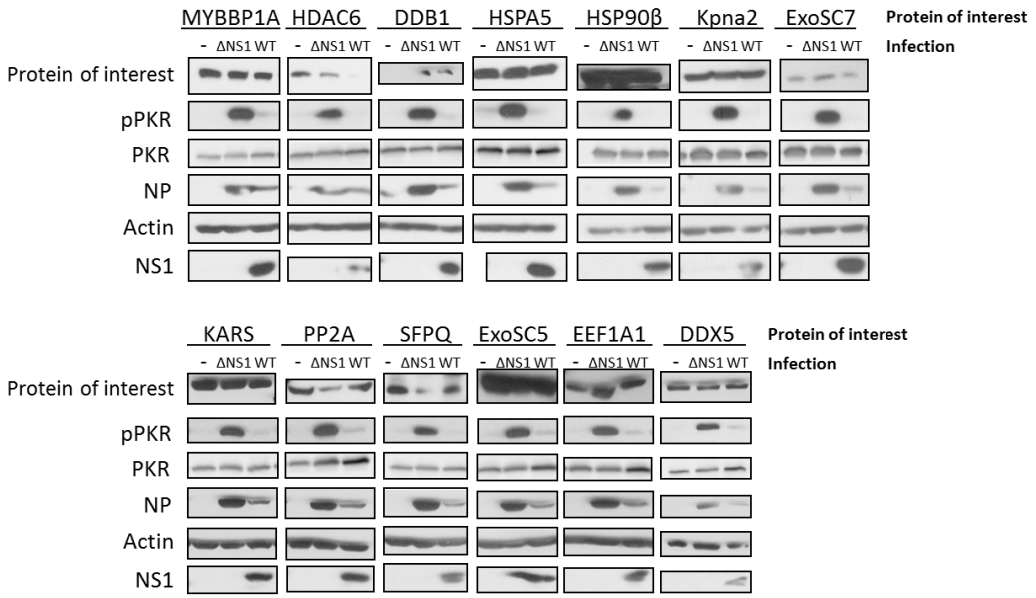

Figure 7.1. Overexpression of 14 identified PKR interaction partners does not affect phosphorylation of endogenous PKR. A 293T cells were transfected with expression vectors for tagged versions of MYPPP1A, HDAC6, DDB1, HSPA5, HSP90β, KPNA2, ExoSC7, KARS, PP2A, SFPQ, ExoSC5, EEF1A1 or DDX5 and infected with influenza A/PR/8 WT virus, ΔNS1 virus or non-infected. 16 h p.i. cells were lysed and analysed by SDS PAGE and immunoblotting using tag-specific or the indicated antibodies. Representative experiment of n = 4.

Supplementary tables

Study	Number of elements	Elements
Blalock et al., 2013; Li et al., 2011; Thesis	2	EIF6 DHX9
Blalock et al., 2013; Thesis	5	ACTB GRWD1 C7orf50 KPNA2 TUBB
Blalock et al., 2013; Li et al., 2011	9	PPP1CC GNL3 LYAR HNRNPCL1 NOP2 HIST1H1C NOC3L HNRNPC TOP1
Thesis	40	PRKCSH DECR1 DDB1 YWHAH RDX DDX5 CD2BP2 MSN VIM SRSF7 SFPQ EIF2S1 CBS HSPA9 EXOSC2 EXOSC7 HSPA1A PRMT1 EXOSC6 SKIV2L2 HSPA5 C14orf166 PPP2R1A SRSF5 SRSF1 CCT8 HPRT1 EZR HSP90AB1 EXOSC5 ISOC2 MYBBP1A LRRC59 KHSRP PWP1 EEF1A1 IGF2BP1 GRSF1 HDAC6 HSP90AA1
Li et al., 2011	25	PRKRA MOV10 FARSB EBNA1BP2 CCDC124 STAU2 DICER1 GTPBP4 PURA KCTD17 TOLLIP GLTSCR2 PABPC4 SSB FTSJ3 XRN2 ZNF346 FARSA CCNA2 DHX30 EDC4 TARBP2 IFRD1 CDK3 STAU1
Blalock et al., 2013	120	RPL10 RPL10L HSPD1 YBX1 RPL23 SRSF2 CBX5 PP1CB YLPM1 ACTA2 DDX1 HNRPM TAF15 CCDC137 HBA SSRP1 SMARCA4 BMS1 BUB3 RPL26 HIST1H2A WDR43 RPL34 MYST2 DHX37 SON TUBA4A RRP36 EWSR1 TPX2 KPNA4 NPM U2AF1 HSP8 DKC1 RRP15 SUB1 TUBB3 HNRNPD SMARCC2 MAGEB1 AHCTF1 U2AF2 SYNCRIP SMARCA5 SMARCC1 GNB2L1 TUBB2A RPL36 RPL3 EBNA1BP ADAR1 RIF1 ILF3 LARP1 SRP14 TUBA1A COIL HIST1H2AA DBPA CHD1 RUVBL2 HNRPDL RBBP4 ILF2 ELAVL1 GLYR1 ARID2 SPTAN1 POLDIP3 RPL22 RPL32 HIST1H2AC RPS10L KRR1 ACTL6A PINX1 RPL35 RPS10 BAT1 RPS26 NOL12 NGND RUVBL1 SNRPA1 RPS19 RPL27A DX39B RBM19 DDX54 RSL24D1 POTEF TUBB4 HBD CDCA5 CENPF BCLAF1 NUSAP1 H1F0 TRA2B SMARCA1 TUBA1B RRP1 EIF4A1 PBRM1 EIF4A3 SURF6 THOC2 PA2G4 SRRM1 UTP3 PPP1CA PPAN HIST1H2AB SLC25A5 C1orf77 TUBB2C SRSF6 SNRPD2 DCD

Table 7.1. Result table of Venn diagram analysis. Lists of 137 PKR binding proteins from Blalock *et al.* and 36 high confidence candidate proteins (HCIP) for Flag-PKR from Li *et al.* were compared to 47 PKR interacting proteins from this thesis [223, 224] with a Venn diagram calculation tool [227].

Identified proteins from single SILAC experiments

Replicate 1

Gene name	Description	Score	Coverage	Unique peptides	Ratio WT/ Mock	Ratio ΔNS1/ Mock
TUBB	Tubulin beta chain	18,26	25,23	8	1,653	2,257
HSP90AA1	Heat shock protein HSP 90-alpha	30,51	15,30	2	0,894	0,293
EIF2S1	Eukaryotic translation initiation factor 2 subunit 1	5,15	10,16	3	1,806	2,642
EIF6	Eukaryotic translation initiation factor 6	14,91	31,43	5	1,986	2,284
YWHAH	14-3-3 protein eta	57,90	31,71	3	8,197	8,212
EZR	Ezrin	46,70	22,35	7	1,942	4,223
ACTB	Actin, cytoplasmic 1	27,12	29,33	8	1,872	2,622
EXOSC2	Exosome complex component RRP4	27,59	45,05	8	1,846	2,843
EEF1A1	Elongation factor 1-alpha 1	4,69	6,71	3	1,713	1,918
RDX	Radixin	22,90	15,27	3	1,074	6,848
GRWD1	Glutamate-rich WD repeat-containing protein 1	28,65	28,92	7	1,618	2,017
EXOSC7	Exosome complex component RRP42	12,36	13,40	3	1,748	2,668
PRKCSH	Glucosidase 2 subunit beta	6,67	6,25	3	7,662	7,726
PRMT1	Protein arginine N-methyltransferase 1	6,75	9,42	3	1,652	2,288
EXOSC6	Exosome complex component MTR3	17,93	27,21	6	1,634	2,208
SFPQ	Splicing factor, proline- and glutamine-rich	28,51	17,40	8	1,700	2,466
HDAC6	Histone deacetylase 6	16,63	3,87	3	2,430	3,505

Gene name	Description	Score	Coverage	Unique peptides	Ratio WT/ Mock	Ratio ΔNS1/ Mock
CBS	Cystathionine beta-synthase					
DDX5	Probable ATP-dependent RNA helicase DDX5					
GRSF1	G-rich sequence factor 1	11,25	14,37	4	2,163	2,121
ISOC2	Isochorismatase domain-containing protein 2, mitochondrial	9,42	29,76	3	2,157	1,714
SRSF7	Serine/arginine-rich splicing factor 7					
EXOSC5	Exosome complex component RRP46	12,92	19,15	4	1,700	1,867
KPNA2	Importin subunit alpha-1	6,97	7,18	3	0,962	2,212
PWP1	Periodic tryptophan protein 1 homolog	9,69	10,98	3	0,689	0,471
SRSF1	Serine/arginine-rich splicing factor 1					
CD2BP2	CD2 antigen cytoplasmic tail-binding protein 2	10,44	15,84	5	1,181	2,048
DDB1	DNA damage-binding protein 1	5,44	7,02	7	0,951	3,577
EIF2AK2	Interferon-induced, double-stranded RNA-activated protein kinase	568,27	41,56	22	1,007	0,396
HSP90AB1	Heat shock protein HSP 90-beta	34,19	18,78	3	0,887	0,344
PPP2R1A	Serine/threonine-protein phosphatase 2A 65 kDa regulatory subunit A alpha isoform					
DHX9	ATP-dependent RNA helicase A	35,67	12,44	12	1,322	1,030
IGF2BP1	Insulin-like growth factor 2 mRNA-binding protein 1					
LRRC59	Leucine-rich repeat-containing protein 59					

Gene name	Description	Score	Coverage	Unique peptides	Ratio WT/ Mock	Ratio ΔNS1/ Mock
C14orf166	UPF0568 protein C14orf166	5,86	11,89	2	0,735	5,543
CCT8	T-complex protein 1 subunit theta					
HPRT1	Hypoxanthine-guanine phosphoribosyltransferase	16,58	16,51	3	0,652	0,444
HSPA9	Stress-70 protein, mitochondrial	108,87	40,21	21	1,021	0,698
HSPA1A	Heat shock 70 kDa protein 1A/1B	6,81	13,42	5	0,739	0,906
MSN	Moesin	18,44	13,69	3	0,951	7,979
KHSRP	Far upstream element-binding protein 2					
VIM	Vimentin	5,46	6,22	3	1,012	4,357
HSPA5	78 kDa glucose-regulated protein	94,62	37,00	16	1,036	1,237
C7orf50	Uncharacterized protein C7orf50	14,58	39,18	4	0,951	2,228
DECR1	2,4-dienoyl-CoA reductase, mitochondrial	27,51	28,06	7	1,554	1,429
SRSF5	Serine/arginine-rich splicing factor 5					
MYBBP1A	Myb-binding protein 1A	15,48	4,59	4	1,221	0,967
SKIV2L2	Superkiller viralicidic activity 2-like 2					

Table 7.2. Detailed data for proteins identified as PKR binding partners in replicate 1. .

Replicate 2

Gene name	Description	Score	Coverage	Unique peptides	Ratio WT/ Mock	Ratio ΔNS1/ Mock
TUBB	Tubulin beta chain	90,96	47,52	5	1,116	1,108
HSP90AA1	Heat shock protein HSP 90-alpha	86,57	22,68	5	1,067	0,931
EIF2S1	Eukaryotic translation initiation factor 2 subunit 1	35,69	49,84	13	0,981	1,088
EIF6	Eukaryotic translation initiation factor 6	17,20	36,33	5	1,049	0,887
YWHAH	14-3-3 protein eta	65,60	34,55	3	12,562	11,626
EZR	Ezrin	119,65	40,78	15	1,439	0,987
ACTB	Actin, cytoplasmic 1	56,24	43,20	11	0,833	0,964
EXOSC2	Exosome complex component RRP4	69,86	49,15	9	0,939	1,053
EEF1A1	Elongation factor 1-alpha 1	72,14	22,73	9	1,050	1,040
RDX	Radixin	79,43	27,62	8	1,200	0,984
GRWD1	Glutamate-rich WD repeat-containing protein 1	40,87	41,26	10	0,852	0,889
EXOSC7	Exosome complex component RRP42	32,28	28,87	6	0,957	1,055
PRKCSH	Glucosidase 2 subunit beta	35,71	18,94	9	1,124	1,074
PRMT1	Protein arginine N-methyltransferase 1	29,19	17,73	6	1,112	1,092
EXOSC6	Exosome complex component MTR3	27,99	43,75	8	0,974	1,023
SFPQ	Splicing factor, proline- and glutamine-rich	18,32	14,14	6	0,916	0,849
HDAC6	Histone deacetylase 6	12,70	3,87	3	1,759	1,581
CBS	Cystathionine beta-synthase	29,35	17,60	6	1,094	1,068
DDX5	Probable ATP-dependent RNA helicase DDX5	15,79	11,40	6	0,991	0,961

Gene name	Description	Score	Coverage	Unique peptides	Ratio WT/ Mock	Ratio ΔNS1/ Mock
GRSF1	G-rich sequence factor 1	30,76	21,67	6	0,752	0,756
ISOC2	Isochorismatase domain-containing protein 2, mitochondrial	24,59	52,68	5	0,978	1,150
SRSF7	Serine/arginine-rich splicing factor 7	6,06	24,79	6	1,707	1,103
EXOSC5	Exosome complex component RRP46	12,00	15,32	3	0,919	1,109
KPNA2	Importin subunit alpha-1	15,76	13,80	6	1,243	0,981
PWP1	Periodic tryptophan protein 1 homolog	16,91	15,57	5	0,905	0,826
SRSF1	Serine/arginine-rich splicing factor 1	11,68	21,37	5	1,734	1,192
CD2BP2	CD2 antigen cytoplasmic tail-binding protein 2	18,31	23,17	6	0,939	0,827
DDB1	DNA damage-binding protein 1	18,94	11,49	9	0,834	0,984
EIF2AK2	Interferon-induced, double-stranded RNA-activated protein kinase	931,08	43,74	25	0,932	0,952
HSP90AB1	Heat shock protein HSP 90-beta	105,24	27,90	8	1,005	0,929
PPP2R1A	Serine/threonine-protein phosphatase 2A 65 kDa regulatory subunit A alpha isoform	34,67	19,02	8	0,995	1,017
DHX9	ATP-dependent RNA helicase A	37,86	11,57	12	0,973	1,025
IGF2BP1	Insulin-like growth factor 2 mRNA-binding protein 1	20,49	16,64	7	0,989	0,929
LRRC59	Leucine-rich repeat-containing protein 59	13,29	14,66	5	0,948	0,813
C14orf166	UPF0568 protein C14orf166	10,63	19,26	4	1,135	0,907
CCT8	T-complex protein 1 subunit theta	31,39	15,69	8	1,001	1,046

Gene name	Description	Score	Coverage	Unique peptides	Ratio WT/ Mock	Ratio ΔNS1/ Mock
HPRT1	Hypoxanthine-guanine phosphoribosyltransferase	17,58	33,49	6	1,049	1,133
HSPA9	Stress-70 protein, mitochondrial	423,50	53,46	32	0,815	0,846
HSPA1A	Heat shock 70 kDa protein 1A/1B	426,65	63,65	24	1,257	1,021
MSN	Moesin	93,68	31,89	12	1,197	1,049
KHSRP	Far upstream element-binding protein 2	26,21	18,28	8	0,836	0,781
VIM	Vimentin	11,59	14,81	6	0,671	1,160
HSPA5	78 kDa glucose-regulated protein	303,97	56,27	30	1,079	1,152
C7orf50	Uncharacterized protein C7orf50	10,16	29,38	3	0,781	0,791
DECR1	2,4-dienoyl-CoA reductase, mitochondrial	43,79	51,04	13	0,867	1,186
SRSF5	Serine/arginine-rich splicing factor 5	16,79	16,54	4	2,010	1,391
MYBBP1A	Myb-binding protein 1A	9,98	4,52	4	1,009	0,991
SKIV2L2	Superkiller viralicidic activity 2-like 2	6,30	2,21	2	0,889	1,180

Table 7.3. Detailed data for proteins identified as PKR binding partners in replicate 2. .

Replicate 3

Gene name	Description	Score	Coverage	Unique peptides	Ratio WT/ Mock	Ratio ΔNS1/ Mock
TUBB	Tubulin beta chain					
HSP90AA1	Heat shock protein HSP 90-alpha	25,42	16,80	4	0,999	0,949
EIF2S1	Eukaryotic translation initiation factor 2 subunit 1	8,39	27,62	8	0,944	0,450
EIF6	Eukaryotic translation initiation factor 6	8,61	31,84	4	1,000	10,941
YWHAH	14-3-3 protein eta	38,35	36,59	3	0,992	0,108
EZR	Ezrin	38,43	20,14	9	1,000	10,054
ACTB	Actin, cytoplasmic 1	27,67	25,87	8	1,000	0,572
EXOSC2	Exosome complex component RRP4	15,90	43,69	8	1,000	10,145
EEF1A1	Elongation factor 1-alpha 1	37,95	22,94	9	0,940	0,101
RDX	Radixin	16,33	11,15	4	1,762	0,327
GRWD1	Glutamate-rich WD repeat-containing protein 1	20,51	29,82	7	1,000	10,672
EXOSC7	Exosome complex component RRP42	7,48	9,28	2	1,000	100,000
PRKCSH	Glucosidase 2 subunit beta					
PRMT1	Protein arginine N-methyltransferase 1	6,97	9,42	3	1,000	3,192
EXOSC6	Exosome complex component MTR3	7,14	25,37	5	1,000	9,846
SFPQ	Splicing factor, proline- and glutamine-rich	8,28	5,66	3	1,000	100,000
HDAC6	Histone deacetylase 6	5,27	3,13	3	1,000	4,562
CBS	Cystathionine beta-synthase	12,19	17,06	5	1,000	100,000
DDX5	Probable ATP-dependent RNA helicase DDX5	13,93	11,24	5	1,000	7,234

Gene name	Description	Score	Coverage	Unique peptides	Ratio WT/ Mock	Ratio ΔNS1/ Mock
GRSF1	G-rich sequence factor 1	7,22	6,04	2	0,805	0,839
ISOC2	Isochorismatase domain-containing protein 2, mitochondrial	8,51	17,07	2	1,620	3,006
SRSF7	Serine/arginine-rich splicing factor 7	10,24	21,85	5	1,000	100,000
EXOSC5	Exosome complex component RRP46	13,20	9,36	2	46,485	7,499
KPNA2	Importin subunit alpha-1	9,70	14,18	6	1,000	4,960
PWP1	Periodic tryptophan protein 1 homolog	8,35	8,58	4	1,000	3,888
SRSF1	Serine/arginine-rich splicing factor 1	3,99	9,27	2	1,000	8,586
CD2BP2	CD2 antigen cytoplasmic tail-binding protein 2					
DDB1	DNA damage-binding protein 1					
EIF2AK2	Interferon-induced, double-stranded RNA-activated protein kinase	304,58	44,28	21	1,074	0,094
HSP90AB1	Heat shock protein HSP 90-beta	31,71	22,24	7	1,000	100,000
PPP2R1A	Serine/threonine-protein phosphatase 2A 65 kDa regulatory subunit A alpha isoform	13,15	9,85	4	0,881	1,073
DHX9	ATP-dependent RNA helicase A	28,15	14,17	14	1,000	4,698
IGF2BP1	Insulin-like growth factor 2 mRNA-binding protein 1	9,06	12,13	5	1,000	7,329
LRRC59	Leucine-rich repeat-containing protein 59	11,55	12,05	4	1,000	100,000
C14orf166	UPF0568 protein C14orf166	16,19	33,20	6	1,000	100,000
CCT8	T-complex protein 1 subunit theta	5,24	4,01	2	1,000	10,599

Gene name	Description	Score	Coverage	Unique peptides	Ratio WT/ Mock	Ratio ΔNS1/ Mock
HPRT1	Hypoxanthine-guanine phosphoribosyltransferase	11,82	20,64	4	1,000	9,926
HSPA9	Stress-70 protein, mitochondrial	54,67	38,14	22	1,000	6,512
HSPA1A	Heat shock 70 kDa protein 1A/1B	78,83	42,43	18	1,000	6,448
MSN	Moesin	13,31	8,49	3	1,000	4,796
KHSRP	Far upstream element-binding protein 2	7,86	6,75	4	1,000	4,839
VIM	Vimentin	12,64	20,17	9	1,000	3,605
HSPA5	78 kDa glucose-regulated protein	64,83	33,49	16	1,503	3,818
C7orf50	Uncharacterized protein C7orf50					
DECR1	2,4-dienoyl-CoA reductase, mitochondrial	15,41	18,51	6	0,979	0,092
SRSF5	Serine/arginine-rich splicing factor 5					
MYBBP1A	Myb-binding protein 1A	13,17	5,27	6	0,749	0,092
SKIV2L2	Superkiller viralicidic activity 2-like 2					

Table 7.4. Detailed data for proteins identified as PKR binding partners in replicate 3. .

Replicate 4

Gene name	Description	Score	Coverage	Unique peptides	Ratio WT/ Mock	Ratio ΔNS1/ Mock
TUBB	Tubulin beta chain	49,81	37,61	12	0,360	1,240
HSP90AA1	Heat shock protein HSP 90-alpha	14,52	9,29	2	3,846	5,061
EIF2S1	Eukaryotic translation initiation factor 2 subunit 1	58,88	53,65	14	100,000	1,000
EIF6	Eukaryotic translation initiation factor 6	4,78	15,92	3	100,000	1,000
YWHAH	14-3-3 protein eta	90,05	48,37	7	0,125	0,778
EZR	Ezrin	37,22	21,50	8	0,376	2,236
ACTB	Actin, cytoplasmic 1	52,34	37,33	11	0,010	0,010
EXOSC2	Exosome complex component RRP4	49,11	47,44	10	100,000	1,000
EEF1A1	Elongation factor 1-alpha 1	31,18	22,29	9		
RDX	Radixin	13,84	12,01	3	0,265	2,051
GRWD1	Glutamate-rich WD repeat-containing protein 1	14,99	19,51	5	100,000	1,000
EXOSC7	Exosome complex component RRP42	40,39	34,36	8	100,000	1,000
PRKCSH	Glucosidase 2 subunit beta					
PRMT1	Protein arginine N-methyltransferase 1	33,07	25,76	9	0,265	0,907
EXOSC6	Exosome complex component MTR3	20,38	39,34	9	100,000	1,000
SFPQ	Splicing factor, proline- and glutamine-rich	16,53	13,44	6	100,000	1,000
HDAC6	Histone deacetylase 6	20,10	7,57	6	100,000	1,000
CBS	Cystathionine beta-synthase	4,41	5,81	2	100,000	1,000
DDX5	Probable ATP-dependent RNA helicase DDX5	15,36	14,50	7	100,000	1,000

Gene name	Description	Score	Coverage	Unique peptides	Ratio WT/ Mock	Ratio ΔNS1/ Mock
GRSF1	G-rich sequence factor 1	8,73	12,92	4	100,000	1,000
ISOC2	Isochorismatase domain-containing protein 2, mitochondrial					
SRSF7	Serine/arginine-rich splicing factor 7	19,40	21,85	5	100,000	1,000
EXOSC5	Exosome complex component RRP46	11,80	15,32	3	100,000	1,000
KPNA2	Importin subunit alpha-1	16,21	16,45	7	100,000	1,000
PWP1	Periodic tryptophan protein 1 homolog	13,00	14,57	5	5,209	1,000
SRSF1	Serine/arginine-rich splicing factor 1	20,26	30,24	7	100,000	1,000
CD2BP2	CD2 antigen cytoplasmic tail-binding protein 2	3,98	10,26	3	100,000	1,000
DDB1	DNA damage-binding protein 1	6,53	5,61	5	100,000	1,000
EIF2AK2	Interferon-induced, double-stranded RNA-activated protein kinase	611,80	43,38	24	0,068	1,167
HSP90AB1	Heat shock protein HSP 90-beta	12,77	12,15	3	0,074	1,000
PPP2R1A	Serine/threonine-protein phosphatase 2A 65 kDa regulatory subunit A alpha isoform	10,38	6,45	3	1,003	7,227
DHX9	ATP-dependent RNA helicase A	86,66	26,93	26	0,114	0,887
IGF2BP1	Insulin-like growth factor 2 mRNA-binding protein 1	20,92	16,81	7	0,100	0,744
LRRC59	Leucine-rich repeat-containing protein 59	14,92	16,29	5	0,117	0,763
C14orf166	UPF0568 protein C14orf166					
CCT8	T-complex protein 1 subunit theta	25,93	24,82	12	0,131	0,747

Gene name	Description	Score	Coverage	Unique peptides	Ratio WT/ Mock	Ratio ΔNS1/ Mock
HPRT1	Hypoxanthine-guanine phosphoribosyltrans-ferase					
HSPA9	Stress-70 protein, mitochondrial	60,80	35,49	19	0,989	0,933
HSPA1A	Heat shock 70 kDa protein 1A/1B	83,46	46,18	18	0,109	1,176
MSN	Moesin	17,75	9,01	2	1,688	1,348
KHSRP	Far upstream element-binding protein 2					
VIM	Vimentin	30,90	32,19	14	0,010	0,011
HSPA5	78 kDa glucose-regulated protein	59,61	40,67	17	0,267	1,000
C7orf50	Uncharacterized protein C7orf50					
DECR1	2,4-dienoyl-CoA reductase, mitochondrial	65,18	56,42	14	0,158	1,000
SRSF5	Serine/arginine-rich splicing factor 5	24,18	27,57	6	0,059	0,528
MYBBP1A	Myb-binding protein 1A	43,19	19,65	17	5,483	1,000
SKIV2L2	Superkiller viralicidic activity 2-like 2	14,32	8,73	7	100,000	1,000

Table 7.5. Detailed data for proteins identified as PKR binding partners in replicate 4. .

Selbstständigkeitserklärung

Hiermit erkläre ich, die Dissertation selbstständig und nur unter Verwendung der angegebenen Hilfen und Hilfsmittel angefertigt zu haben. Ich habe mich anderwärts nicht um einen Doktorgrad beworben und besitze einen entsprechenden Doktorgrad nicht. Ich erkläre die Kenntnisnahme der dem Verfahren zugrunde liegenden Promotionsordnung der Mathematisch-Naturwissenschaftlichen Fakultät I der Humboldt-Universität zu Berlin vom 06. Juli 2009.

Berlin, den 30.06.2016

Sandra Sänger